

In presenting the dissertation as a partial fulfillment of the requirements for an advanced degree from the Georgia Institute of Technology, I agree that the Library of the Institute shall make it available for inspection and circulation in accordance with its regulations governing materials of this type. I agree that permission to copy from, or to publish from, this dissertation may be granted by the professor under whose direction it was written, or, in his absence, by the Dean of the Graduate Division when such copying or publication is solely for scholarly purposes and does not involve potential financial gain. It is understood that any copying from, or publication of, this dissertation which involves potential financial gain will not be allowed without written permission.

---

3/17/65

b

AN INVESTIGATION INTO THE MEASUREMENT  
OF LONG PERIOD, LOW AMPLITUDE, TORSIONAL VIBRATIONS  
BY MEANS OF A SERVO TORSIONAL VIBROGRAPH

A THESIS

Presented to

The Faculty of the Graduate Division

by

Sydnor Hummer Byrne, Jr.

In Partial Fulfillment  
of the Requirements for the Degree  
Doctor of Philosophy  
in the School of Mechanical Engineering

Georgia Institute of Technology

April, 1967

AN INVESTIGATION INTO THE MEASUREMENT  
OF LONG PERIOD, LOW AMPLITUDE, TORSIONAL VIBRATIONS  
BY MEANS OF A SERVO TORSIONAL VIBROGRAPH

Approved: \_\_\_\_\_

Chairman \_\_\_\_\_

Date approved by Chairman: \_\_\_\_\_

*April 18, 1967*

## ACKNOWLEDGMENTS

The author wishes to express his sincere appreciation to all those individuals who have had an influence on his professional development.

The author wishes to thank expressly his father and mother, Dr. and Mrs. S. H. Byrne, whose encouragement made possible his academic achievements. He would also like to thank Dr. J. P. Vidosic for his basic foundation on the graduate level and his assistance in his capacity as head of the School of Mechanical Engineering.

The author would like to thank his wife for her encouragement and labor which made the completion of this work possible.

At the start of the research for this dissertation Dr. T. Nakada and Dr. K. G. Picha were of great help in the formulation of the basic idea for the research. Since then Dr. H. L. Johnson, the faculty advisor for this dissertation, has with patience and understanding helped the author. Dr. E. Harrison is particularly thanked for his help in the experimental part of the investigation. Appreciation is also extended to Dr. Harrison and Dr. W. J. Lnenicka for their helpful comments in reviewing the work.

Without the help of Messrs. H. O. Foster, L. A. Cavelli, R. J. Collins, and D. W. Kiebel the mechanical prototype of the servo torsional vibrograph could not have been constructed.

The author is greatly indebted to the National Aeronautics and

Space Administration for the financial assistance during his doctoral program.

## TABLE OF CONTENTS

	Page
ACKNOWLEDGMENTS. . . . .	ii
LIST OF TABLES . . . . .	vi
LIST OF ILLUSTRATIONS. . . . .	vii
SUMMARY. . . . .	x
Chapter	
I. INTRODUCTION. . . . .	1
Definition of the Problem	
Literature Search and Historical Background	
Investigation Procedure	
II. ANALYTICAL INVESTIGATION. . . . .	11
Derivation of Basic Equations	
General Description	
Description of the Servo Vibrograph Network	
Basic Theoretical Equations	
Frequency Response Equations	
Optimum Frequency Response	
Stability and Impulse Response	
Characteristic Equation	
Damping Characteristics of the Servo Vibrograph System	
Root Loci and the Stability of the System	
III. EXPERIMENTAL INVESTIGATION. . . . .	69
General Procedure	
Prototype Construction	
Operation and Design Refinement	
Experimental Procedure	
Frequency Response Tests	
Transient Tests	
Frequency Response Characteristics	
Transient Response Characteristics	

Chapter	Page
IV. CONCLUSIONS AND SUGGESTIONS FOR FURTHER RESEARCH. . . . .	83
Conclusions	
Suggestions for Further Research	
APPENDIX	
A. EXPERIMENTAL DATA . . . . .	89
B. PROTOTYPE CONSTRUCTION. . . . .	98
C. SUGGESTED DESIGN MODIFICATIONS. . . . .	106
D. SENSITIVITY ANALYSIS USING SENSITIVITY FUNCTION . . . . .	107
E. SAMPLE COMPUTER PROGRAMS. . . . .	114
LITERATURE CITED . . . . .	125
OTHER REFERENCES . . . . .	128
VITA . . . . .	130

## LIST OF TABLES

Table		Page
1.	Component Transfer Functions. . . . .	18
2.	Root Locus Characteristic Point Locations . . . . .	63
3.	Root Locus Characteristic Point Locations . . . . .	64
4.	Root Locus Characteristic Point Locations . . . . .	65
5.	Parts List. . . . .	104

## LIST OF ILLUSTRATIONS

Figure	Page
1. Basic Vibrograph. . . . .	3
2. Frequency Response of the Basic Vibrograph. . . . .	3
3. Schematic of the Servo Torsional Vibrograph . . . . .	13
4. Servo Vibrograph Block Diagram. . . . .	15
5. Servo Vibrograph Block Diagram with Transfer Functions. . .	15
6. Theoretical Frequency Response. . . . .	22
7. Frequency Response Characteristics. . . . .	25
8. Influence of the Damping Constant ( $C_1$ ) on the 10 Per Cent Amplitude Error Frequency. . . . .	33
9. Influence of the Damping Constant ( $C_1$ ) on the 10 Per Cent Phase Angle Error Frequency. . . . .	34
10. Influence of the Damping Constant ( $C_1$ ) on the Frequency of the Maximum . . . . .	35
11. Influence of the Servo Motor Time Constant ( $T_m$ ) on the 10 Per Cent Amplitude Error Frequency. . . . .	36
12. Influence of the Servo Motor Time Constant ( $T_m$ ) on the 10 Per Cent Phase Angle Error Frequency. . . . .	37
13. Influence of the Servo Motor Time Constant ( $T_m$ ) on the Frequency of the Maximum . . . . .	38
14. Influence of the Tachometer Feedback Constant ( $K_t$ ) on the 10 Per Cent Amplitude Error Frequency. . . . .	40
15. Influence of the Tachometer Feedback Constant ( $K_t$ ) on the 10 Per Cent Phase Angle Error Frequency. . . . .	41
16. Influence of the Tachometer Feedback Constant ( $K_t$ ) on the Frequency of the Maximum . . . . .	42
17. Influence of the Gamma Gain ( $\gamma$ ) on the 10 Per Cent Amplitude ( $Z$ ) and 10 Per Cent Phase Angle ( $A$ ) Error Frequencies ( $\beta = 0$ ) . . . . .	44

Figure	Page
18. Influence of the Gamma Gain ( $\gamma$ ) on the 10 Per Cent Amplitude (Z) and 10 Per Cent Phase Angle (A) Error Frequencies ( $\beta = 1.0$ ) . . . . .	45
19. Influence of the Beta Gain ( $\beta$ ) on the Value of the Optimum Gamma Gain ( $\gamma$ ) for Several Values of the Alpha Gain ( $\alpha$ ). . . . .	47
20. Influence of the Beta Gain ( $\beta$ ) on the 10 Per Cent Amplitude Error Frequency . . . . .	49
21. Influence of the Beta Gain ( $\beta$ ) on the 10 Per Cent Phase Angle Error Frequency . . . . .	50
22. Influence of the Beta Gain ( $\beta$ ) on the Frequency of the Maximum . . . . .	51
23. Root Locus Plots for the Servo Vibrograph (for Variable Gamma). . . . .	62
24. Root Locus for Optimum Values of the Parameters Plotted on Three Scales . . . . .	67
25. Prototype of the Servo Torsional Vibrograph . . . . .	70
26. Sample Output of the Servo Vibrograph . . . . .	90
27. Frequency Response of the Servo Vibrograph. . . . .	91
28. Frequency Response of the Servo Vibrograph. . . . .	92
29. Frequency Response of the Servo Vibrograph. . . . .	93
30. Frequency Response with Saturated Amplifiers. . . . .	94
31. Theoretical Response of the Servo Vibrograph to a Unit Impulse . . . . .	95
32. Transient Response of the Servo Vibrograph. . . . .	96
33. Transient Response of the Servo Vibrograph. . . . .	97
34. Top View of the Servo Torsional Vibrograph Prototype. . . . .	99
35. Front View of the Servo Torsional Vibrograph Prototype. . . . .	100
36. Driving Motor and Gear Box for the Sine Generator . . . . .	101

Figure	Page
37. Amplifiers for the Servo Vibrograph . . . . .	102
38. Servo System for the Servo Vibrograph . . . . .	103
39. Sensitivity of the Servo Vibrograph . . . . .	112

## SUMMARY

The principal objective of this work was a study of the analytical and experimental characteristics of the servo torsional vibrograph, the investigation of which has been made by considering the frequency and impulse responses of the device.

A device was needed to measure long period, low amplitude torsional vibrations which occur in large rotary machinery. To measure this vibration, a vibrograph is required which has an extremely long natural period, has a convenient output, and is not so large as to affect the efficiency and operation of the machinery. To achieve this objective, a servo feedback system was designed which, when added to a basic vibrograph, increased its natural period and improved its response characteristics. The basic torsional spring-mass system was modified by artificially decreasing the spring constant with a servo system. The servo system reduced the spring's relative displacement and by its action decreased the spring constant and the natural frequency.

Three amplifiers supplied the required action of the servo system. The principal feedback amplifier and the servo amplifier were in the main feedback path. In order to provide a stable null point an additional amplifier was used in a feedback path around the servo amplifier; tachometer feedback was also provided around the servo amplifier.

All analyses were based on linear analytical models of the system. In the frequency response analysis two criteria were used to find the optimum value for the parameters; the 10 per cent amplitude

error frequency and the 10 per cent phase angle error frequency. The frequency of the maximum amplitude was also calculated but was not used as a design criterion. The error frequencies were found for a wide range of all the parameters in order to optimize the frequency response. An equation was found for the optimum value of the servo amplifier gain, and the best value for each of the other parameters was found.

Using the sensitivity function, the feedback system was proved to be insensitive to small unexpected changes in the values of the parameters.

The root locus technique was used to investigate the stability of the system. For all positive values of each of the parameters the system was found to be stable. An equation was found for the optimum value of the parameters for critically-damped vibrometer action. This action is necessary when the device is to be used for the measurement of aperiodic inputs.

The experimental investigation was undertaken in order to determine the validity of the mathematical model and to determine the problems which would arise in a prototype of the device. For values of the parameters, which were in the linear range of the components, the theoretical response was found to duplicate the actual response very closely in the tests for the frequency response and the transient response.

The principle of the servo torsional vibrograph was proved by the investigation to be of practical value and the design, with small design modifications, could be used in practice for the measurement of very long period, low amplitude, torsional vibrations.

## CHAPTER I.

INTRODUCTIONDefinition of the Problem

This work is concerned with the investigation and design of a torsional vibrograph whose natural period and characteristics have been modified by means of a servo system. Vibrographs are instruments for measuring the displacement of vibrating bodies and the instrument under investigation was designed to measure torsional or angular vibrations of long period and low amplitude. In general the vibrograph is designed to have a low natural frequency so that the ratio of the frequency of the vibration to be measured to the natural frequency of the instrument will be as high as possible.

For this reason, in the measurement of a rotational or torsional vibration, it is necessary to have a torsional spring-mass system whose period is much longer than the period of the vibration to be measured. Much has been done to extend the use of the torsional vibrograph to higher frequencies, principally with application to the internal combustion engine (1,2,3,4,5). However, very little research has been conducted toward extending the range of the torsional vibrograph to long periods. A need has arisen to extend the range to lower frequencies in order to measure torsional vibrations in large gear hobbing machines and other large rotary machinery. In the area of celestial navigation and seismic study there is also a great need for devices which are capable

of measuring torsional vibrations of very long period.

The schematic of the basic vibrograph appears in Figure 1. In its simplest form it is composed of three basic elements: the spring with constant  $K$ , the mass  $M$ , and the viscous damper with constant  $C'$ . The input vibration  $X$  causes the mass to oscillate with the motion  $W$  and the relative motion  $Z$ :

When the input to the spring-mass system is a sine wave, the ratio of the input to output motion is expressed by the following equation:

$$\frac{Z}{X} = \frac{\left(\frac{\omega}{\omega_n}\right)^2}{\left[1 - \left(\frac{\omega}{\omega_n}\right)^2\right]^2 + \left(\frac{C'}{C_c} \frac{\omega}{\omega_n}\right)^2} \quad \text{ARCTAN} \frac{\frac{-2 C' \omega}{C_c \omega_n}}{1 - \left(\frac{\omega}{\omega_n}\right)^2}$$

where,

$\omega$  = input frequency

$\omega_n$  = natural undamped frequency of the system

$C'$  = damping constant

$C_c$  = critical damping constant.

When values computed from this equation are plotted versus frequency the graphs in Figure 2 result.

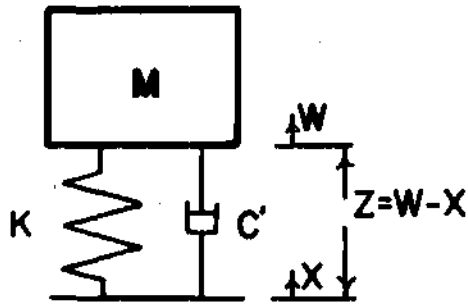


Figure 1. Basic Vibrograph

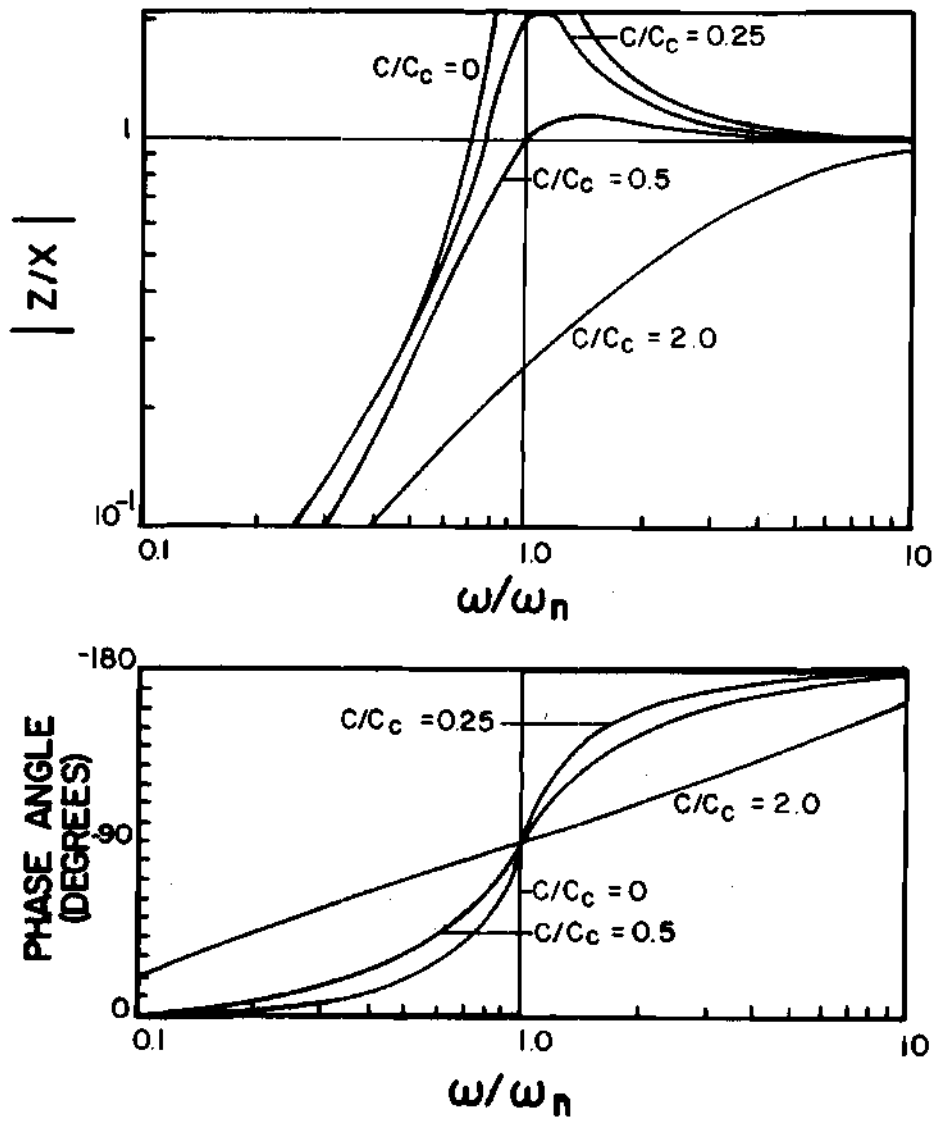


Figure 2. Frequency Response of Basic Vibrograph

From the graph most of the important characteristics of the vibrograph can be deduced. As the frequency ratio increases the magnitude of  $Z/X$  approaches unity and its phase angle approaches  $-180$  degrees. Thus the impressed motion is duplicated by the motion of the mass relative to the vibrating body and base of the vibrograph, lagging it by  $180$  degrees. In the limit it can be said that the suspended mass is motionless and the relative motion is the motion of the vibrating object.

The amount of damping required to produce a good vibrograph is subject to two contradictory factors. An ideal vibrograph would have the phase angle close to  $180$  degrees for all frequencies above the natural frequency since, if the phase angle does vary, there will be distortion of superimposed waveforms of different frequencies due to their difference in phase angle. From this consideration a minimum amount of damping is desirable. However if there is little or no damping then, as the vibration changes in frequency or amplitude, there will be insufficient damping to damp out the unwanted transient vibrations which will result and distort the output. In the basic vibrograph a compromise must be reached between these two opposing characteristics.

The basic problem which initiated this research was the desire to create a device for measuring the rotational irregularity of the master gear in a hobbing machine. If this vibration could be precisely measured, a signal could be fed back to the cutting apparatus through appropriate components and thereby nullify the error which would have been made in the generated gear. For this task a vibrograph of long natural period is needed since the master gear irregularities encountered are of very low frequency. At the present time there is no suitable

device discussed in the literature other than the one presented here which is capable of measuring this low amplitude, long period vibration.

In order to produce a vibrograph which will have an extremely long natural period, have convenient output for the apparatus, and yet not be so large as to affect the efficiency and operation of the machinery, a servo feedback system was chosen. In order to decrease the natural frequency of a basic spring-mass system, either the spring constant must be decreased or the moment of inertia of the mass must be increased. The servo torsional vibrograph is augmented by a servo system which effectively decreases the spring constant and thus lengthens the period of the instrument to any period which is desired within the stability of the device.

#### Literature Search and Historical Background

Previous research in the measurement of low amplitude, long period torsional vibrations by means of a vibrograph is almost nonexistent. However, the measurement of translational vibrations has received a great deal of research, particularly with respect to seismic instruments.

Most of the material on the measurement of low amplitude translational vibrations occurs in the field of seismology. Seismic waves, except for local shocks, are of very low magnitude and vary widely in period. An instrument is needed which has a very high magnification (100 to 100,000) and has characteristics which are close to the theoretical and constant over long periods of time.

Many different types of instruments have been produced which

function according to varied principles (6,7,8,9). In the past, the trend was toward very large masses supported by weak springs with critical damping, these being excellent examples of an elementary vibrograph. Current practice in seismology puts the emphasis on a measuring instrument whose response can be completely predicted. No longer is it a requirement that the output of the seismograph be linear since the seismic record is analyzed by digital techniques which use the response characteristics of the instrument to deduce the actual ground motions. Also, current seismographs do not in general measure the actual displacement of the ground. Most have outputs which are proportional to the velocity or acceleration of the seismic motion. Seismographs almost always use critical damping to eliminate transient vibrations of the instrument's seismic mass.

On the other hand, for a vibrograph an output which is proportional to the output is desired for simplicity and ease of utilization of the output signal. However, much insight can be gained by the study of the techniques and instruments of seismology.

Early in this century, work was started on the electromagnetic seismograph which derives its name from the type of pickup it uses. The current from the pickup is fed to a very sensitive galvanometer which registers its motion either by means of a light beam-mirror arrangement or electronically. The output of the galvanometer is proportional to the velocity of the ground motion. The galvanometer has a pronounced effect on the seismograph and thus the two have to be considered as a complete system. By changing the galvanometer characteristics, the frequency response of the basic seismograph can be

altered, producing a marked change of natural period. Much work has been done on predicting the transfer function of these seismographs (10,11,12,13,14,15,16,17,18), the time domain solution of the systems (9,10,15,19), and the frequency response (18,20,21).

Several seismographs have been designed which use feedback to alter their response characteristics. Feedback is used to flatten their response, change their natural period, and add to the ruggedness and stability of the instruments.

Feedback proportional to velocity fed to a coil-magnet assembly was used by Fleming (22) and Tucker (23) to flatten the response curves of a seismograph. Both instruments have an output which is proportional to acceleration and use feedback to alter the damping characteristics of the instrument. Tucker also decreased the natural period by means of feedback. He developed the characteristic transfer function, simplified it, and predicted the response of the instrument.

Sutton and Latham (24) made a complete analysis of a lunar feedback-controlled seismometer. The feedback was used to shape the response of the system and to compensate for long-term drift. Output was again proportional to acceleration. Feedback was passed through a low pass filter to a coil and magnet assembly which provided force on the seismic mass thus acting to restore the mass toward its electrical center position.

Another type of long period seismograph is the one designed by Gilman (25). A permanent magnet on the frame surrounded a coil which was attached to a simple pendulum and a constant current was passed through the coil. The coil-magnet combination was polarized to produce

a force on the mass opposite in direction to the gravitational restoring force. This resulted in a lengthened period, but instability resulted at long periods because of an uneven magnetic field caused by the presence of magnetic impurities.

Sheffield (26) developed an electronic vertical long period seismograph which achieved long-period seismograph action through magnetic field support of the seismic mass and electronic feedback. A two-mass, two-degree-of-freedom system was developed which had the seismic mass almost entirely supported by means of a constant magnetic field in order to reduce the size of the spring which was needed to support the mass. Feedback was introduced to produce a force on a second mass which was positioned between the seismic mass and the base. The combined action of the two magnets produced a seismic device of long period which very closely duplicated the action of a normal seismograph.

Another method of lengthening the period of the electromagnetic seismograph is the use of a shunt capacitor between the transducer coil and the galvanometer; period increases of a magnitude of ten can be obtained (27,28,29).

Limited research has been done outside the field of seismology. The most important papers are by Matsushama and Nakada (30,31) and Nakada, Asakura, Fukuda and Watanabe (32) which concern an electro-mechanical system which was developed to measure translational vibrations of long period. A pendulum was produced whose period was lengthened by means of a servo system. The paper (30) included a theoretical analysis for one particular system; damping was not considered, and a first order model for the servo system was used. Included was a

description of a practical model which was only moderately successful because of the marked dependence of the response on the angular misalignment of the base.

The investigation of devices which measure rotational vibrations of low frequency has been totally neglected because of the great interest in high frequency phenomena and also because of the predominant interest of seismologists in translatory vibrations. For seismic feedback systems very little analytical work has been done toward either optimization of the designs or determination of the maximum stable increase in natural period. Seismic systems based on magnetic components are generally not applicable to industrial applications because of their sensitivity to changes in gain in the amplifier, nonlinear flux fields, and their sensitivity to changes in magnetic flux caused by slight changes in voltage.

#### Investigation Procedure

The initial phase of this research dealt with the theoretical investigation of the servo torsional vibrograph. Primary interest was focused on a study of the frequency and impulse responses. Each parameter of importance was varied and its effect on the frequency response noted. In this manner a complete characterization of the effect of each variable under consideration was obtained and from this large amount of data the best or optimum design was selected. The transient behavior was investigated to find the best compromise for the damped phase angle characteristics of the instrument. Also investigated for a wide range of parameters were the sensitivity to small unforeseen changes in the parameters and the stability of the device by means of root loci.

In the experimental phase of the research, a prototype was built which had characteristics in the middle-range of the variables which were to be investigated. Since a complete parameter study was to be undertaken, it was deemed impossible to conduct the study on the machine itself since the range of the variables would be too great. Thus it was decided that the prototype would be built just to verify the theoretical equations which would be used for the parameter study and to find out what problems would develop in the investigation of a practical model of the system.

## CHAPTER II

## ANALYTICAL INVESTIGATION

Derivation of Basic EquationsGeneral Description

For the analytical investigation of the servo torsional vibrograph it was necessary to set up a mathematical model of the system. This model was constructed by first finding the transfer function of each component of the system. A transfer function is defined as the ratio of the Laplace transform of the output variable to the transform of the input variable with all initial conditions assumed to be zero. Each transfer function is based on the assumption that all components have linear characteristics.

It was desired to construct a stable system which would decrease the natural frequency and enhance the characteristics of a basic torsional spring-mass system. The equation for the natural frequency of a simple torsional spring-mass system is:

$$\omega_n = \sqrt{\frac{K}{J}}$$

where,

$\omega_n$  = natural undamped frequency

K = spring constant of torsional spring

J = moment of inertia of the mass.

Therefore, for a fixed mass, it is necessary to reduce the spring constant to obtain any decrease in natural frequency. Since there is a limit to the size decrease of the spring in question and there are weight and size restrictions for the mass, it is necessary to decrease the spring constant artificially.

In order to accomplish this reduction, it is necessary to move the spring support in the same direction as the motion of the inertial mass, thus reducing the spring displacement and the spring constant. A servo system was used to accomplish this motion. This servo system consists of the basic spring-mass system, three electronic displacement transducers, two amplifiers, and a servo motor-amplifier. Figure 3, on the following page, shows a schematic representation of the system:

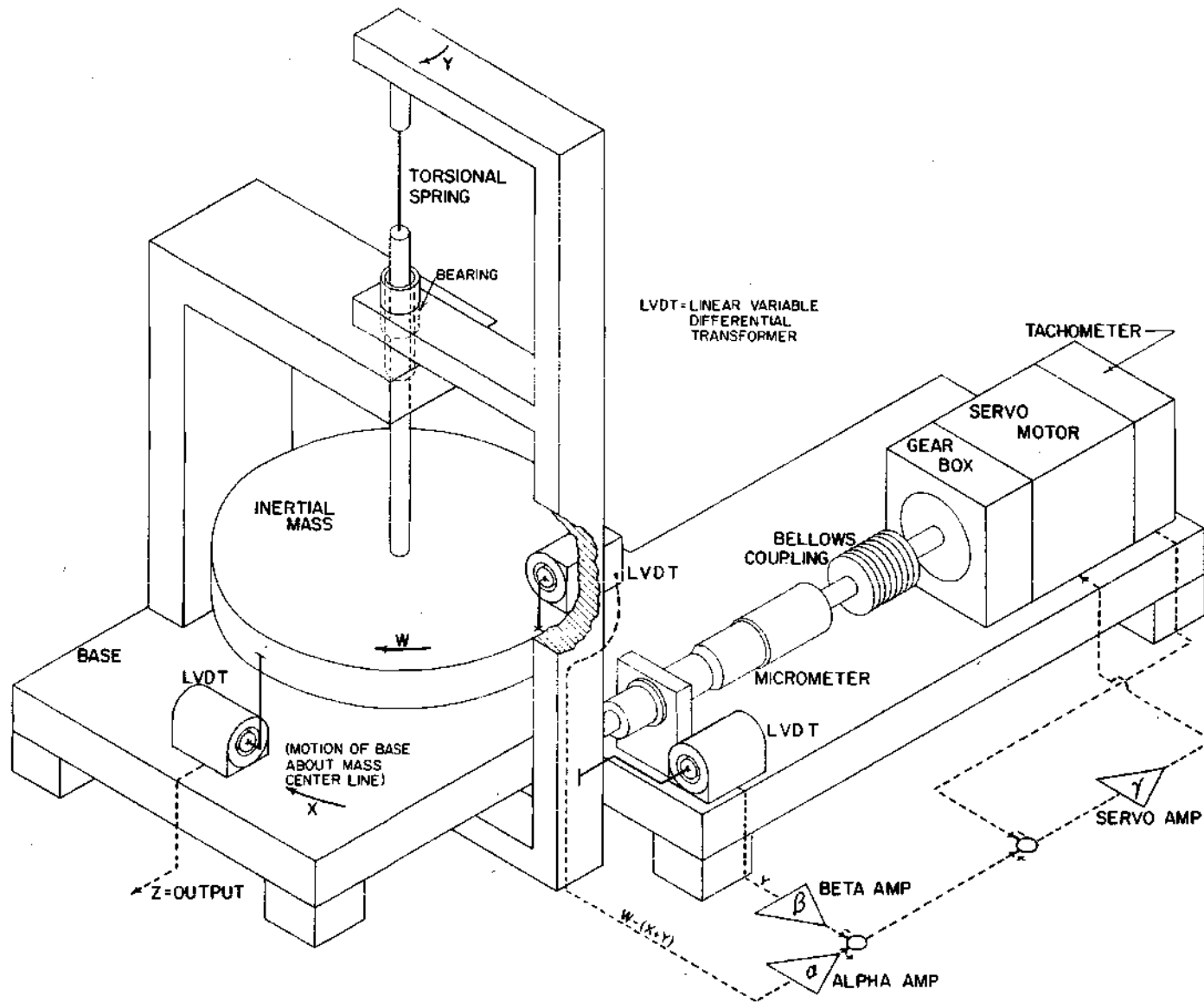


Figure 3. Schematic of the Servo Torsional Vibrograph.

### Description of the Servo Vibrograph Network (Figure 3)

The desired motion of the spring base is produced by the alpha network which measures at its source the relative motion between the inertial mass and the spring support. The signal from the transducer is fed through the high gain alpha amplifier to the servo motor-amplifier. From the servo motor the rotary motion is reduced in speed, changed in direction, and applied to the spring base. The alpha network is the basic natural frequency reduction mode and all other circuitry is added to modify the characteristics of the instrument and to add to its stability.

The beta network is added to correct for drift in the alpha circuit and to keep the instrument in its neutral position. The tachometer feedback is supplied to add damping to the servo motor-amplifier circuit and to add to its stability. The output transducer measures the relative motion between the inertial mass and the base of the instrument and is fed directly to a recorder. In operation, the machine is placed with its vertical centerline coincident with the centerline of the rotary motion which is to be analyzed.

If the motion to be sampled has a constant velocity, then the vibrometer will have no output. But, if the basic motion has a torsional vibration superimposed upon it, then the inertial mass will be displaced and the servo system actuated. The output will then be directly proportional to the input vibration.

### Basic Theoretical Equations

From the schematic drawing of the system (Figure 3), the block diagram in Figure 4 can be deduced.



The block diagram of the system represents all the electrical and mechanical interconnections which are present in the system. For the spring-mass system in Figure 1 the velocity of relative motion is:

$$\frac{dZ}{dt} = \frac{dW}{dt} - \frac{dX}{dt} \quad (1)$$

and the differential equation of the motion of the system is:

$$J \frac{d^2W}{dt^2} + C' \frac{dZ}{dt} + KZ = 0 \quad (2)$$

where,

W = motion of the inertial mass

X = motion of the spring support

Z = relative motion between the mass and the spring base, or

$$Z = W - X \quad (3)$$

J = moment of inertia of the mass

Y = servo motion.

Substituting Equation (1) and (3) into (2) and eliminating Z, the following differential equation is obtained:

$$J \frac{d^2W}{dt^2} + C' \frac{dW}{dt} + KW = \frac{C'dX}{dt} + KX \quad (4)$$

and with initial conditions equal to zero, the transfer function is:

$$\frac{W}{X} = \frac{C's + K}{Js^2 + C's + K}$$

$$= \frac{C_1 s + \omega_n^2}{s^2 + C_1 s + \omega_n^2}$$

where,

$$C_1 = C/J$$

$$\omega_n = \sqrt{K/J}$$

$s$  = Laplacian operator

For all other components the standard linear representation will be used (33). The transfer functions for each component are presented in Table 1.

The diagram in Figure 5 is a representation of the linearized system which will be used for the analysis of the servo system.

The system can be simplified using standard block diagram reduction techniques (33). The components in the H-network (Figure 5) can be reduced to

$$H = \frac{\alpha T_1 \gamma Km P}{Tm s^2 + (1 + Kt Km \gamma)s + \beta T_2 \gamma Km P}$$

and if

$$G = \frac{C_1 s + \omega_n^2}{s^2 + C_1 s + \omega_n^2}$$

Table 1. Component Transfer Functions

Component	Transfer Function	Comment
Spring Mass System	$\frac{C_1 s + \omega_n^2}{s^2 + C_1 s + \omega_n^2}$	
Amplifier gains		Set Constants
Alpha	$\alpha$	
Beta	$\beta$	
Gamma	$\gamma$	
Linear differential transformers		
Alpha	$T_1$	Inherent Constant of Device
Beta	$T_2$	
Output	$T_3$	
Tachometer Generator	$K_t \times s$	Proportional to velocity where $K_t$ = constant of proportionality
Gears	$P$	Gear ratio
Servo motor	$\frac{K_m}{s + s^2 T_m}$	Where, $K_m = \frac{kk}{F_m - m}$ $T_m = \frac{J_m}{F_m - m}$ and $J_m$ = Motor Inertia $kk = \frac{\text{Blocked motor torque at rated voltage}}{\text{Rated voltage}}$ $F_m = \text{Motor viscous friction}$ $m = \frac{\text{Blocked rotor torque}}{\text{No load speed}}$

the diagram can be reduced to the following transfer function which represents the entire system.

$$Z/X = \frac{(G - 1)(H + 1)}{1 - H(G - 1)}$$

or if the values of G and H are introduced, the final result is obtained. Equation (5) represents this transfer function.

$$Z/X = \frac{-s^2(Tm s^2 + (1 + Km Kt \gamma) s + (\alpha T_1 + \beta T_2) Km P \gamma)}{Tm s^4 + (1 + Km Kt \gamma + C_1 Tm) s^3 + (\omega_n^2 Tm + (\alpha T_1 + \beta T_2) Km P \gamma + C_1 (1 + Km Kt \gamma)) s^2 + (\omega_n^2 (1 + Km Kt \gamma) + C_1 Km P \gamma \beta T_2) s + \omega_n^2 Km P \gamma \beta T_2} \quad (5)$$

and if

$$A = 1 + Km Kt \gamma$$

$$B = (\alpha T_1 + \beta T_2) Km P \gamma$$

$$C = 1 + Km Kt \gamma + C_1 Tm$$

$$D = \omega_n^2 Tm + (\alpha T_1 + \beta T_2) Km P \gamma + C_1 (1 + Km Kt \gamma)$$

$$E = \omega_n^2 (1 + Km Kt \gamma) + C_1 Km P \gamma \beta T_2$$

$$F = \omega_n^2 Km P \gamma \beta T_2$$

then

$$Z/X = \frac{Tm s^4 + A s^3 + B s^2}{Tm s^4 + C s^3 + D s^2 + E s + F} \quad (6)$$

### Frequency Response Equations

The steady state response of any system to a sinusoidal input can be calculated by replacing the Laplace operator  $s$  in the transfer function with  $j\omega$  where  $\omega$  is the input frequency and  $j$  is the complex operator. The transfer function is transformed by this substitution to a new sinusoidal transfer function which is in general a complex function of the frequency and can be most conveniently represented by a magnitude and a phase angle.

Equation (6) can now be transformed into a sinusoidal transfer function by the transformation  $s = j\omega$ . The magnitude of the transfer function is

$$|Z/X| = \frac{\sqrt{(Tm\omega^4 - B\omega^2)^2 + (A\omega^3)^2}}{\sqrt{(Tm\omega^4 - D\omega^2 + F)^2 + (-C\omega^3 + E\omega)^2}} \quad (7)$$

at a phase angle of

$$\phi = \text{ARCTAN}(A\omega/(-Tm\omega^2+B)) - \text{ARCTAN}(1-C\omega^3+E\omega)/(Tm\omega^4-D\omega^2+f) \quad (8)$$

or in another form the phase angle is

$$\phi = \text{ARCTAN} \left( \frac{-[(CTm-ATm)\omega^5 - (BC+ETm-DA)\omega^3 + (BE-AF)\omega]}{-[Tm^2\omega^6 + (AC-TmD-TmB)\omega^4 + (FTm + BD-AE)\omega^2 - BF]} \right) \quad (9)$$

If the input frequency is allowed to approach infinity it can be seen that for any value of the parameters

$$\lim_{\omega \rightarrow \infty} \left| \frac{Z}{X} \right| / \phi = 1 / -180 \text{ degrees}$$

Therefore if the input frequency is large the ratio of the output motion to input motion will approach unity at a phase angle of 180 degrees, and the output will duplicate the input, lagging it by 180 degrees.

When representative values are substituted into Equations (7) and (9) a sample graph of the frequency response can be calculated. The values for a plot of this type were obtained from a computer program for the Burroughs 5500 which appears in the Appendix. The following constants were assumed as a representative sample for the frequency response curves which appear in Figure 6.

$$\alpha = 100, 1000, \text{ and } 5000$$

$$\gamma = 5000$$

$$\beta = 10$$

$$C_1 = 0.1 \text{ 1/second}$$

$$\omega_n = 1.0 \text{ cycle/second}$$

$$Kt = 0.00031 \text{ volt/radian/sec}$$

$$T_m = 0.013 \text{ radian/sec}$$

$$K_m = 3.05 \text{ radian/sec/volt}$$

$$P = 6.9 \times 10^{-6}$$

The constants were approximately those of the experimental machine.

Figure 6 appears on the following page:

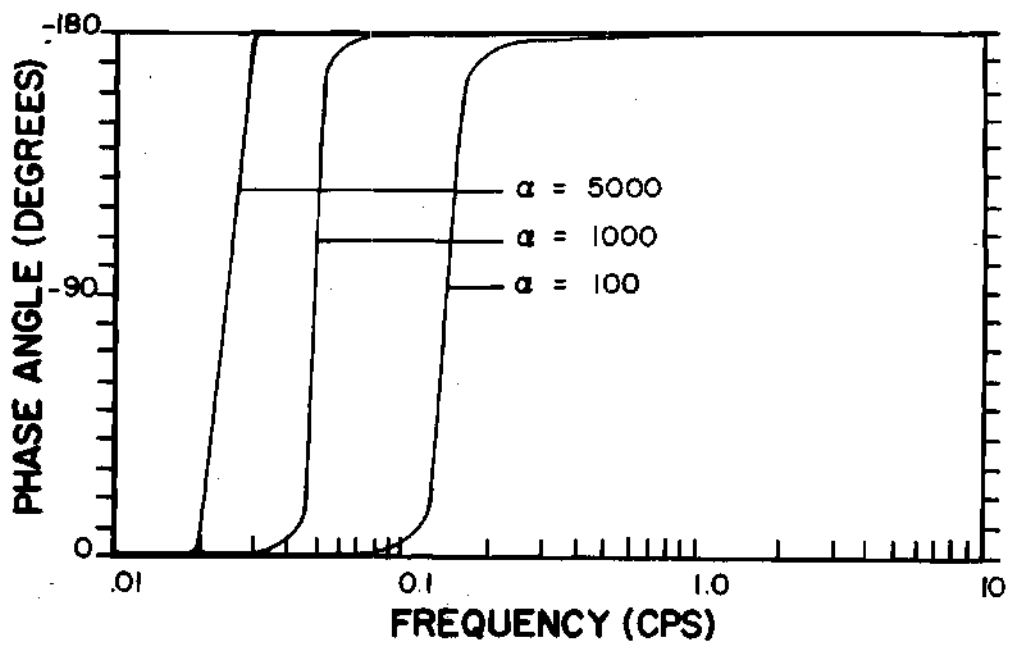
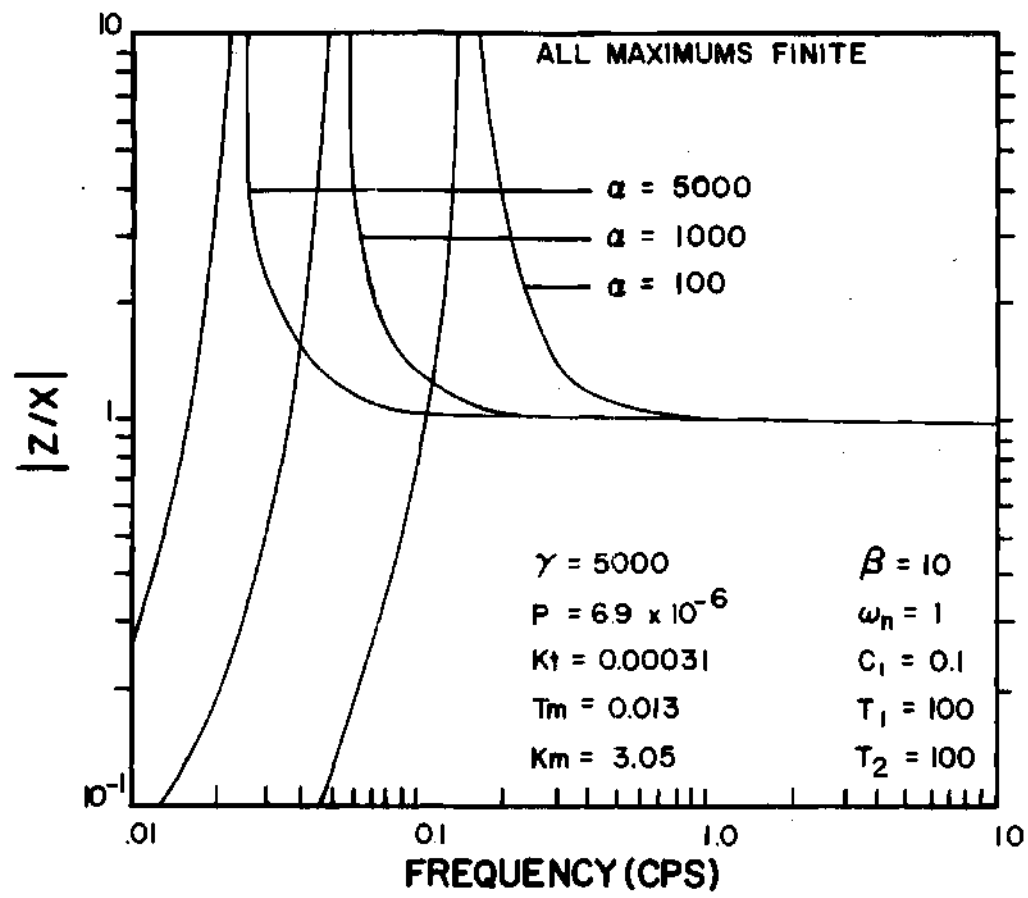


Figure 6. Theoretical Frequency Response

### Optimum Frequency Response

For the parameters whose frequency response is pictured in Figure 6 a decrease in natural frequency can be noted for each increase in alpha gain. An extension of this procedure would be to graph the frequency response for a wide range of values for each of the parameters. However, for the large number of parameters involved this would be too cumbersome. The alternate method selected was that of choosing certain properties of the frequency response curve which were found by means of the electronic computer for each set of variables.

With reference to Figure 6, the frequency response and its accompanying phase angle have the same general shape respectively for each value of alpha. This situation is true for all variations of the parameters. At low frequencies the frequency response begins at a very low number, rises to a maximum as the frequency increases and then decreases toward unity. The phase angle starts at zero and decreases to -180 degrees. For the parameter study the following four characteristics were found for each curve:

1. Frequency at which the amplitude is a maximum with the amplitude and phase angle at this frequency;
2. Frequency for a phase angle of 90 degrees with the amplitude at this point;
3. The 10 per cent amplitude error frequency and the corresponding phase angle;
4. The 10 per cent phase angle error frequency and the corresponding amplitude.

Hereafter the 10 per cent amplitude error frequency and 10 per cent phase angle error frequency will be abbreviated 10%AME frequency and 10%PHAE frequency, respectively. The characteristics are graphically illustrated in Figure 7, which appears on page 25.

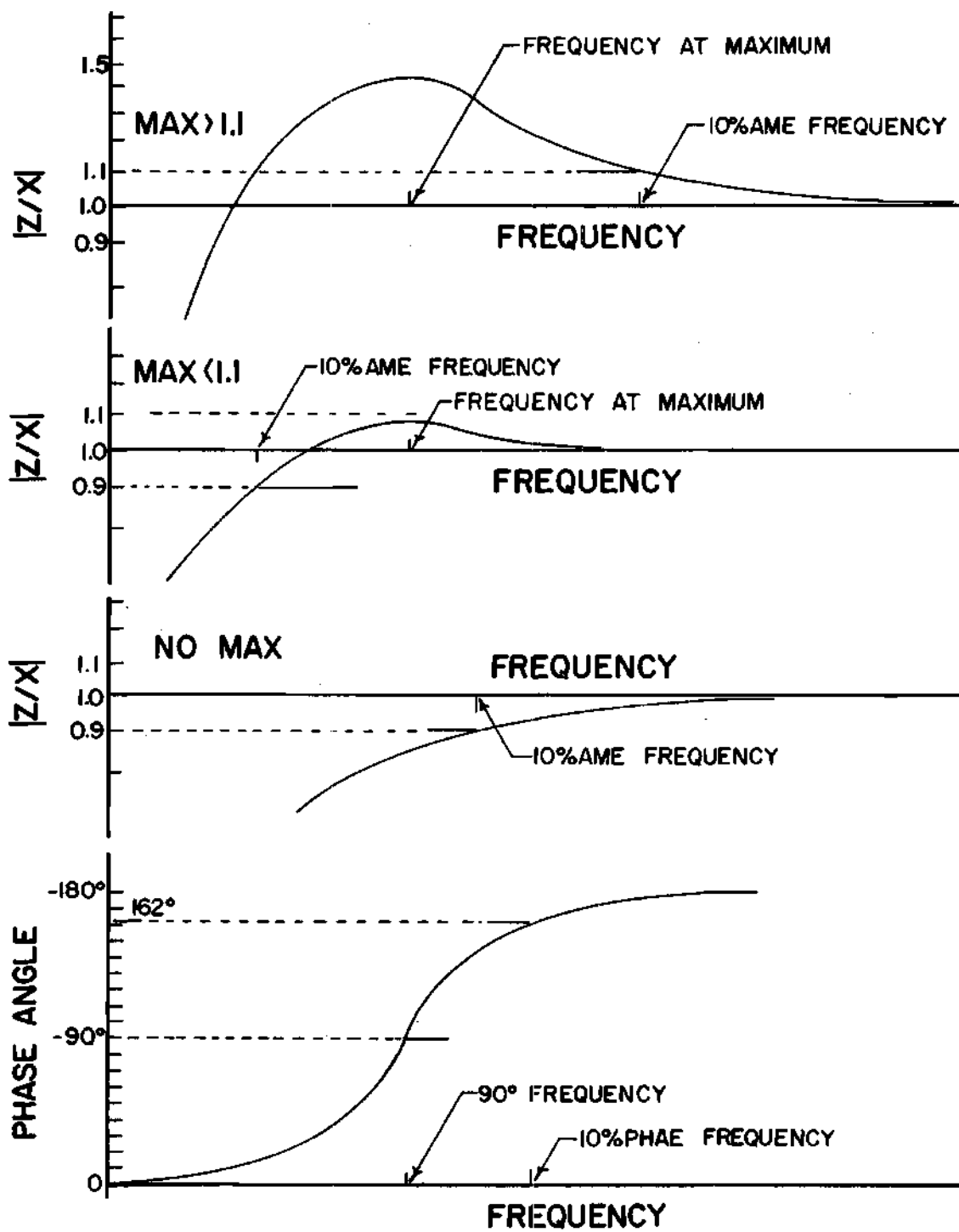


Figure 7. Frequency Response Characteristics

The 90-degree point was selected because the natural undamped frequency of the basic vibrograph (Figure 2) always occurs at a phase angle of 90 degrees. Thus, if the simple case can be extended to this more complicated system, a pseudo natural undamped frequency for the servo vibrograph can be found.

Since the vibrograph is designed to be used in the range of frequencies above the natural frequency, the natural frequency of the instrument is of less interest than the response of the system at the point where it is to be used. In industrial control of large rotary machinery, an instrument of this type could have a maximum error of 10 per cent without seriously affecting the end use. Thus, a 10 per cent-error criterion is the most important aspect of the performance of the instrument. If, however, a different per cent-error criterion were to be selected, although the exact lower bound of the accuracy would be incorrect, the optimized parameters would still be the best that are obtainable.

In order to find the maximum of the function in Equation (7), the iterative technique of interval-halving was selected. In this procedure the frequency and value of the maximum amplitude are obtained from Equation (7) and the phase angle for this frequency from Equation (9).

The 10%AME and 10%PHAE frequency were also found by means of interval-halving. The 10%AME frequency was obtained from

$$\left| \frac{\sqrt{(Tm\omega^4 - B\omega^2)^2 + (A\omega^3)^2}}{\sqrt{(\omega^4 - D\omega^2 + F)^2 + (-C\omega^3 + E\omega)^2}} - 1 \right| = 0.1$$

which was solved for the value of frequency to the right of the maximum (if such existed) which solved the equation. From Equation (9) the corresponding phase angle was calculated.

For the 10%PHAE frequency, Equation (9) was set equal to 162 degrees and solved for the corresponding frequency. The amplitude at this frequency was calculated by means of Equation (7).

The frequency at which the phase angle reaches 90 degrees was calculated by equating the denominator of Equation (9) to zero. The equation was solved by Newton's method and the corresponding amplitude was calculated by means of Equation (7).

Each of the system parameters was varied throughout the range of possible values in order to optimize the performance of the instrument. Five of the 11 variables were not varied.  $K_m$ ,  $T_1$  and  $T_2$  were held constant since they are in the same uninterrupted forward path of the block diagram as  $\gamma$ ,  $\alpha$ , and  $\beta$ , respectively. The natural undamped frequency ( $\omega_n$ ) was held constant since it is simply a reference point for the system and would be made as low as possible in any practical model in order to get the lowest possible natural frequency.  $P$  was also held constant since its increase or decrease would simply change the effective servo amplifier gain. The five constants above were set for the parameter study at the following values:

$$\omega_n = 1 \text{ cps} \quad (10)$$

$$K_m = 1 \text{ rad/sec/volt}$$

$$T_1 = 100 \text{ volts/radian}$$

$$T_2 = 100 \text{ volts/radian}$$

$$P = 7 \times 10^{-6}$$

The values for the variable parameters were chosen so that they varied in value about the middle of the range for commercially obtainable components. The widest latitude was allowed for the constants alpha and gamma since these are the gains of the amplifiers and can be changed easily. The beta gain was allowed to vary only at low values. The following were the values for the parameter study:

$$\alpha = 10, 25, 50, 100, 250, 500, 750, 1000, 2000, 3000, 4000, 5000, 10000;$$

$$\gamma = 10, 25, 50, 100, 250, 500, 750, 1000, 2000, 3000, 4000, 5000, 10000;$$

$$\beta = 0, 0.01, 0.1, 1.0, 10;$$

$$C_1 = 0, 0.1, 0.5, 1.0; \quad \text{l/second}$$

$$K_t = 0, 0.01, 0.025, 0.1; \quad \text{volt/radian/second}$$

$$T_m = 0.001, 0.01, 0.1. \quad \text{radian/second}$$

Every combination of all the variables was used to provide a complete study. The complete operation was carried out on the Burrough's 5500 computer which made in the entire process over eight million separate calculations. The computer program and a sample output appear in the Appendix. From the output of the computer approximately 365,000 frequency response characteristic numbers were obtained. Since there was such a massive amount of data only a small portion can be presented

here. The curves in Figures 8 through 22 were chosen to represent the frequency response characteristics because they are representative of the larger data set.

The graphs each have one of the response characteristics on the ordinate versus a system parameter on the abscissa. In plotting the curves all the system parameters were held constant except the one on the abscissa. In addition to the parameters in Equations (10) and the variable on the abscissa, all graphs have the following parameters in common:

$$\beta = 1.0 \quad (0.01-10) \quad (11)$$

$$C_1 = 0.1 \quad (0.0-1.0) \quad \text{l/second}$$

$$Kt = 0.0 \quad (0.0-0.1) \quad \text{volt/radian/second}$$

$$Tm = 0.01 \quad (0.001-0.1) \quad \text{radian/second}$$

The range for each parameter is listed beside its standard value. Each figure contains 16 curves for all combinations of  $\alpha = 10, 100, 1000, 10000$  and  $\gamma = 10, 100, 1000, 10000$ . For each variable parameter (i.e.,  $\beta$ ,  $C_1$ ,  $Kt$  and  $Tm$ ) the 10%AME, 10%PHAE, and natural frequencies were plotted. The 90-degree point was not included since it was found to add no useful information.

In each of the graphs in Figures 8 through 22, dotted lines show portions of each curve in which the maximum value of the amplitude of  $Z/X$  is less than 1.1 (Figure 7). This convention is not used on the 10%PHAE curves since it has no significance. On several of the plots of the 10%AME frequency a jump occurs: this discontinuity occurs when the value of the maximum amplitude decreases below 1.1 and the 10%AME amplitude changes from 1.1 to 0.9 with a resulting jump in the 10%AME

frequency. The influence of each of the parameters on the frequency response characteristics is only discussed for significant values of gamma and alpha (i.e., values that are large enough to have the desired effect on the instrument). The minimum frequency at which a vibration can be measured accurately is determined from the larger value of the 10%AME and 10%PHAE frequencies. The Key to Figures 8 through 22 appears on the following page:

Key to Figures 8 through 22

For	a	$\gamma = 10$	$\alpha = 10$
	b	$\gamma = 100$	$\alpha = 10$
	c	$\gamma = 1000$	$\alpha = 10$
	d	$\gamma = 10,000$	$\alpha = 10$
	e	$\gamma = 10$	$\alpha = 100$
	f	$\gamma = 100$	$\alpha = 100$
	g	$\gamma = 1000$	$\alpha = 100$
	h	$\gamma = 10,000$	$\alpha = 100$
	i	$\gamma = 10$	$\alpha = 1000$
	j	$\gamma = 100$	$\alpha = 1000$
	k	$\gamma = 1000$	$\alpha = 1000$
	l	$\gamma = 10,000$	$\alpha = 1000$
	m	$\gamma = 10$	$\alpha = 10,000$
	n	$\gamma = 100$	$\alpha = 10,000$
	o	$\gamma = 1000$	$\alpha = 10,000$
	p	$\gamma = 10,000$	$\alpha = 10,000$
A1 (for angle)	Z1 (for amplitude)	$\alpha = 10$	
A2 (for angle)	Z2 (for amplitude)	$\alpha = 100$	
A3 (for angle)	Z3 (for amplitude)	$\alpha = 1000$	
A4 (for angle)	Z4 (for amplitude)	$\alpha = 10,000$	

Two parameters,  $C_1$  (the damping constant) and  $T_m$  (the servo motor time constant) have little effect on the frequency response of the instrument (Figures 8 through 13). As  $C_1$  increases from zero to one, the 10%AME frequency decreases very slightly and the 10%PHAE frequency and the frequency of the maximum increase slightly. As  $T_m$  increases from 0.001 to 0.1 the 10%AME, 10%PHAE and maximum's frequencies all decrease. Since both the factors have so little effect on the error frequencies their value should be set by the nature of the components.

Figures 8 through 13 appear on the following pages:

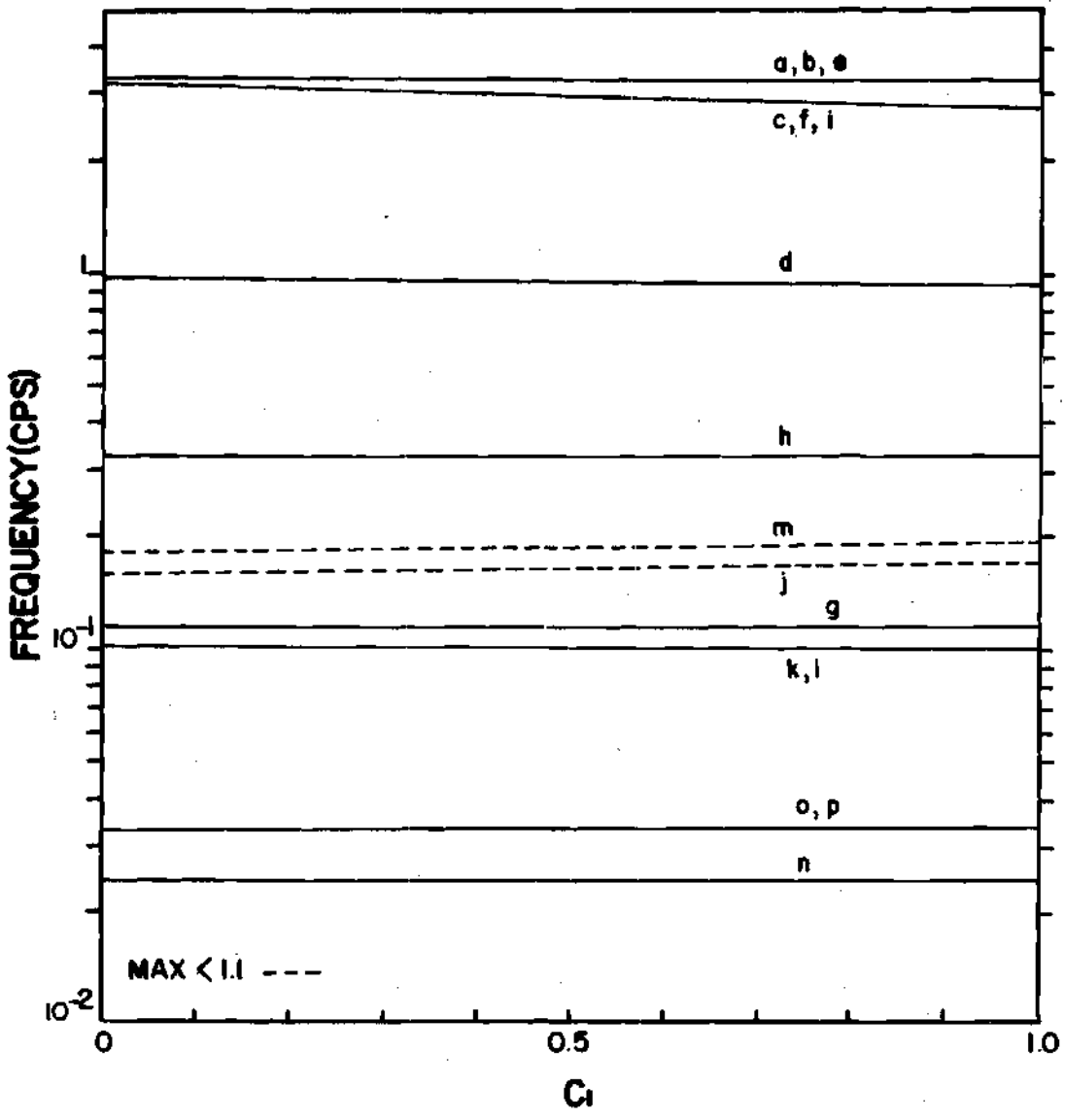


Figure 8. Influence of Damping Constant (C<sub>1</sub>) on the 10 Per Cent Amplitude Error Frequency

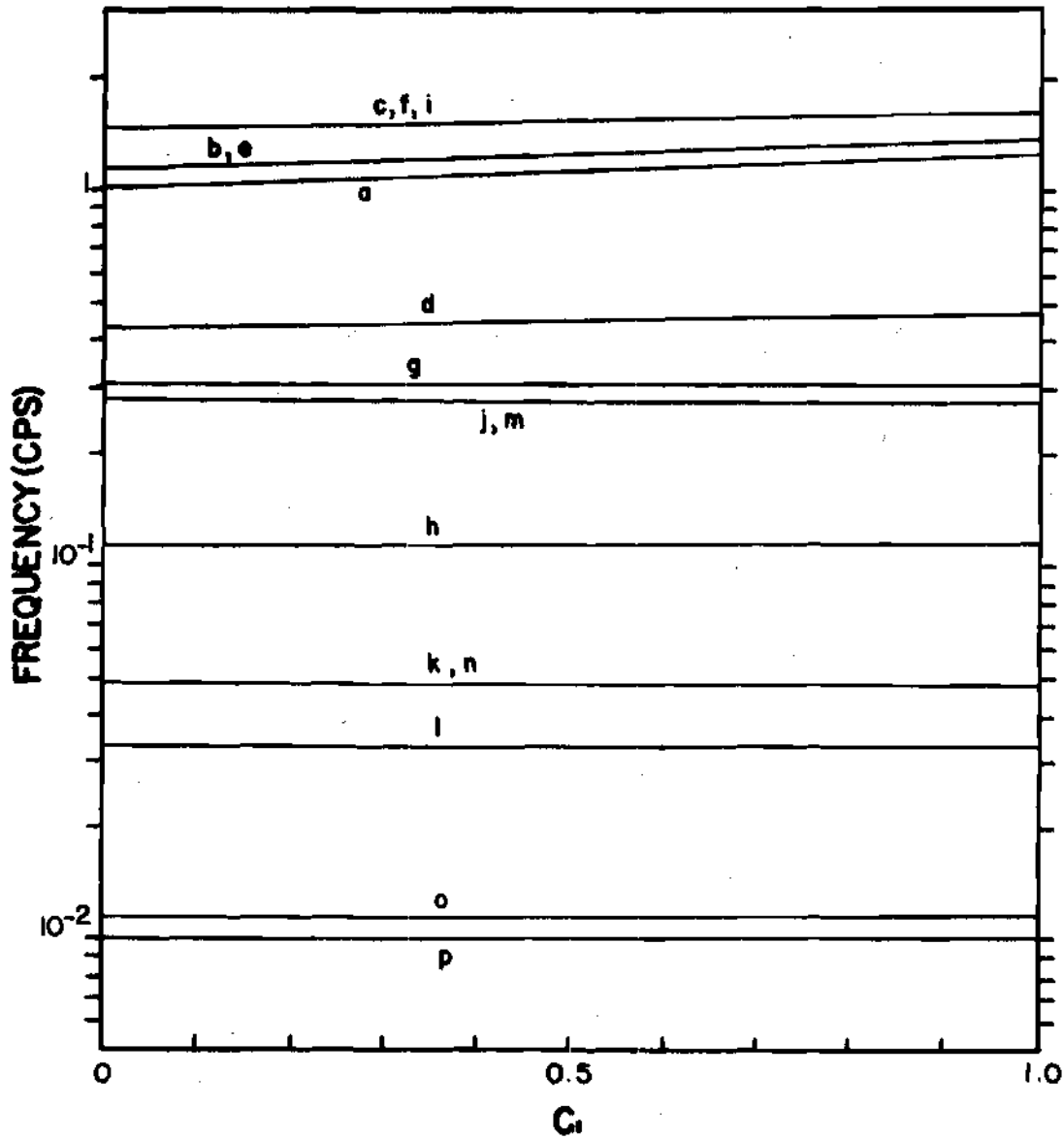


Figure 9. Influence of the Damping Constant ( $C_1$ ) on the 10 Per Cent Phase Angle Error Frequency

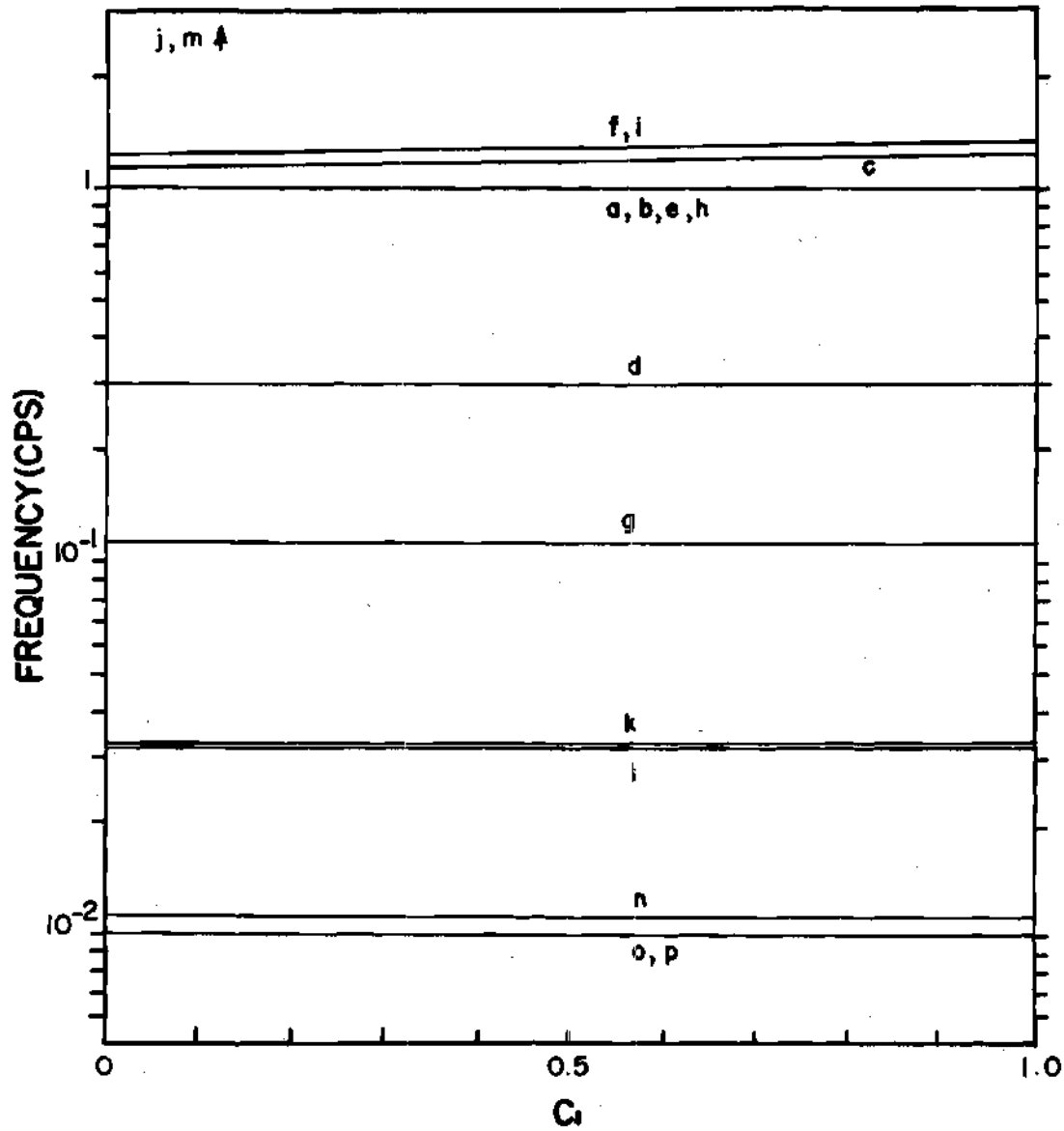


Figure 10. Influence of the Damping Constant ( $C_1$ ) on the Frequency of the Maximum

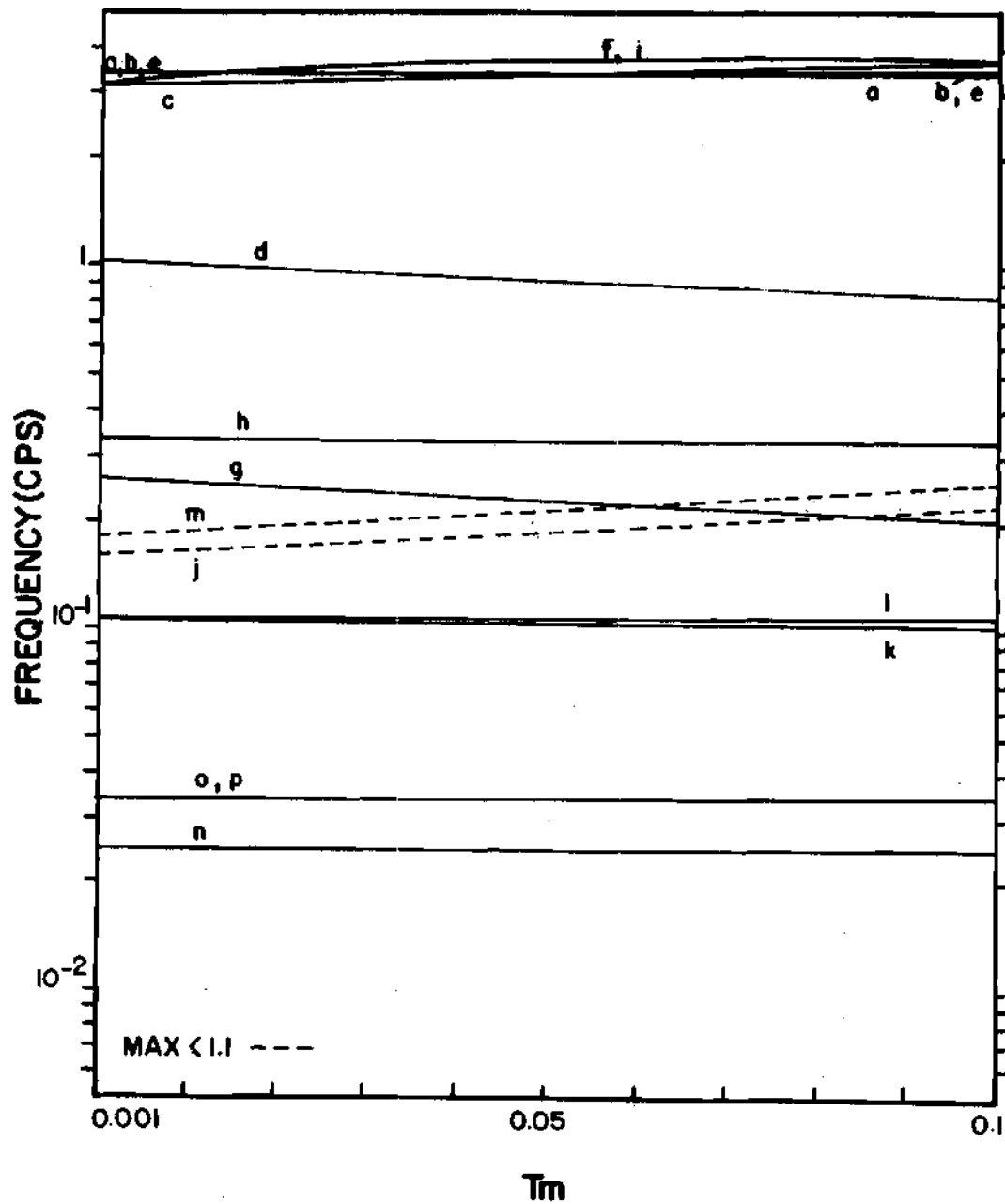


Figure 11. Influence of the Servo Motor Time Constant ( $T_m$ ) on the 10 Per Cent Amplitude Error Frequency

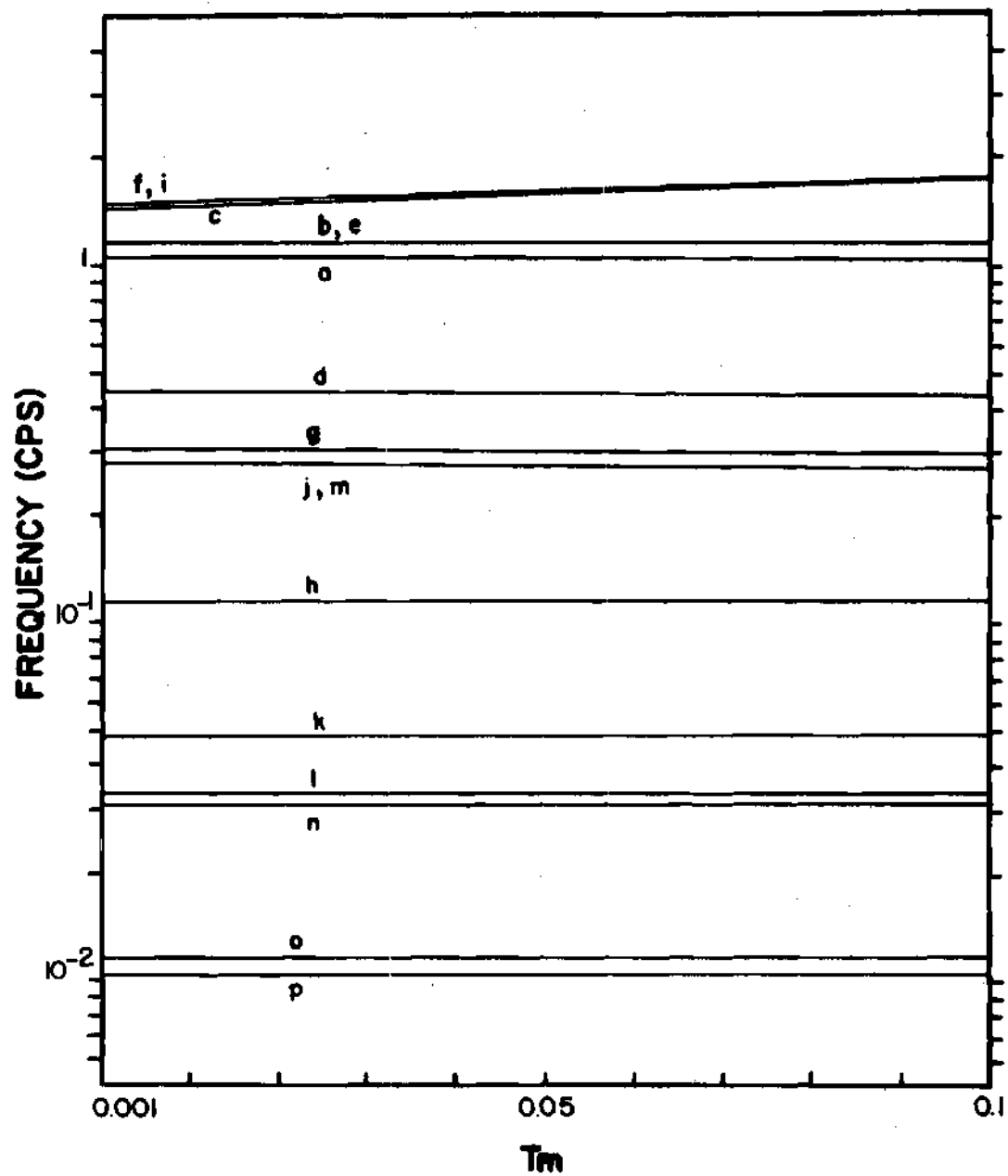


Figure 12. Influence of the Servo Motor Time Constant ( $T_m$ ) on the 10 Per Cent Phase Angle Error Frequency

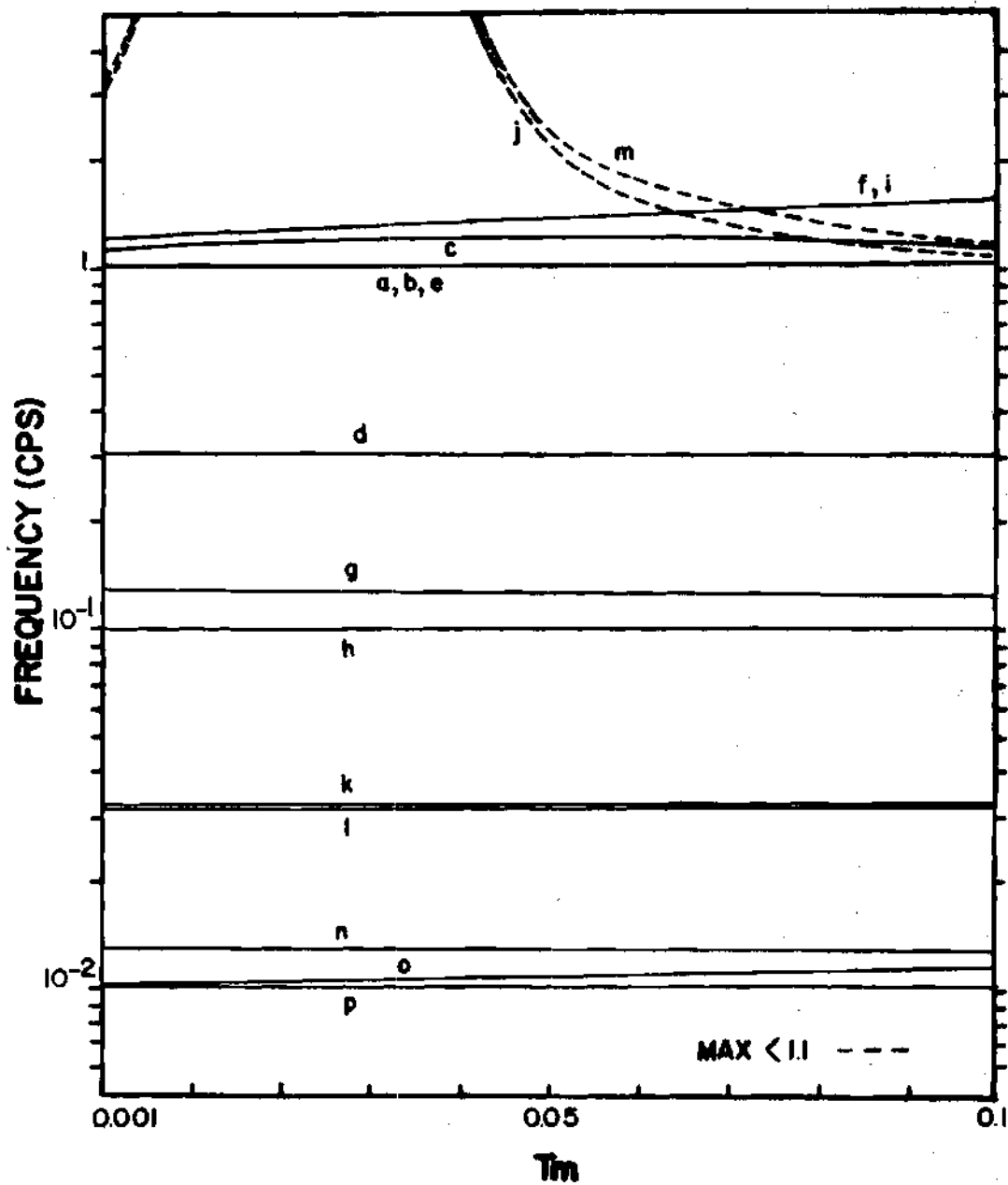


Figure 13. Influence of the Servo Motor Time Constant ( $T_m$ ) on the Frequency of the Maximum

The changes in the frequency response characteristics are more pronounced for the tachometer feedback constant ( $K_t$ ) (Figures 14, 15, and 16). As  $K_t$  increases, the value of the maximum and the 10%PHAE frequency both increase. The 10%AME frequency decreases, undergoes the 1.1-0.9 discontinuity and then increases. The optimum value for the tachometer constant should be less than 0.005 volts/radian/sec and set at a value which will damp out unwanted chatter and other nonlinear effects of the servo amplifier-motor system.

Figures 14 through 16 appear on the following pages:

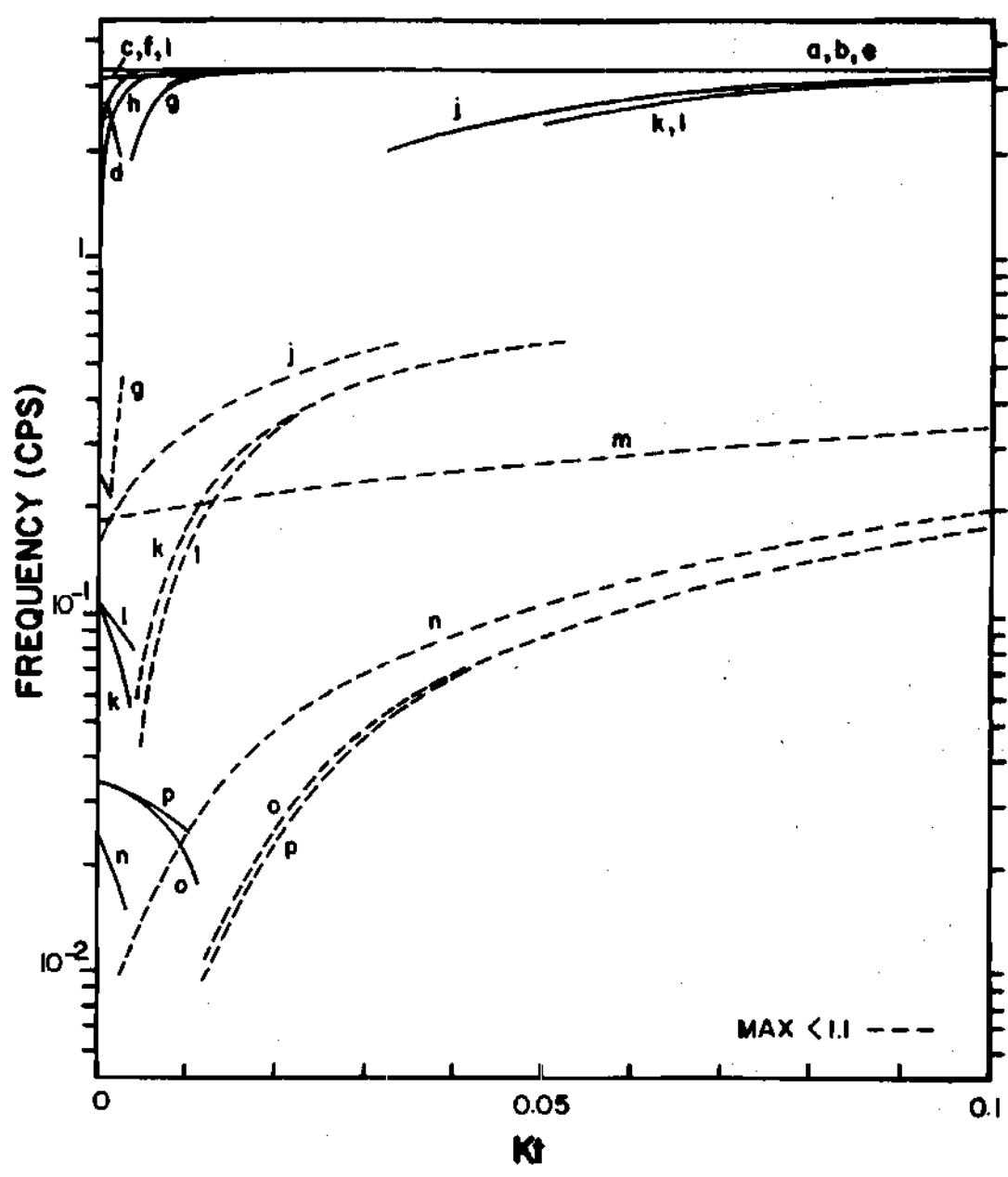


Figure 14. Influence of the Tachometer Feedback Constant ( $K_t$ ) on the 10 Per Cent Amplitude Error Frequency

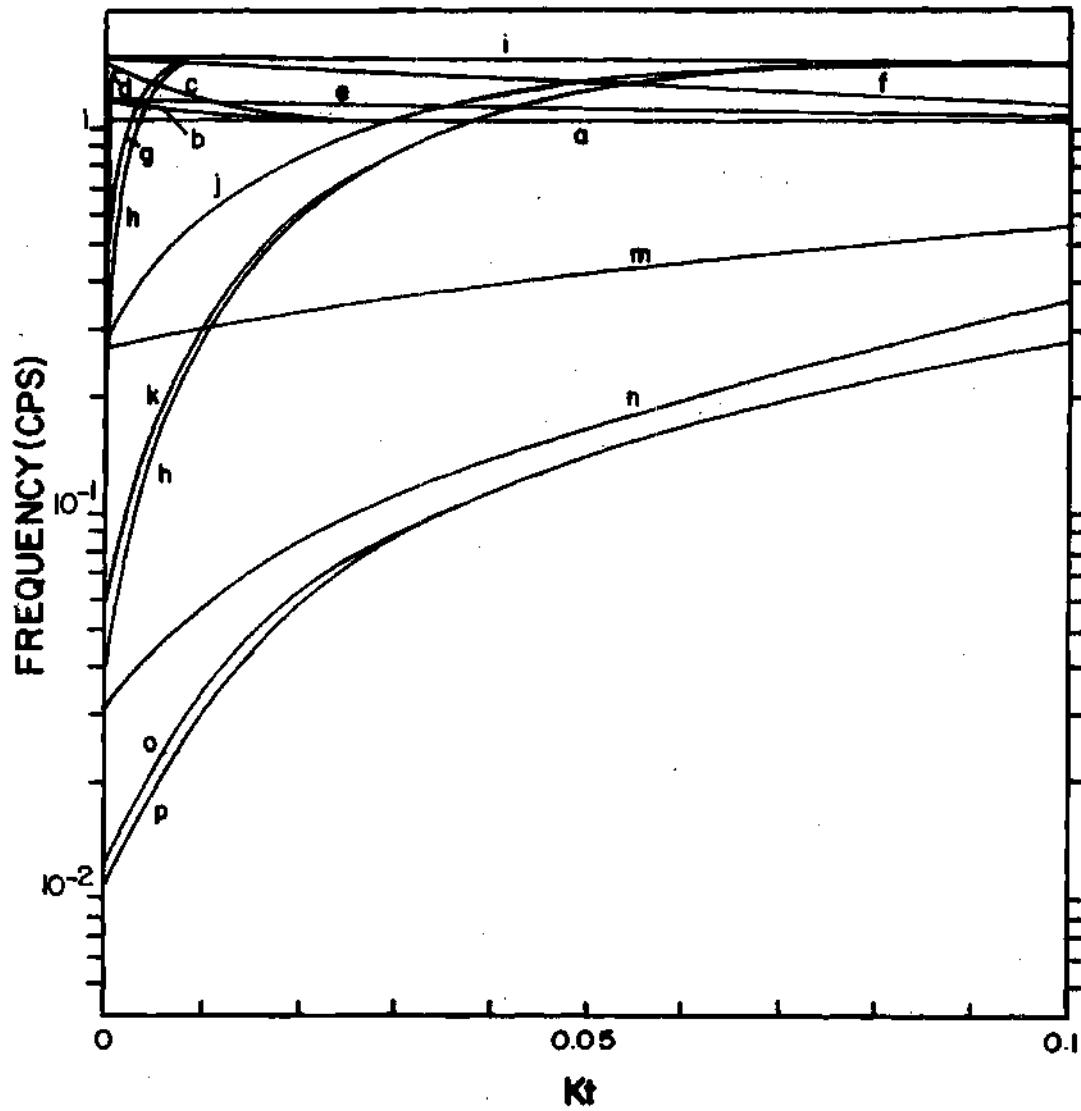


Figure 15. Influence of the Tachometer Feedback Constant ( $K_t$ ) on the 10 Per Cent Phase Angle Error Frequency

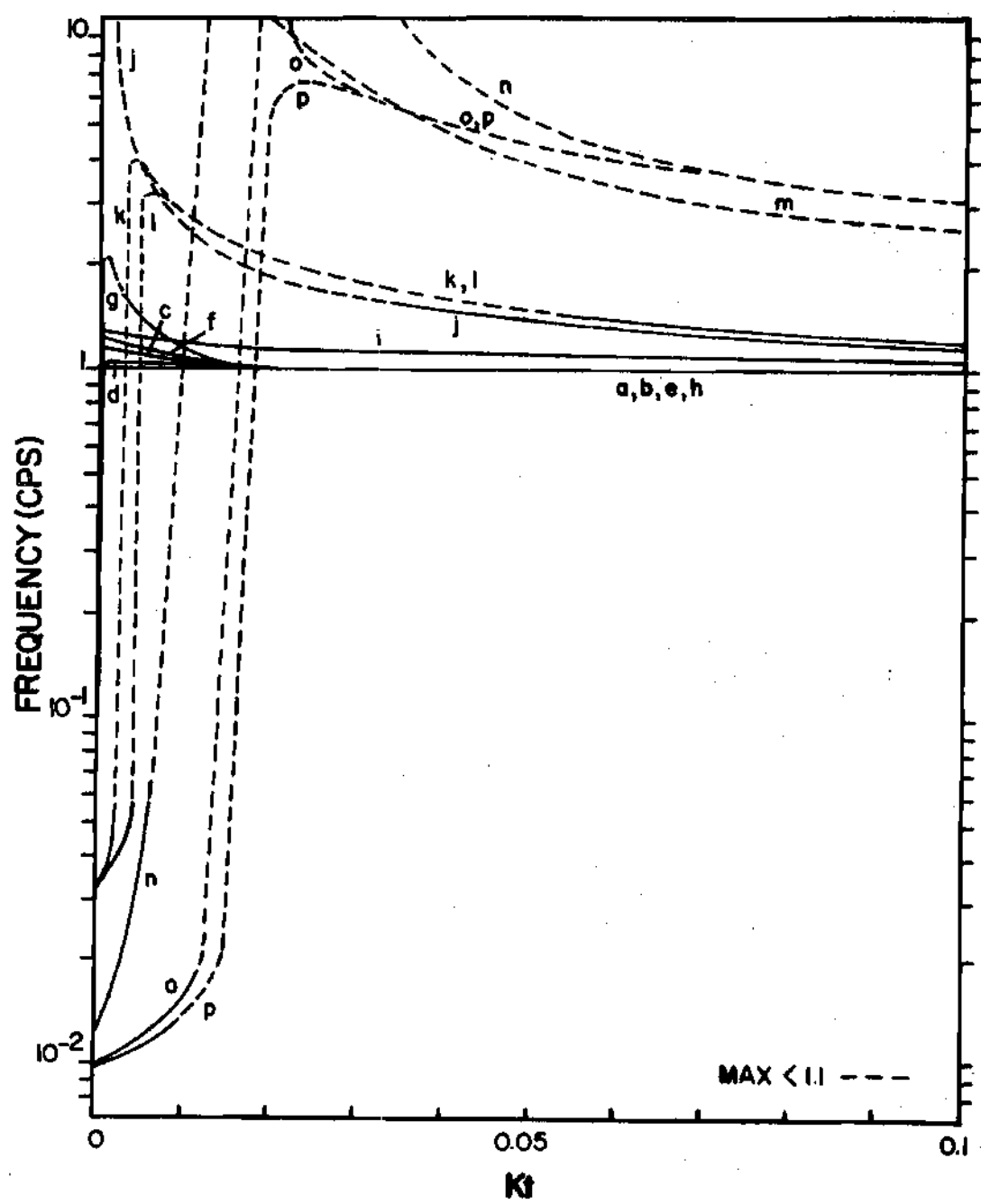


Figure 16. Influence of the Tachometer Feedback Constant (Kt) on the Frequency of the Maximum

In addition to the curves in Figures 8 through 16, it was necessary to plot five more curves in order to completely analyze the system. Since a small number of values for alpha and gamma were plotted in different combinations, another set of curves was needed to find the optimum value for the two. Gamma (the servo amplifier gain) was plotted on the abscissa for values of the null amplifier gain,

$$\beta = 0.0, 0.01, 0.1, 1.0, 10.0$$

for individual values of the principal feedback gain,

$$\alpha = 10, 100, 1000, 10000$$

Only values of

$$\beta = 0.0 \text{ and } 1.0$$

appear through the range of alphas in Figure 17 and 18 as representative of the entire set. The curve for the frequency of the maximum will not be presented since it was not used as a design criterion.

Figures 17 and 18 appear on the following pages:

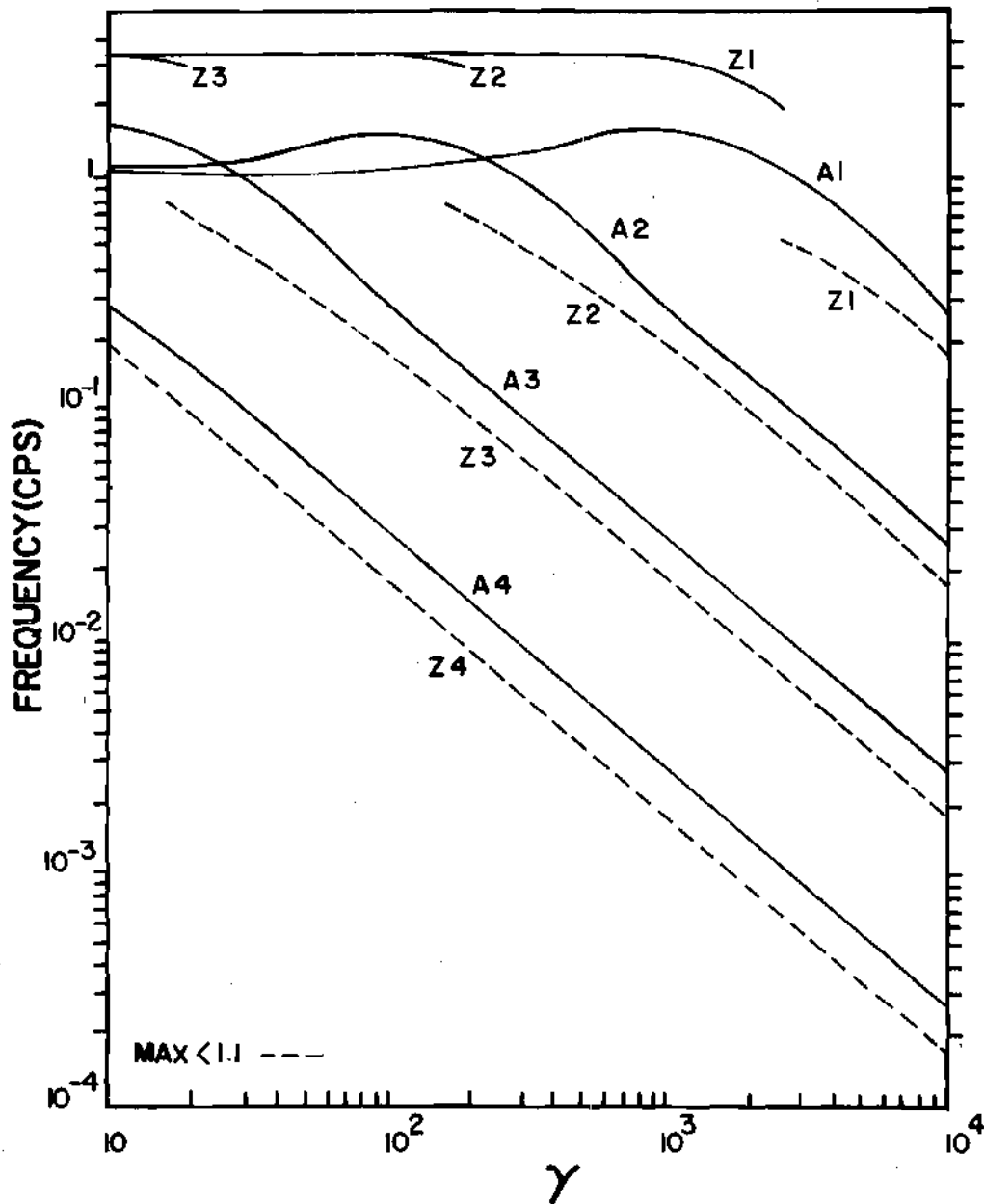


Figure 17. Influence of the Gamma Gain ( $\gamma$ ) on the 10 Per Cent Amplitude (Z) and 10 Per Cent Phase Angle (A) Error Frequencies ( $\beta = 0$ )

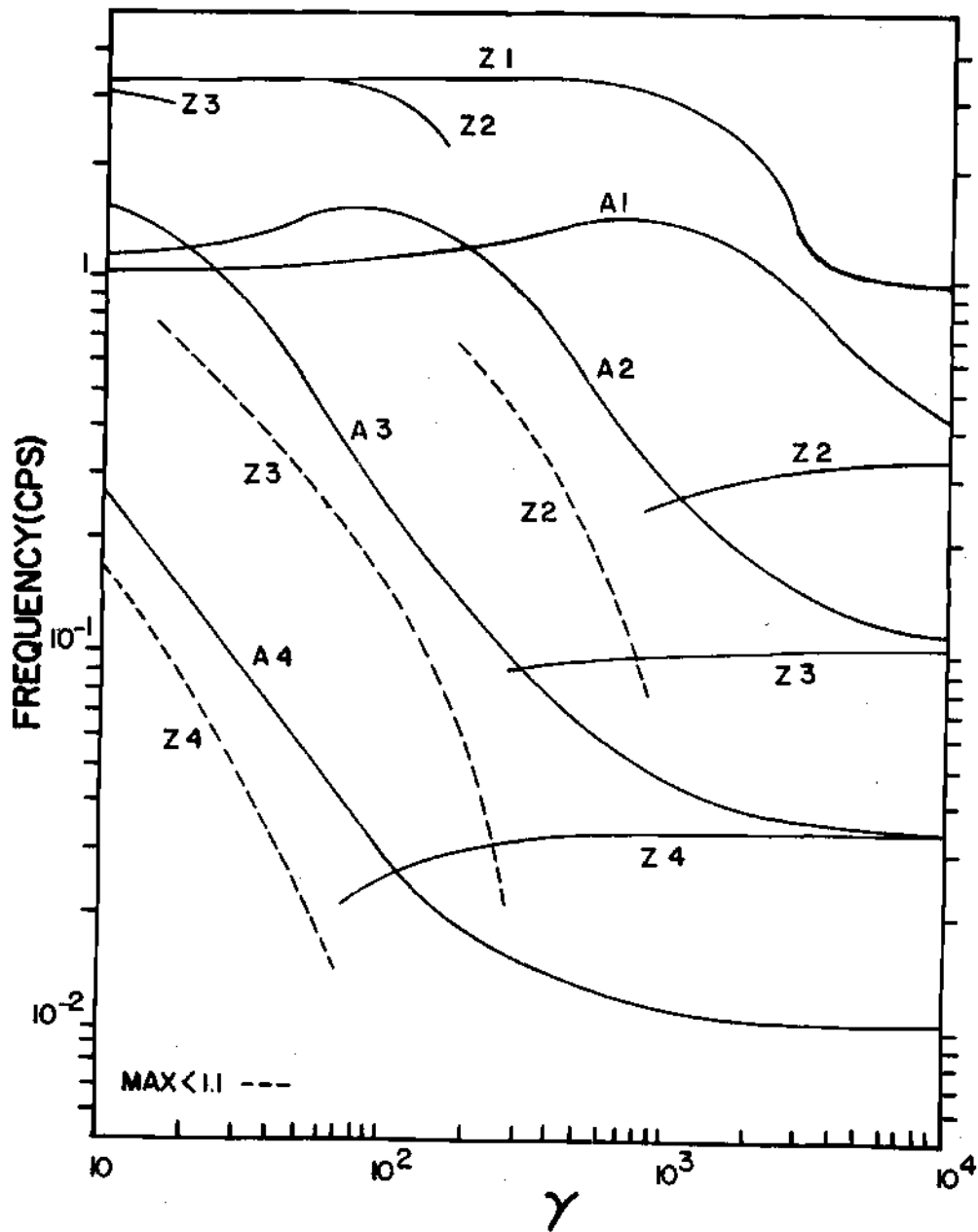


Figure 18. Influence of the Gamma Gain ( $\gamma$ ) on the 10 Per Cent Amplitude (Z) and 10 Per Cent Phase Angle (A) Error Frequencies ( $\beta = 1.0$ )

As the principal feedback gain ( $\alpha$ ) increases, the 10%AME, 10%PHAE, and the maximum's frequency all decrease.

The changes in the frequency response due to changes in the gamma gain for larger values of  $\alpha$  and  $\beta$  are of particular interest. As gamma is increased (Figure 18), the 10%AME frequency decreases through two discontinuities and then increases. The 10%PHAE frequency decreases as gamma increases for higher values of  $\alpha$  and gamma.

One of the most significant points of Figure 18 is the value of gamma where the 10%AME and 10%PHAE frequency curves intersect. At this point the amplitude of the maximum is at a low value, the 10%AME frequency is almost at its minimum, and the phase angle error is at its highest acceptable limit. If this value for gamma is obtained for a wide range of  $\alpha$  and  $\beta$  and is plotted on the ordinate versus  $\beta$  on the abscissa with a separate curve for each  $\alpha$ , the curves in Figure 19 result. Each curve is a straight line on the log-log coordinate system (straight lines would also result if  $\alpha$  were on the ordinate). Thus, the value for the optimum gain for gamma can be expressed as a function of  $\beta$ ,  $\alpha$ , and the servo motor gain constant ( $K_m$ ).

$$\gamma = \frac{12,000}{K_m \alpha^{1/2} \beta^{1/2}} \quad (12)$$

which holds for  $\beta \geq 0.01$ ,  $\alpha \geq 50$ ,  $T_1 = 100$  volts/radian, and  $T_2 = 100$  volts/radian.

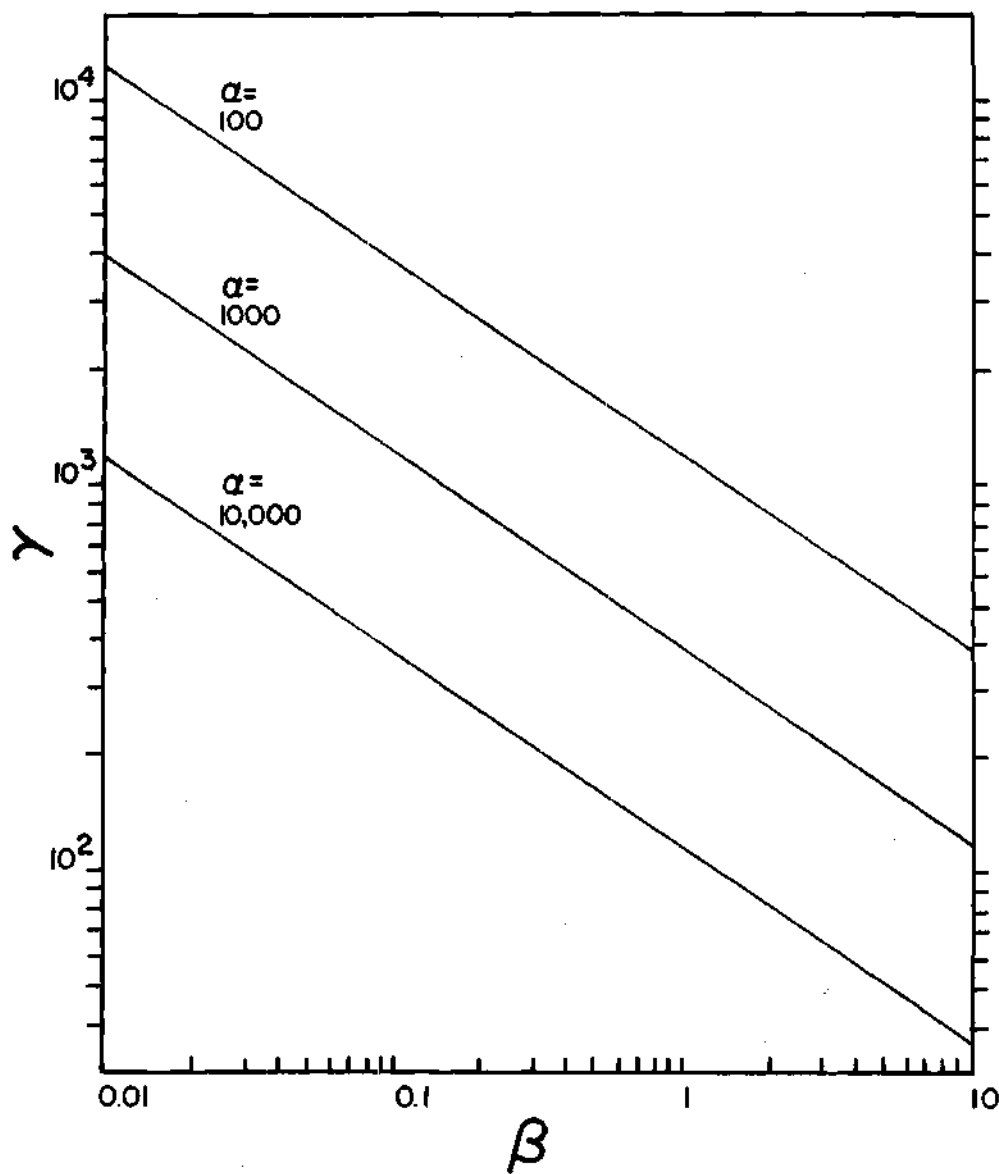


Figure 19. Influence on the Beta Gain ( $\beta$ ) on the value of the Optimum Gamma Gain ( $\gamma$ ) for Several Values of the Alpha Gain ( $\alpha$ )

As the null feedback amplifier's gain ( $\beta$ ) is decreased, the value of the maximum's amplitude and frequency decrease until the maximum disappears (Figures 17 and 22). The 10%AME frequency decreases with an increase in  $\beta$  until the 0.9-1.1 discontinuity appears and then it increases (Figure 20). The 10%PHAE frequency increases for the whole range as  $\beta$  increases (Figure 21). The values of the parameters from the criterion for the optimum servo amplifier gain ( $\gamma$ ) produce a maximum amplitude greater than 1.1. Thus the smallest value of  $\beta$  which will keep the servo vibrograph in its null position will be the best.

Figures 20 through 22 appear on the following pages:

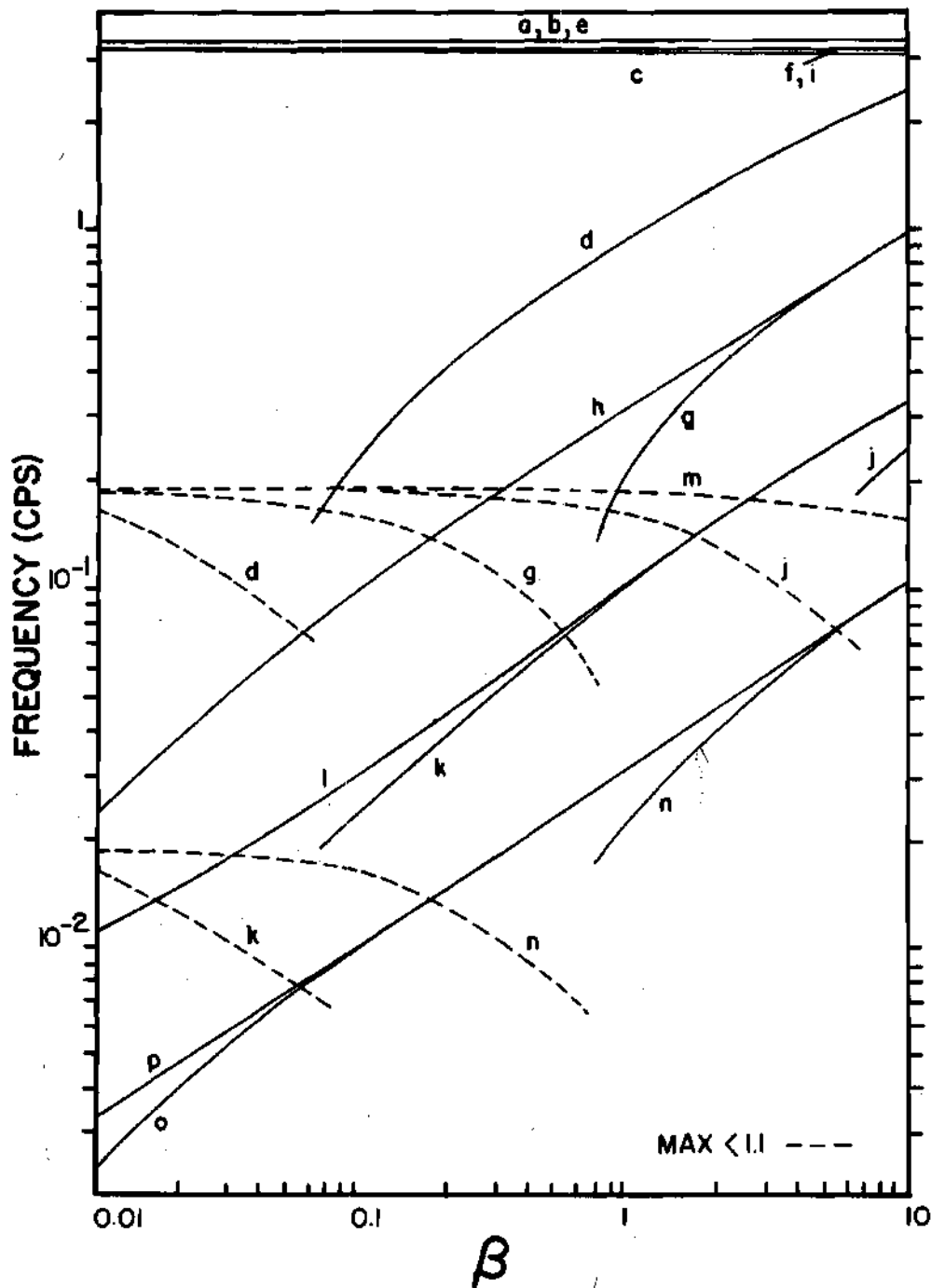


Figure 20. Influence of the Beta Gain ( $\beta$ ) on the 10 Per Cent Amplitude Error Frequency

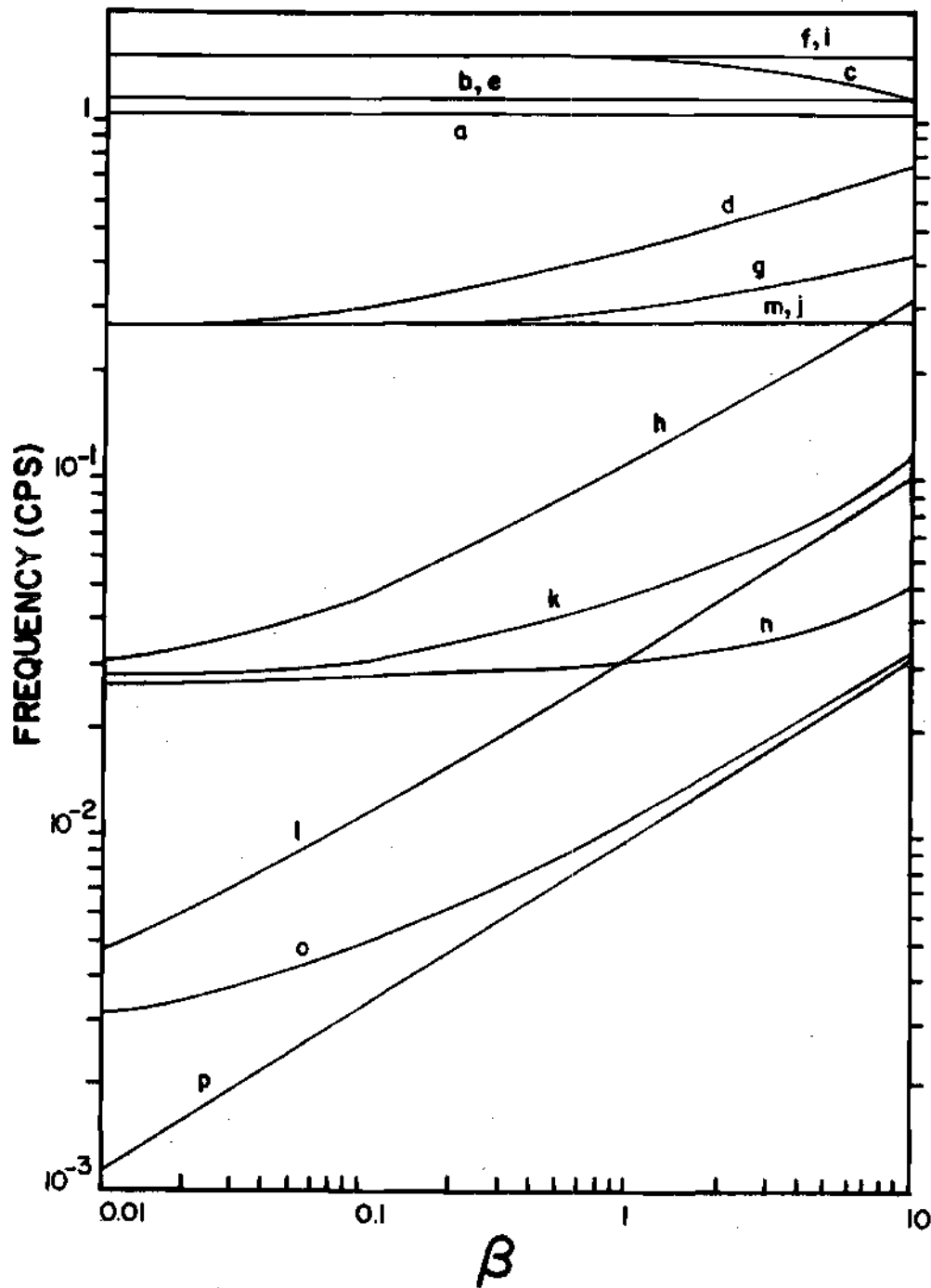


Figure 21. Influence of the Beta Gain ( $\beta$ ) on the 10 Per Cent Phase Angle Error Frequency

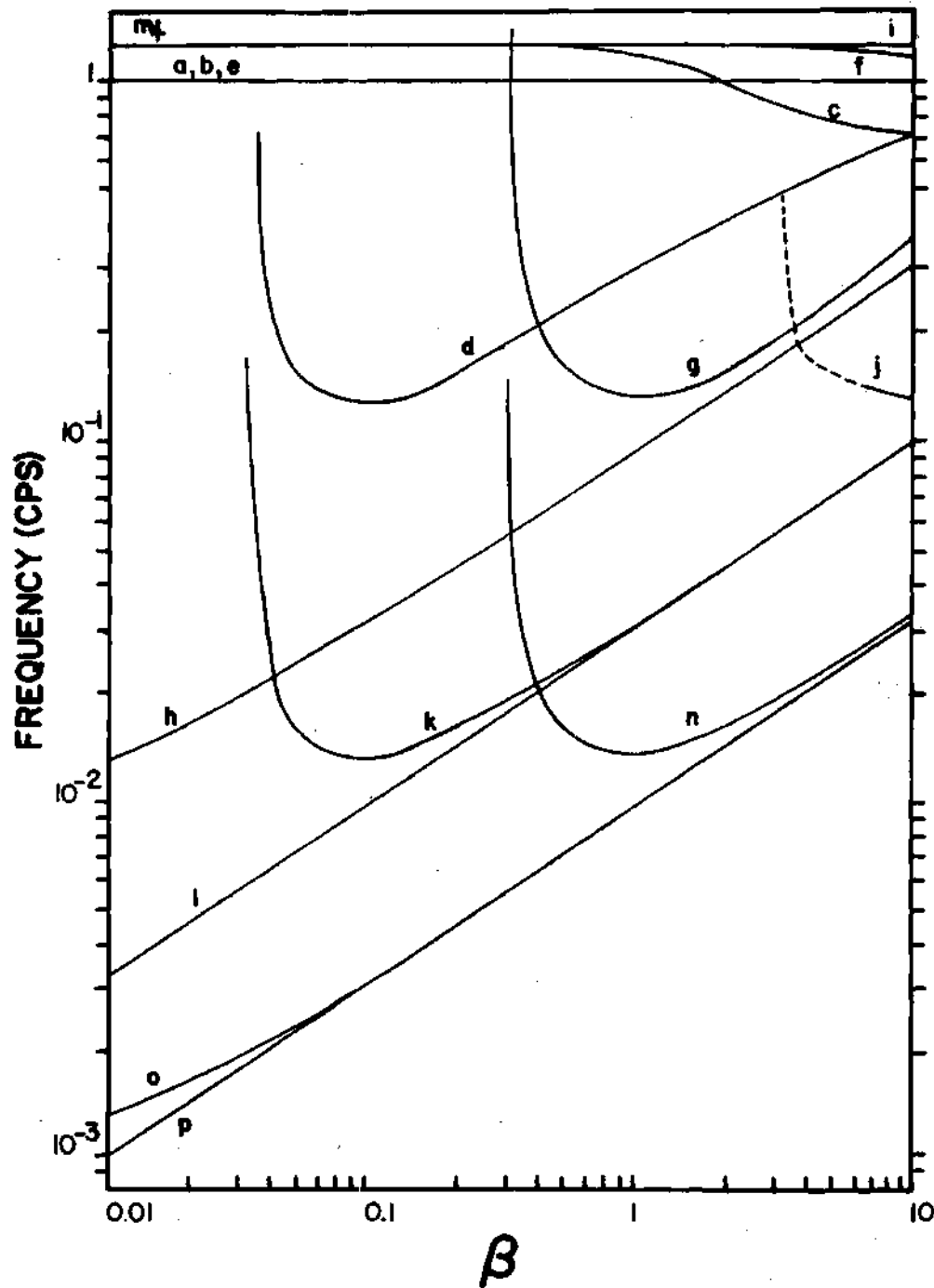


Figure 22. Influence of the Beta Gain ( $\beta$ ) on the Frequency of the Maximum

In order to investigate the sensitivity of the servo vibrograph to small changes in each of the parameters, the sensitivity function with respect to amplitude ( $Z/X$ ) was employed. The values of the sensitivity function were found to be quite small, thus showing that the sensitivity of the amplitude to small changes in the parameters is quite small (Appendix D).

The sensitivity with respect to the 10%AME frequency cannot be found in a closed form. It can, however, be found approximately from the optimization graphs on the preceding pages. At the optimum values of each of the parameters, a 10 per cent change in:

$K_t$  produces approximately a 1 per cent change in the 10%AME frequency;

$\beta$  produces approximately a 5 per cent change in the 10%AME frequency;

$\gamma$  produces approximately a 1 per cent change in the 10%AME frequency;

$\alpha$  produces approximately a 1 per cent change in the 10%AME frequency;

and the changes for  $T_m$  and  $C_1$  are negligible.

Thus, excepting the natural frequency of the vibrograph, the gain of the null amplifier produces the largest percentage of change in the 10%AME frequency.

## Stability and Impulse Response

### Characteristic Equation

The equation

$$Tm s^4 + Cs^3 + Ds^2 + Es + F = 0 \quad (13)$$

which is the denominator of Equation (6) is called the characteristic equation of the servo vibrograph. For the particular case in which all the constants have specified values, it is a rational function with constant coefficients and thus its roots will be real numbers, complex conjugate numbers or a combination of the two. The impulse response of the system can be calculated by taking the inverse transform of Equation (6). If any of the roots of Equation (13) have positive real parts the system will be unstable because of the resulting increasing exponential term in the inverse transform.

### Damping Characteristics of the Servo Vibrograph System

Since the characteristic equation is of the fourth order, it will have four roots. There are several possible combinations which can result:

1. Four equal real roots;
2. Two sets of distinct real roots;
3. Three equal and one distinct real roots;
4. Four distinct real roots;
5. Two equal conjugate complex pairs;
6. Two distinct conjugate complex pairs;

7. One conjugate complex pair and two equal real roots;
8. One conjugate complex pair and two distinct real roots.

If the characteristic equation has repeated roots (cases 1, 2, 3, 5 and 7), then some terms of the impulse response will have time as a functional multiplier. If there are complex roots (cases 5, 6, 7, and 8), the impulse response will have terms with a sinusoidal multiplier and if there is a real part to any of the roots, the impulse response will have terms with an exponential multiplier (possible for all cases).

Case one is of particular interest if the wave form of the input vibration is of a random nature with no harmonic component. This case is analogous to critical damping in a simple vibrograph, in that the decay is at a maximum rate but no oscillation occurs. Any set of real roots which are not all equal will have at least one smaller real root. If it is assumed that the characteristic equation has four equal real roots of value  $R$  then the characteristic equation with these four roots would be

$$(s + R)^4 = s^4 + 4Rs^3 + 6R^2s^2 + 4R^3s + R^4 \quad (14)$$

In order to have the four real roots in Equation (14), each coefficient must equal its corresponding value in

$$s^4 + Cs^3/T_m + Ds^2/T_m + Es/T_m + F/T_m = 0 \quad (15)$$

or

$$4R = C/T_m \quad (16)$$

$$6R^2 = D/T_m \quad (17)$$

$$4R^3 = E/T_m \quad (18)$$

$$R^4 = F/T_m \quad (19)$$

Solving Equations (16), (17), (18), and (19) for R, then

$$R = \frac{C}{4T_m} = \frac{4D}{6C} = \frac{6E}{4D} = \frac{4F}{E}$$

or

$$3C^2 = 8DT_m \quad (20)$$

$$CD = 6ET_m \quad (21)$$

$$CE = 16FT_m \quad (22)$$

Solving Equations (21) and (22) for  $\beta'$  if

$$M = \frac{1 + \gamma K_m K_t}{T_m} \quad (23)$$

$$\alpha' = \frac{(T_1 \alpha + T_2 \beta) P K_m \gamma}{T_m} \quad (24)$$

$$\beta' = \beta \frac{T_2 P \gamma Km}{T_m} \quad (25)$$

and the values of C, D, E, and F are substituted then

$$\beta' = \frac{M\alpha' + C_1 M^2 + C_1 \omega_n^2 + C_1 \alpha' + C_1^2 M - 5M\omega_n^2}{6C_1} \quad (26)$$

$$\beta' = \frac{\omega_n^2 M^2 + \omega_n^2 MC_1}{16\omega_n^2 - MC_1 - C_1^2} \quad (27)$$

Eliminating  $\beta'$  from Equations (26) and (27) and solving for  $\alpha'$  then

$$\alpha' = \frac{(\omega_n^2 M^2 + \omega_n^2 MC_1)6C_1 - (C_1 M^2 + C_1 \omega_n^2 + C_1^2 M - 5M\omega_n^2)(16\omega_n^2 - MC_1 - C_1^2)}{(16\omega_n^2 - MC_1 - C_1^2)(M + C_1)} \quad (28)$$

Also solving Equation (20) for  $\alpha'$  then

$$\alpha' = \frac{3M^2 + 3C_1^2 - 8\omega_n^2 - 2C_1 M}{8} \quad (29)$$

Elimination of  $\alpha'$  from Equations (28) and (29) results in the final equation:

$$C_1 M^4 + 4M^3(C_1^2 - 4\omega_n^2) + 6M^2 C_1(-8\omega_n^2 + C_1^2) \quad (30)$$

$$+ 4M(-12C_1^2 \omega_n^2 + 64\omega_n^2 + C_1^4) + C_1^3(C_1^2 - 16\omega_n^2) = 0$$

The equation can be factored into the following:

$$(M + C_1 + 4\omega_n)(M + C_1 - 4\omega_n)(C_1 M^2 + 2C_1^2 M - 16M\omega_n^2 + C^3) = 0 \quad (31)$$

and from this the roots are:

$$M = -C_1 \pm 4\omega_n \quad (32)$$

$$M = \frac{8\omega_n^2 - C_1^2 \pm 4\omega_n \sqrt{4\omega_n^2 - C_1^2}}{C_1} \quad (33)$$

As an example of the range of values that can result from the roots of Equations (32) and (33) if

$$\omega_n = 1 \text{ cps} = 6.28 \text{ rad/sec}$$

$$C_1 = 0.1 \text{ 1/sec}$$

$$Kt = 0$$

$$P = 7 \times 10^{-6}$$

then the following of the variables can be calculated (excluding negative values of the roots).

$$M_1 = 2.5$$

$$M_2 = 6300$$

$$Tm_1 = 1/25$$

$$Tm_2 = 1/6300$$

$$R_1 = 6.25$$

$$R_2 = 1575$$

$$\alpha_1' = 195$$

$$\alpha_2' = 1.49 \times 10^7$$

$$\begin{array}{ll}
 \beta_1 = 39.2 & \beta_2 = 1.56 \times 10^9 \\
 \beta_1 \gamma_1 = 2240 & \beta_2 \gamma_2 = 3.54 \times 10^8 \\
 \alpha_1 \gamma_1 = 9000 & \alpha_2 \gamma_2 = -3.51 \times 10^8
 \end{array}$$

The subscripts are for the first and second roots in Equations (32) and (33), respectively. The second root for M is much too large and for this case yields a negative value of the product  $\gamma\alpha$ . The other root is a possible solution.

The impulse response for the case when all four roots are equal and real is:

$$\begin{aligned}
 F(t) = \frac{1}{24 T_m} [ & (T_m R^4 - AR^3 + BR^2)t^3 e^{-Rt} & (34) \\
 & + 4(-4 T_m R^3 + 3AR^2 - 2RB)t^2 e^{-Rt} \\
 & + 12(6 T_m R^2 - 3AR + B)te^{-Rt} \\
 & + 24(-4 T_m R + A)e^{-Rt} ] + 1
 \end{aligned}$$

where,

t = time

R = root

F(t) = impulse response

For the case in which all the roots are real and distinct, the impulse response is of the form

$$F(t) = A_1 e^{-R_1 t} + A_2 e^{-R_2 t} + A_3 e^{-R_3 t} + A_4 e^{-R_4 t} + 1 \quad (35)$$

where,

$$A_i = \frac{[(R_i^4 + (A/Tm)(-R_i)^3 + (B/Tm)(R_i)^2](R_i - R_i)}{(R_1 - R_i)(R_2 - R_i)(R_3 - R_i)(R_4 - R_i)}$$

for  $i = 1, 2, 3, 4$ , and

$R_i$  = roots of characteristic equation.

Equations (34) and (35) approach one as  $t$  approaches infinity.

If there are complex roots of the characteristic equation, the impulse response will take the following form:

$$F(t) = \dots + A' e^{at} \sin(bt + \psi) + 1 \quad (36)$$

where,

$a$  = real part of the complex conjugate root.

$b$  = positive imaginary part of the complex conjugate root

$$A' = \frac{(s + a - jb)(s + a + jb)(s^4 + (A/Tm)s^3 + (B/Tm)s^2)}{(s + a - jb)(s + a + jb)(s + R_1)(s + R_2)}$$

$b$

evaluated at  $s = a + jb$ .

$\psi$  = phase angle of  $A'$ .

### Root Loci and the Stability of the System

If  $\gamma$  were varied from zero to infinity (all other constants remaining constant) and at each value of  $\gamma$  the roots of the

characteristic equation were found, a locus of these roots could be plotted with real values on the abscissa and imaginary values on the ordinate. If any value of the locus appeared with a positive real part, the system would be unstable at this point because of the increasing exponential in the impulse response. The value of the imaginary part of any point on the locus represents the natural damped frequency of the component and the value of the real part is proportional to the damping of the impulse response due to that particular root. Thus, for high values on the real axis, the component which corresponds to the particular root dies out very quickly and large values on the imaginary axis represent large natural damped frequencies.

Thus to investigate the transient response and stability of the servo vibrograph, the root loci with respect to gamma were determined for a range of values of all the parameters. In order to find the path of the root locus for each set of parameters an electronic computer was used to find the roots of the characteristic equation for a finite number of values of gamma. Plotting the value of these roots forms a root locus. The routine for finding the roots (both simple and complex) of a polynomial is a standard program at the Georgia Institute of Technology's Rich Computer Center and will not be presented here.

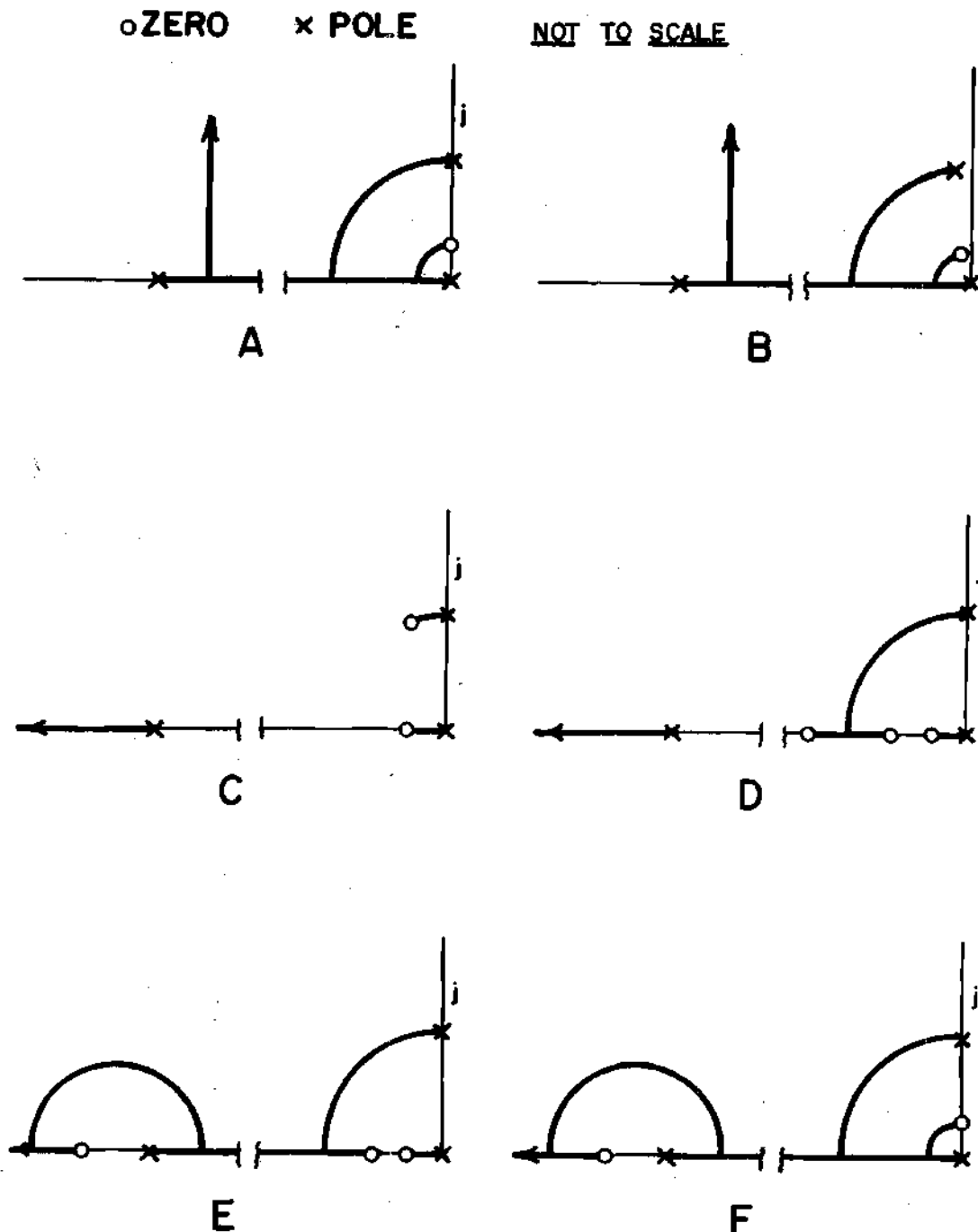
For a wide range of all the parameters the root locus was found and plotted. Each parameter was varied through the range of values for the frequency response study although in larger steps because of the slow convergence of the program. In no instance, for positive values of the parameters, did the root locus have a value which was in the positive real half of the root locus plot.

Presented in Tables 2, 3, and 4 is a sample of the results obtained. The value at gamma equal zero and infinity are respectively called poles and zeros. A root locus plot starts at each of the poles and proceeds to one of the zeros which may be finite or infinite. There must be an equal number of poles and zeros. In Figure 23 a diagram of all the root loci corresponding to the values in the tables is presented. A breakaway point occurs when the locus converges to a point and breaks away from the original curve at right angles to it.

When  $C_1$  is zero the pole is at a value of 6.28 which is the natural frequency of the basic vibrograph in radians (i.e., 1 cps). The value of the pole is unaffected by changes in the gains. The only parameters which affect the pole are the natural frequency and the damping ( $C_1$ ).  $C_1$  serves to move the pole off the imaginary axis. The values at 100 and zero are just limit points as gamma approaches zero and at zero do not really exist.

The emergence of breakaway points can best be described by examining the movement of the zeros as the parameters change.  $T_m$  has little effect on the root locus for the values considered here.  $C_1$  tends to move the pole and the zero which are on the imaginary axis in plot A slightly to the left as in plot B (Figure 23).

With no damping, an increase in beta increases the imaginary coordinate of the zero which is on the imaginary axis, and an increase in alpha decreases this zero point. With damping, the zero moves upward to the left with increasing beta and downward to the right with increasing alpha. Thus increasing beta increases the limit of the natural frequency and the damping while increasing alpha decreases the



ALL ROOT LOCI ARE SYMMETRIC WITH RESPECT TO THE REAL AXIS

Figure 23. Root Locus Plots for the Servo Vibrograph  
(for Variable Gamma)

Table 2. Root Locus Characteristic Point Locations

$\zeta_n=1$   $C_n=0$   $K_f=0$   $T_m=0.01$   $K_m=1.0$   $P=7 \times 10^{-6}$   $T_1=100$   $T_2=100$

	$\alpha=100$			$\alpha=1000$			$\alpha=10,000$			
	ZEROS		BREAKAWAY PTS.	ZEROS		BREAKAWAY PTS.	ZEROS		BREAKAWAY PTS.	
	REAL	IMAG	REAL GAIN	REAL	IMAG	REAL GAIN	REAL	IMAG	REAL GAIN	
$\beta=0.01$	0.00@ 0	6.28@-2	-6.28@-2/4.49@ 3	0.00@ 0	1.99@-2	-1.99@-2/1.42@ 3	0.00@ 0	6.28@-3	-6.28@-3/4.49@ 2	
	0.00@ 0	-6.28@-2	-6.75@ 0/1.67@ 2	0.00@ 0	-1.99@-2	-6.75@ 0/1.67@ 1	0.00@ 0	-6.28@-3	-6.75@ 0/1.67@ 0	
			-4.92@ 1/3.63@ 2			-4.92@ 1/3.63@ 1			-4.92@ 1/3.63@ 0	
		ROOT LOCUS PLOT			ROOT LOCUS PLOT			ROOT LOCUS PLOT		
		A			A			A		
$\beta=0.1$	0.00@ 0	1.99@-1	-1.99@-1/1.42@ 3	0.00@ 0	6.28@-2	-6.28@-2/4.49@ 2	0.00@ 0	1.99@-2	-1.99@-2/1.42@ 2	
	0.00@ 0	-1.99@-1	-6.74@ 0/1.68@ 2	0.00@ 0	-6.28@-2	-6.75@ 0/1.68@ 1	0.00@ 0	-1.99@-2	-6.76@ 0/1.68@ 0	
			-4.92@ 1/3.63@ 2			-4.92@ 1/3.63@ 1			-4.92@ 1/3.63@ 0	
		ROOT LOCUS PLOT			ROOT LOCUS PLOT			ROOT LOCUS PLOT		
		A			A			A		
$\beta=1$	0.00@ 0	6.25@-1	-6.34@-1/4.48@ 2	0.00@ 0	1.99@-1	-1.99@-1/1.42@ 2	0.00@ 0	6.28@-2	-6.28@-2/4.49@ 1	
	0.00@ 0	-6.25@-1	-6.63@ 0/1.65@ 2	0.00@ 0	-1.99@-1	-6.74@ 0/1.68@ 1	0.00@ 0	-6.28@-2	-6.75@ 0/1.68@ 0	
			-4.92@ 1/3.59@ 2			-4.92@ 1/3.63@ 1			-4.92@ 1/3.63@ 0	
		ROOT LOCUS PLOT			ROOT LOCUS PLOT			ROOT LOCUS PLOT		
		A			A			A		
$\beta=10$	0.00@ 0	1.89@ 0	-2.39@ 0/1.47@ 2	0.00@ 0	6.25@-1	-6.34@-1/4.48@ 1	0.00@ 0	1.99@-1	-1.99@-1/1.42@ 1	
	0.00@ 0	-1.89@ 0	-5.28@ 0/1.39@ 2	0.00@ 0	-6.25@-1	-6.63@ 0/1.65@ 1	0.00@ 0	-1.99@-1	-6.74@ 0/1.68@ 0	
			-4.93@ 1/3.29@ 2			-4.92@ 1/3.59@ 1			-4.92@ 1/3.63@ 0	
		ROOT LOCUS PLOT			ROOT LOCUS PLOT			ROOT LOCUS PLOT		
		A			A			A		
	POLES:	REAL	IMAG	REAL	IMAG	REAL	IMAG	REAL	IMAG	NOTE: @ a = x 10 <sup>a</sup>
		0.00@ 0	0.00@ 0	0.00@ 0	6.28@ 0	0.00@ 0	-6.28@ 0	-1.00@ 2	0.00@ 0	

Table 3. Root Locus Characteristic Point Locations

$\alpha=1$   $C_1=0.5$   $K_1=0$   $T_m=0.01$   $K_m=1.0$   $P=7 \times 10^{-6}$   $T_1=100$   $T_2=100$

	$\alpha=100$				$\alpha=1000$				$\alpha=10,000$			
	ZEROS		BREAKAWAY PTS.		ZEROS		BREAKAWAY PTS.		ZEROS		BREAKAWAY PTS.	
	REAL	IMAG	REAL	GAIN	REAL	IMAG	REAL	GAIN	REAL	IMAG	REAL	GAIN
$\beta=0.01$	-2.50@-5	6.28@-2	-6.28@-2/4.48@ 3		-2.50@-6	1.99@-2	-1.99@-2/1.42@ 3		-2.50@-7	6.28@-3	-6.28@-3/4.49@ 2	
	-2.50@-5	-6.28@-2	-6.73@ 0/1.61@ 2		-2.50@-6	-1.99@-2	-6.74@ 0/1.61@ 1		-2.50@-7	-6.28@-3	-6.74@ 0/1.61@ 0	
			-4.94@ 1/3.59@ 2				-4.94@ 1/3.59@ 1				-4.94@ 1/3.59@ 0	
	ROOT LOCUS PLOT				ROOT LOCUS PLOT				ROOT LOCUS PLOT			
	B				B				B			
$\beta=0.1$	-2.50@-4	1.99@-1	-1.98@-1/1.42@ 3		-2.50@-5	6.28@-2	-6.28@-2/4.48@ 2		-2.50@-6	1.99@-2	-1.99@-2/1.42@ 2	
	-2.50@-4	-1.99@-1	-6.72@ 0/1.61@ 2		-2.50@-5	-6.28@-2	-6.73@ 0/1.61@ 1		-2.50@-6	-1.99@-2	-6.74@ 0/1.61@ 0	
			-4.94@ 1/3.59@ 2				-4.94@ 1/3.59@ 1				-4.94@ 1/3.59@ 0	
	ROOT LOCUS PLOT				ROOT LOCUS PLOT				ROOT LOCUS PLOT			
	B				B				B			
$\beta=1$	-2.48@-3	6.25@-1	-6.29@-1/4.46@ 2		-2.50@-4	1.99@-1	-1.98@-1/1.42@ 2		-2.50@-5	6.28@-2	-6.28@-2/4.48@ 1	
	-2.48@-3	-6.25@-1	-6.62@ 0/1.58@ 2		-2.50@-4	-1.99@-1	-6.72@ 0/1.61@ 1		-2.50@-5	-6.28@-2	-6.73@ 0/1.61@ 0	
			-4.94@ 1/3.56@ 2				-4.94@ 1/3.59@ 1				-4.94@ 1/3.59@ 0	
	ROOT LOCUS PLOT				ROOT LOCUS PLOT				ROOT LOCUS PLOT			
	B				B				B			
$\beta=10$	-2.27@-2	1.89@ 0	-2.30@ 0/1.45@ 2		-2.48@-3	6.25@-1	-6.29@-1/4.46@ 1		-2.50@-4	1.99@-1	-1.98@-1/1.42@ 1	
	-2.27@-2	-1.89@ 0	-5.40@ 0/1.35@ 2		-2.48@-3	-6.25@-1	-6.62@ 0/1.58@ 1		-2.50@-4	-1.99@-1	-6.72@ 0/1.61@ 0	
			-4.95@ 1/3.26@ 2				-4.94@ 1/3.56@ 1				-4.94@ 1/3.59@ 0	
	ROOT LOCUS PLOT				ROOT LOCUS PLOT				ROOT LOCUS PLOT			
	B				B				B			
	POLES:	REAL	IMAG	REAL	IMAG	REAL	IMAG	REAL	IMAG	NOTE: @ a - x 10 <sup>a</sup>		
		0.00@ 0	0.00@ 0	-2.50@-1	6.28@ 0	-2.50@-1	-6.28@ 0	-1.00@ 2	0.00@ 0			

Table 4. Root Locus Characteristic Point Locations

$\omega_n=1$   $\zeta=0$   $K_f=0.025$   $T_m=0.01$   $K_m=1.0$   $P=7 \times 10^{-6}$   $T_1=100$   $T_2=100$

	$\alpha=100$			$\alpha=1000$				$\alpha=10,000$			
	ZEROS		BREAKAWAY PTS.	ZEROS		BREAKAWAY PTS.		ZEROS		BREAKAWAY PTS.	
	REAL	IMAG		REAL	IMAG	REAL	GAIN	REAL	IMAG	REAL	GAIN
$\beta=0.01$	-2.80@-4	0.00@ 0	NONE	-2.80@-4	0.00@ 0	-6.53@ 0	3.05@ 1	-2.81@-4	0.00@ 0	-6.73@ 0	1.76@ 0
	-1.40@ 0	6.13@ 0		-1.49@ 0	0.00@ 0			-1.41@-1	0.00@ 0	-5.49@ 1	4.47@ 0
	-1.40@ 0	-6.13@ 0		-2.65@ 1	0.00@ 0			-2.80@ 2	0.00@ 0	-5.04@ 2	3.64@ 2
			ROOT LOCUS PLOT			ROOT LOCUS PLOT				ROOT LOCUS PLOT	
			C			D				E	
$\beta=0.1$	-2.80@-3	0.00@ 0	NONE	-2.81@-3	0.00@ 0	-6.53@ 0	3.05@ 1	-2.86@-3	0.00@ 0	-6.73@ 0	1.76@ 0
	-1.40@ 0	6.12@ 0		-1.49@ 0	0.00@ 0			-1.38@-1	0.00@ 0	-5.49@ 1	4.47@ 0
	-1.40@ 0	-6.12@ 0		-2.65@ 1	0.00@ 0			-2.80@ 2	0.00@ 0	-5.04@ 2	3.64@ 2
			ROOT LOCUS PLOT			ROOT LOCUS PLOT				ROOT LOCUS PLOT	
			C			D				E	
$\beta=1$	-2.81@-2	0.00@ 0	NONE	-2.86@-2	0.00@ 0	-6.52@ 0	3.04@ 1	-3.85@-2	0.00@ 0	-6.73@ 0	1.76@ 0
	-1.40@ 0	6.12@ 0		-1.46@ 0	0.00@ 0			-1.03@-1	0.00@ 0	-5.49@ 1	4.47@ 0
	-1.40@ 0	-6.12@ 0		-2.65@ 1	0.00@ 0			-2.80@ 2	0.00@ 0	-5.04@ 2	3.64@ 2
			ROOT LOCUS PLOT			ROOT LOCUS PLOT				ROOT LOCUS PLOT	
			C			D				E	
$\beta=10$	-2.86@-1	0.00@ 0	NONE	-3.84@-1	0.00@ 0	-6.41@ 0	2.94@ 1	-7.04@-2	1.86@-1	-1.99@-1	2.20@ 1
	-1.40@ 0	6.06@ 0		-1.07@ 0	0.00@ 0			-7.04@-2	-1.86@-1	-6.72@ 0	1.75@ 0
	-1.40@ 0	-6.06@ 0		-2.68@ 1	0.00@ 0					-5.49@ 1	4.47@ 0
			ROOT LOCUS PLOT			ROOT LOCUS PLOT				-5.05@ 2	3.64@ 2
			C			D				F	
	POLES:		REAL	IMAG	REAL	IMAG	REAL	IMAG	NOTE: @ a - x 10 <sup>a</sup>		
			0.00@ 0	0.00@ 0	0.00@ 0	6.28@ 0	0.00@ 0	-6.28@ 0	-1.00@ 2	0.00@ 0	

limit.

When tachometer feedback ( $K_t$ ) is added to the system the zeros change their position much more radically. The motion of the zeros can best be represented by referring to Figure 23. With increasing  $K_t$ , the zeros start with positions such as those in Plot A and proceed as follows: A-F-E-D-C. With increasing  $\alpha$  the progression of the zeros is C-D-E-F-A. For large values of  $K_t$  an increase in  $\beta$  has the same effect as an increase in  $\alpha$ , only to a lesser extent for the ranges of  $\beta$  considered here, and for small values of  $K_t$ ,  $\beta$  has just the opposite effect.

The root locus for the optimum values of all the parameters (from the frequency response study) is plotted in Figure 24 (for  $\gamma$  variable). At the optimum value of  $\gamma$ , the values of the roots are:

<u>Real</u>	<u>Imaginary</u>
-0.144	0.136
-0.144	-0.136
-97.4	131.0
-97.4	-131.0

The larger roots have an effect which lasts for only a short time. The smaller roots cause a long-period damped sine wave to appear in the impulse response. Increases in  $\gamma$  cause the impulse response to have a higher frequency and lower damping and decreases in  $\gamma$  cause the opposite effect. Increases in  $\alpha$  cause the gain points of this root locus to be shifted toward the zeros.

$\alpha=1000$

$\omega_n=1.0$  CPS

$T_m=0.01$

$T_1=100$

OPTIMUM  $\gamma=380$

$\beta=1.0$

$C_i=0.1$

$K_m=1.0$

$T_2=100$

x POLE o ZERO

$\gamma$  = VARIABLE (VALUES ON GRAPH)

$K_f=0.0025$

$P=7 \times 10^{-6}$

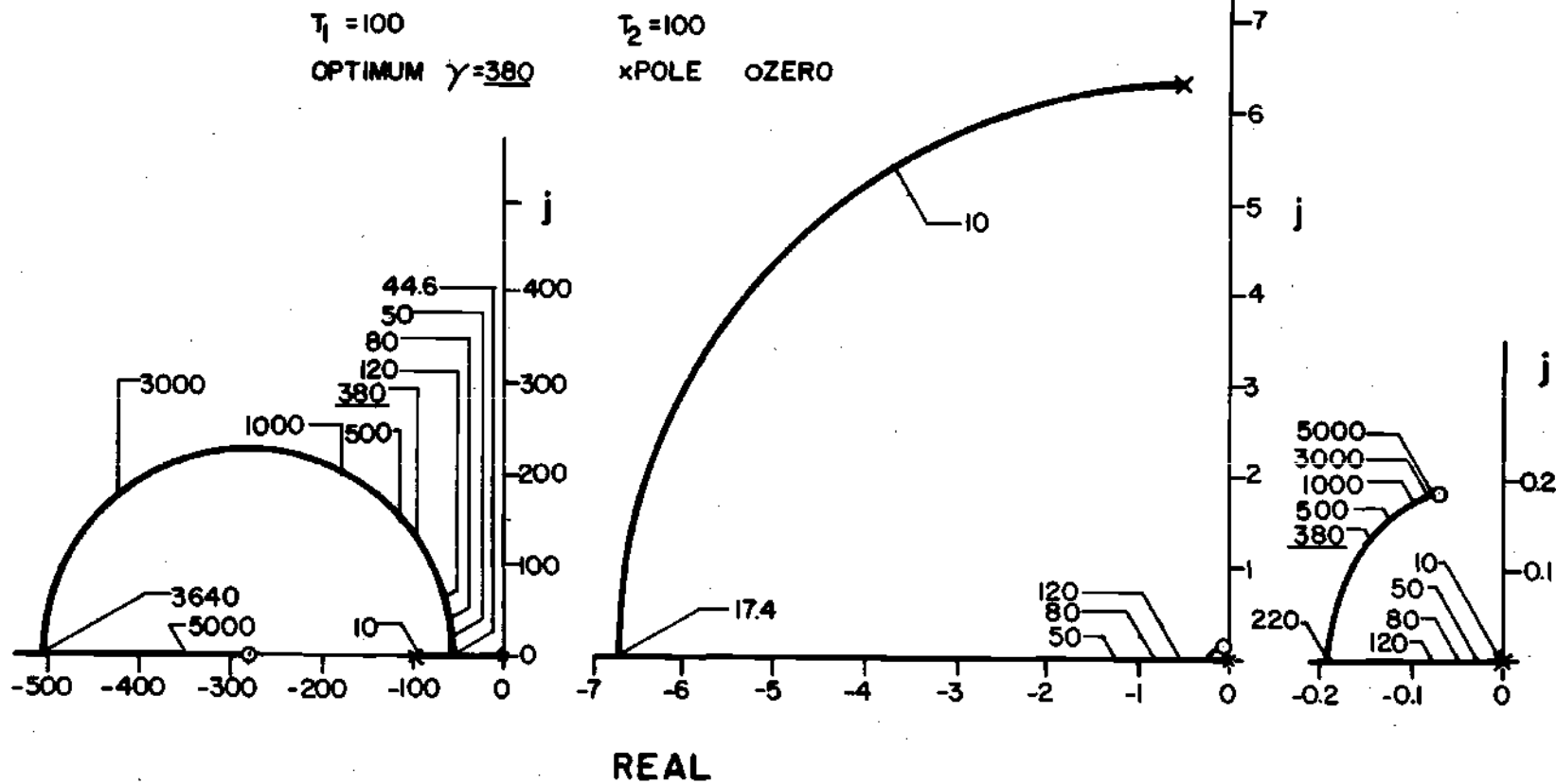


Figure 24. Root Locus for Optimum Values of the Parameters Plotted on Three Scales

Thus, if it is desired to have a frequency response which is not that of a critically damped servo vibrograph, the exact impulse response can be controlled by selecting a suitable location on one of the root loci. For the linear system it can be assumed that the system will be stable for any positive value of all the parameters that might be selected by any design criteria.

## CHAPTER III

### EXPERIMENTAL INVESTIGATION

#### General Procedure

In order to test the theory of the servo torsional vibrograph a prototype was built to verify the basic frequency response equations, check the impulse response, and to find the inherent problems of such a device. In order to test the frequency response of the instrument a sine wave of varying frequency and amplitude was fed into the base of the vibrograph. Several different values of the gains and the tachometer feedback were tried to check the response at different points. The input vibration and output of the vibrometer were plotted by means of a Sanborn two-channel recorder. The impulse response was obtained by tapping the inertial mass of the vibrograph and recording the resulting output.

#### Prototype Construction

The drawings (Figures 34, 35, and 36) show in detail the construction of the servo torsional vibrograph which is pictured in Figure 25. In Figures 37 and 38 the electrical detail drawings are presented.

All the component part numbers which are presented in parenthesis here are designated either on the detail drawings or in the parts list (Table 5). All of the rotary motion measurement for the servo vibrograph is made by means of linear variable differential transformers (LVDT). LVDT (1) measures the relative motion between the vibrometer

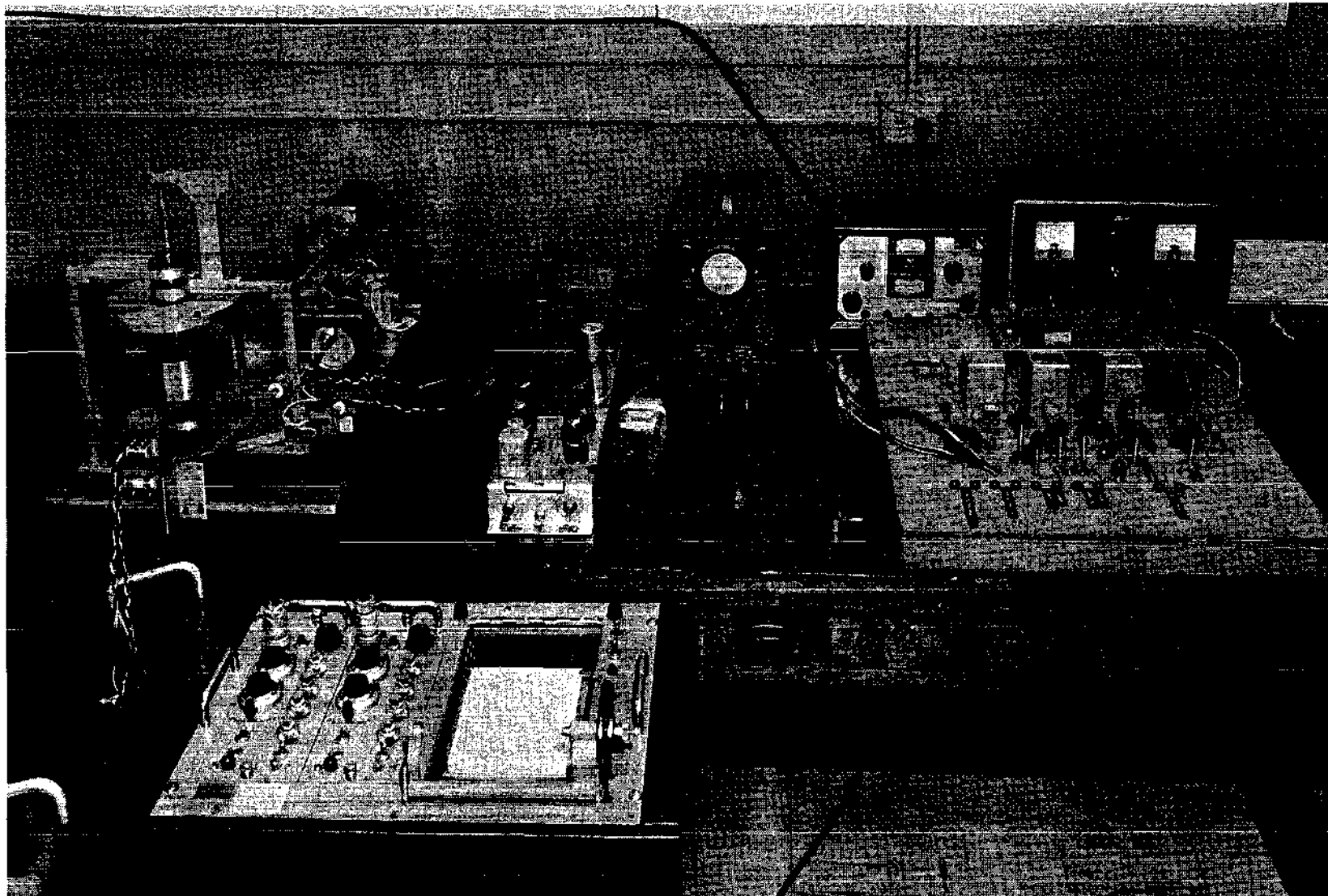


Figure 25. Prototype of the Servo Torsional Vibrograph

base (9) and the inertial mass (14), and LVDT (2) measures the relative motion between the ground plate (15) and the vibrometer base (9). The output of the first is proportional to the output (Z) and that of the second is proportional to the input (X). LVDT (1) and LVDT (2) are independently excited by means of Sanborn recorder preamplifiers and their output is fed to a two-channel Sanborn recorder (31).

The input voltages for the alpha and beta amplification networks are supplied from LVDT (4) and LVDT (3), respectively. Both are excited by means of a signal generator (28) - amplifier (Figure 36) combination at a frequency of nine kilocycles.

The output of LVDT (3) is proportional to the relative motion between the vibrometer base (9) and the spring base (5) and serves to provide a stable null position for the vibrograph. The output of LVDT (4) is proportional to the relative motion between the inertial mass (14) and the spring base (5) and provides the basis for the natural frequency reduction of the servo vibrograph.

The alpha and beta amplifiers (Figure 37) are identical and both have a maximum gain of approximately 5000. From the output transformers of the alpha and beta amplifiers, the two signals are demodulated and then subtracted (i.e., alpha - beta). The filament and plate voltages are obtained from a separate power supply (29).

The D. C. voltage is then fed into the Link servo amplifier (30) which in turn drives the servo motor that is mounted on the vibrograph base (9). The servo motor drives a tachometer generator (22) and a gearbox (19). The voltage from the tachometer is fed back to the second

stage of the servo amplifier. From the gear box the rotary motion is transmitted through a bellows coupling (18) to a micrometer head (16) which converts the rotary motion to a translation of small amplitude. The micrometer motion is transferred to the spring base (5) which rotates about the vibrograph centerline. Attached to the spring base is the torsional spring (6) which transmits the motion of the base to the inertial mass.

All pivots within the vibrograph are precision ball bearings in order to reduce coulomb friction. The weight of the inertial mass is carried by the torsional spring with a provision at the bottom of the center shaft to carry some of the weight by means of a single ball bearing. Since the vibrometer base is cantilevered from the center shaft an additional support is provided by means of a level concentric ball bearing race (12). In order to insure that the vibrometer would not be affected by small misalignments of the base, the inertial mass is balanced by means of the weight (10); leveling screws are also provided (13).

It should be noted that the inertial mass cage, the servo motor support, and the support of LVDT (1) and LVDT (2) are an integral part of the base (9). All LVDT core elements are mounted in such a way that centering and aligning can be accomplished without difficulty.

The input vibration is supplied by means of a nonconcentric circular cam (23) which applies an approximate sine wave to the base of the vibrograph. The cam is propelled by means of a variable speed motor (26) whose speed is reduced by the gearbox (20). In order to isolate the vibrations of the separate gearbox-motor assembly, the motion is

transferred from the assembly to the circular cam by means of a shaft and a set of universal joints (25).

The ground plate (15) is 20-1/4 inches long by 14-1/2 inches wide. The total height of the instrument is 15-3/4 inches and the distance from the instrument's centerline to the centerline of the micrometer-servo motor assembly is 5-3/4 inches.

#### Operation and Design Refinement

In order to keep the servo system at its null position the beta gain has to be set high enough to overcome the drift in the components. Due to the mechanical and electrical drift in the alpha circuit for these particular components, a relatively high value of the beta gain is required (5 to 10). In the experimental model it was necessary to put limit switches on the spring base in order to keep it within the mechanical limits imposed by the bellows coupling (18) and the spring holder (12). The limit switches (not shown) shut off the input voltage when actuated.

The LVDT's have a large dead zone and, at high gains and no input, a high frequency chatter occurred about the null point. This chatter does not affect the output since it is of too high a frequency to actuate the inertial mass. The amplitude of the chatter could be decreased and the frequency increased by the addition of a small amount of tachometer feedback.

The original design featured a spring which was cantilevered from the side of the spring base (5) and fixed to the center shaft. The shaft was supported entirely by the single ball bearing at the bottom of the

central shaft. The cantilevered spring arrangement was not used in the final design because of high friction, spring end support difficulties and high natural frequency. It was replaced by a torsional spring which in addition to supplying a wider range of natural periods, also furnished a support for the mass which was almost frictionless.

The input motor when mounted directly on the ground plate produced comparatively high transverse vibrations in LVDT core mounts. Since the output from the LVDT's were affected by this vibration, it was found necessary to separate the motor-gear box assembly by means of universal joints (25). In order to further isolate the vibrograph from extraneous vibrations, all contact points with the ground are isolated by means of foam rubber.

When the LVDT's are at their null point they do not produce zero A.C. voltage. In order to smooth out the voltage at the null point a variable resistor was added in the circuit before the input of the alpha and beta amplifiers. The center tap voltage of the LVDT is applied to the resistor's variable tap (Figure 37), and the output voltage signal is smoothed by viewing it on an oscilloscope. The second and third variable resistors (left to right in Figure 37) are for gain adjustment.

The demodulator provides phase-sensitive half phase rectification of the A.C. alpha and beta amplifier outputs. The variable resistors in these circuits are for balancing the demodulators.

### Experimental Procedure

#### Frequency Response Tests

At each selected value of the parameters the input vibration was

varied in frequency from the maximum motor speed to the minimum. The frequency was varied in steps and the transient vibrations were allowed to damp out by means of the internal damping of the basic vibrograph and the damping caused by the servo system. After the sinusoidal vibration had reached the steady state condition, the recorder was turned on and the input and output motion was recorded on the Sanborn recorder at a suitable rate of paper feed. An attempt was made to obtain a wide range of values for the output and to test the servo vibrograph until the input frequency was below the natural frequency of the servo system.

In order to set the gains of the alpha and beta amplifiers, the inertial mass is clamped so that it can not move in relation to the ground plate. The micrometer (16) is used to supply an accurate graduated motion for the calibration. The following is the procedure for setting the gain for either the alpha or beta amplifiers.

1. Adjust the demodulator and LVDT voltage supplies at their highest unsaturated value.
2. With alpha and beta amplifiers turned off, null the demodulator output.
3. Turn on either the alpha or beta amplifier.
4. Move the micrometer a small number of thousandths of an inch and convert this to radians.
5. Adjust the variable resistors to obtain the desired D.C. output; always making sure by means of an oscilloscope that the amplifiers are not saturated.

The gain as adjusted above is thus a combination of the LVDT and the amplifier transfer functions. By themselves the LVDT's have a con-

stant transfer function of about 80 volts/radian and thus, to simplify calculations, a constant transfer function of 100 volts/radian is assumed in the overall LVDT-amplifier transfer function. Thus the transfer function as measured is a combination of the LVDT's, the A.C. amplifiers, and the demodulators (i.e., D.C. volts/radian).

Since the amplitude of the output is not of specific interest, only the relative magnitude of the input and output need be considered. With the input amplitude set at a constant value and the inertial mass clamped, the output motion and input motion as measured by the two LVDT's, (1) and (2), are identical. Thus if the two amplitudes were equalized by means of adjustments on the Sanborn recorders, the relative magnitude would be correctly calibrated. The input frequency is determined by referring to a time reference scale on the Sanborn recorder.

In order to calibrate the A.C. tachometer feedback, it was necessary to get its equivalent D.C. input voltage. The method used consisted of first finding the D.C. input voltage-speed curve for the servo amplifier-motor combination by itself and then with tachometer feedback added. At any set speed the input voltage with and without tachometer feedback could be ascertained, and if subtracted, yield the tachometer feedback voltage at that speed. The quotient of the feedback voltage and the speed is the tachometer constant.

In order to find the damping constant  $C_1$  the logarithmic decrement is used as in the following equations:

$$\delta = \log_e \frac{x_{n+1}}{x_n} \quad (37)$$

$$C_1 = \frac{C'}{J} = \frac{2\omega_n \delta}{\sqrt{4\pi^2 + \delta^2}} \quad (38)$$

$$\omega_{nd} = \sqrt{\omega_n^2 - \frac{1}{4} \left(\frac{C'}{J}\right)^2} \quad (39)$$

where,

$\delta$  = Logarithmic decrement.

$\omega_n$  = Natural frequency of the basic vibrograph.

$\omega_{nd}$  = Natural damped frequency of the basic vibrograph.

$C'$  = Damping constant.

$C_1$  = Damping constant as used in servo vibrograph equations.

$J$  = Moment of inertia of the mass.

$X_n$  = Amplitude of the n-th cycle.

In order to find the natural frequency and the logarithmic decrement, the vibrograph is set into motion and the damped vibration is recorded. The natural damped frequency is assumed equal to the natural frequency, and the logarithmic decrement and the damping constant  $C_1$  are determined, Equation (37) and (38), respectively. Then the natural damped frequency is checked by means of Equation (39).

The circular cam assembly has a provision for adjusting the amplitude of the input motion. The minimum amplitude is 0.0155 degrees and the maximum is about 0.65 degrees. Since only low amplitude vibrations are of interest and at high amplitudes the amplifiers will saturate, only the lower range of possible amplitudes were used in the frequency response tests.

### Transient Tests

In place of an impulse response test, a tapping test was used to test the transient response of the servo vibrograph. For an impulse (unity) response, the amplitude would be such that all the amplifiers would be saturated and the recorder would be off scale (Figure 31). Since saturated amplifiers are nonlinear, the impulse response during the first instant of time would not be as predicted by the linear model. Since the components which cause these large amplitude initial vibrations die out in a very short time, only the more important longer lasting vibrations due to the roots with smaller damping need be considered. The remaining root's impulse response generates a simple damped sine wave. In order to compare the theoretical wave to the response of the instrument, the tapping test was used. The tapping test generates the predominant damped sine wave while keeping the danger of saturation to a minimum. The tapping test consists simply of tapping the inertial mass in such a way that the amplitude is low enough to keep all components in the linear range, and recording the resultant damped vibration. The amplitude of the theoretical damped vibration is calculated by the Equations (35) and (36) on the electronic computer. The theoretical curve and the response curve of the instrument are normalized so that they can be compared.

### Frequency Response Characteristics

In the tests of the frequency response of the servo vibrograph the value of the amplitude ratio ( $Z/X$ ) was obtained for a wide range of the parameters. The phase angle could not be obtained accurately

because of its rapidly changing value in a narrow frequency range (Figure 6). Figures 27 through 30 show the frequency response of the prototype together with the theoretical response for several values of the parameters. These figures are representative of the results of all the frequency response tests run on the servo vibrograph.

For low values of the amplitude ratio ( $Z/X$ ), the agreement of the experimental and theoretical response curves is very good. As the input frequency approaches the natural frequency of the servo system, the response of the instrument generally departs from the theoretical curve.

The nonlinearities in the system cause the divergence from the theoretical. The most predominant cause of this divergence is the saturation of the gamma amplifier. At high values of alpha gain (Figure 30) and at frequencies near the natural frequency of the servo vibrograph the input into the gamma amplifier is above the saturation voltage of this particular servo amplifier. When the alpha gain is set at a high enough value to saturate the gamma amplifier at frequencies higher than the natural frequency, a second apparent natural frequency results at a frequency of about two cycles/sec (Figure 30).

The LVDT's had several nonlinearities which affected the response of the system. The lack of response at frequencies below the natural frequency was caused by the dead zone in the LVDT's and the small relative motion between the spring base and the inertial mass. The chatter which was caused by the LVDT dead zone was only evident at frequencies below the natural frequency. The LVDT's also indirectly caused saturation of the alpha amplifier prematurely because of their large residual A.C. voltage at the null point. A small amount of tachometer feedback

tended to inhibit the overloading of the gamma amplifier and also decreased the output's dependence on the chatter of the servo system.

The large amount of beta gain was needed to keep the vibrograph in its null position because of the drift in the alpha amplifier and LVDT. The drift increased with increases in the LVDT input voltage and with increases in alpha gain.

The action of the servo system is very small at high input frequencies and does not affect the output amplitude to any great extent. It does, however, increase the effective damping of the system and eliminates transients quickly. As the system approaches its natural frequency, the servo system displaces the spring base more radically, and the output motion becomes more dependent on the servo action and less on the relative motion of the inertial mass. Thus, at low frequencies below the natural frequency of the basic vibrograph, the principal output motion comes from the servo system.

When the frequency response has a high peak, the servo system tends to limit the experimental response to a lower value than the theoretical as the amplifiers saturate. In the device which is to be used in practice this amplitude limiting feature would be of great value, since it would limit the servo action if an unexpected long period vibration should occur.

The maximum amplitude which the instrument can measure is dependent on the saturation point of the amplifiers and the frequency of the input. The experimental data was all collected at amplitudes near the minimum available input amplitude (0.0155 degrees) in order

to decrease the possibility of saturating the gamma amplifier. At low values of the input amplitude the amplitude ratio ( $Z/X$ ) was constant for equal values of the parameters and different  $Z$  and  $X$  values at the same frequency. The limiting factor to the lowest amplitude vibration which could be measured is the dead zone in the LVDT's; this lower limit is approximately 0.001 degrees.

#### Transient Response Characteristics

The transient response of the servo vibrograph was tested by means of the tapping test. Typical results obtained from the tests are pictured in Figures 32 and 33. In order to compare the results, both the theoretical and experimental values were normalized by assigning one to the value of their first maximum and plotting the damped vibration relative to this point. The theoretical impulse response is presented in Figure 31 for several experimental values of the parameters.

The principal reason for the disagreement of the actual and theoretical curves is the nonlinearities in the system. In the transient test the relative motion between the mass and the spring base was of a greater amplitude than in the frequency response tests. Thus the possibility of saturation was much greater. The addition of tachometer feedback suppressed the saturation and also decreased the system's dependence on the servo system chatter. The chatter and saturation of the gamma amplifier have a pronounced effect on the transient response. As can be seen in Figures 32 and 33 with high gain or no tachometer feedback the natural damped frequency is less than predicted by the

theoretical and the damping is greater. For the tests in which the effective gains were smaller the agreement with the theoretical is very good.

## CHAPTER IV

## CONCLUSIONS AND SUGGESTIONS FOR FURTHER RESEARCH

Conclusions

The theoretical analysis of the servo torsional vibrograph made in this study demonstrated that the servo-augmented vibrograph does improve the response and decrease the natural frequency of a basic torsional vibrograph. For the ranges of the variables which were studied, natural frequency reduction of the order of 100 to 1000 could be obtained.

The frequency response characteristics were in general similar to those of a lightly damped vibrograph with a small maximum amplitude and a desirable phase angle characteristic.

In order to find the optimum value for the parameters with respect to the frequency response, the 10 per cent amplitude error (10%AME) frequency and the 10 per cent phase angle error (10%PHAE) frequency were found for a wide range of the parameters. Thus if the input frequency were above the two minimum required frequencies, the output response would closely duplicate the input vibration for both simple sine waves and superimposed sine waves. The variables which had the greatest effect on the frequency response of the servo vibrograph were the principal feedback amplifier gain ( $\alpha$ ), the null feedback amplifier gain ( $\beta$ ), the servo amplifier gain ( $\gamma$ ), and the tachometer constant ( $K_t$ ). The servo motor time constant ( $T_m$ ) and the damp-

ing of the basic vibrograph ( $C_1$ ) had a much smaller effect on the two frequency response characteristics.

For the optimum performance of the servo vibrograph the following values of the parameters are best:

1. The principal amplifier gain (alpha) should be at the highest value possible.
2. The null feedback amplifier gain (beta) should be at the smallest value which will produce a stable system.
3. The optimum value of the servo amplifier gain (gamma) is given by the following equation:

$$\gamma = \frac{12,000}{K_m \alpha^{1/2} \beta^{1/2}}$$

where the values of the LVDT transfer functions are assumed to be 100 volts/radian,  $\beta \geq 0.01$ , and  $\alpha > 50$ .

4. The tachometer constant should have a value high enough to dampen the inherent chatter of the system but should not exceed 0.005 volt/radian/sec.

5. The values of the servo time constant ( $T_m$ ) and the damping constant of the basic vibrograph ( $C_1$ ) should be set by the nature of the components since they have little effect on the frequency response.

The sensitivity function was analyzed in order to find the effect of the servo vibrograph of small unforeseen changes in the parameters. All the parameters except the natural frequency of the basic vibrograph were found not to affect the sensitivity with respect to amplitude.

(Z/X) to any great extent. The natural frequency can be set and maintained at a specified value and therefore its sensitivity is not important. For the sensitivity with respect to the 10 per cent amplitude error frequency, the null amplifier gain (beta) produced the greatest value excepting the natural frequency. The feedback network of the servo vibrograph decreases the sensitivity of all the parameters to an acceptable level.

If the vibration is expected to be of a periodic nature the transient response is of less importance than the frequency response. The optimum overall response for this case can be obtained by selecting the values for the parameters from the frequency response criteria and then checking the roots of the characteristic equation to insure that sufficient damping is present. If, however, the input vibration is expected to be aperiodic as in seismic work, then the servo vibrograph should be critically damped. In order to accomplish this damping, all the roots of the characteristic equation should be equal; expressions for the values of the parameters which would produce these equal roots are presented in Equations (32) and (33).

In order to determine the stability of the system and to find what effect the parameters had on the transient response, the root locus for many different values of the parameters was calculated. The system was found to be stable for all positive values of all the parameters.

The servo motor time constant ( $T_m$ ) had little effect on the root locus and the damping constant ( $C_1$ ) caused the transient terms to die out more quickly as could be expected. The tachometer feedback constant and the gains of the amplifiers have a pronounced effect on the dominant

transient terms. Their exact effect at any particular value of the parameters has to be determined from the roots of the characteristic equation. These roots and the shape, zeros, poles, and breakaway points change position to such a great extent with small changes in the parameters that no general rule can be derived for determining the effect of the more important parameters on the transient behavior of the system. For the optimum values found in the frequency response study, the impulse response of the system is a long-period damped sine wave and has only one dominant term:

The experimental portion of the investigation was carried out to prove that the mathematical expressions for the frequency response and impulse response were valid and to discover what problems would arise in the prototype of the servo torsional vibrograph. The mathematical model was proved by the experimental investigation to be accurate for all cases in which the components of the system remained in their linear range. Generally the components remained linear at low input and output amplitudes and at gains that were less than the maximum.

The experimental and analytical investigation proved that the servo torsional vibrograph will measure vibrations of long period and low amplitude. Using the principles discussed in this work, a practical model of the servo vibrograph could be produced which would be compact, light in weight and produce an output signal proportional to the vibration to be measured. Its output could easily be utilized by any servo system to control large rotary machinery and thereby increase the accuracy of the finished product from that machine. It is ideally suited for the measurement of very low to moderately high frequency

oscillations of small amplitude.

#### Suggestions for Further Research

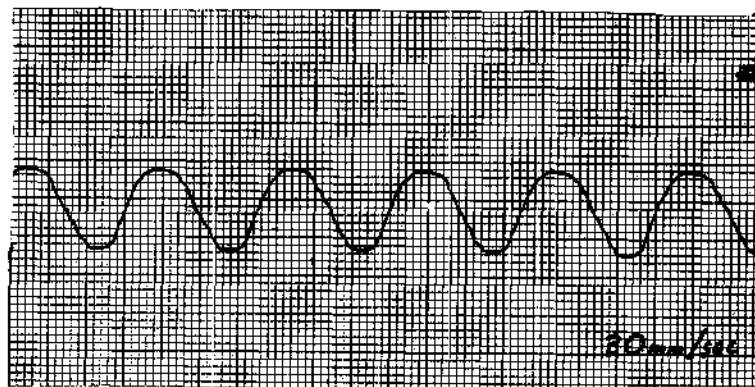
Further research should be directed toward the evolution of a practical design and the utilization of the servo torsional vibrograph. The first reasonable extension of this work would be the inclusion of design refinements into a second generation servo vibrograph which would be of more compact shape, and be of more rugged, foolproof construction. After the practical model of the servo vibrograph has been developed, the next step in the research would be in the application of the vibrograph to its practical uses. The design and implementation of the servo systems necessary to utilize the potential of the servo vibrograph would culminate the research.

Specific design modification suggestions appear in the Appendix (Appendix C).

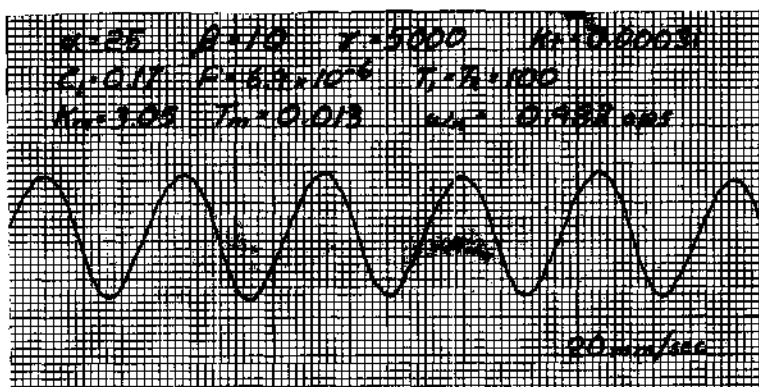
APPENDIX

APPENDIX A

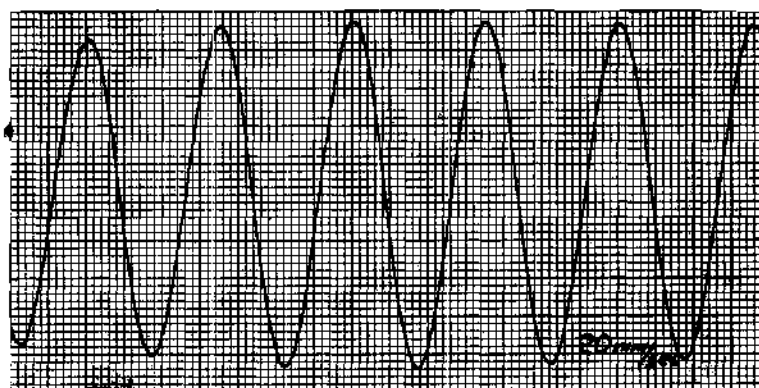
EXPERIMENTAL DATA



Input Signal



Output with Servo System



Output without Servo System

Figure 26. Sample Output of the Servo Vibrograph

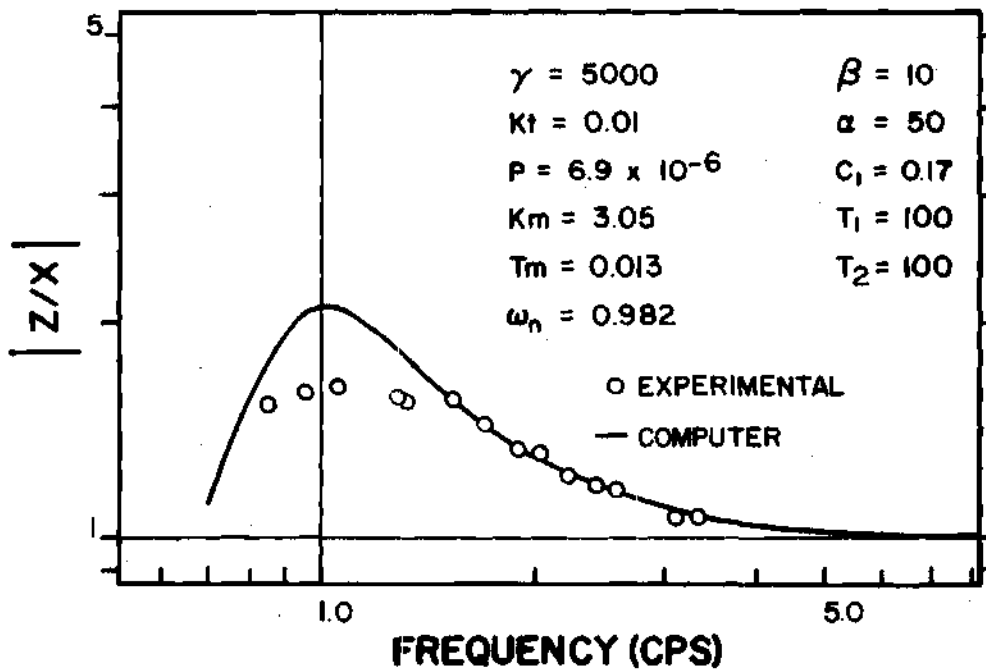
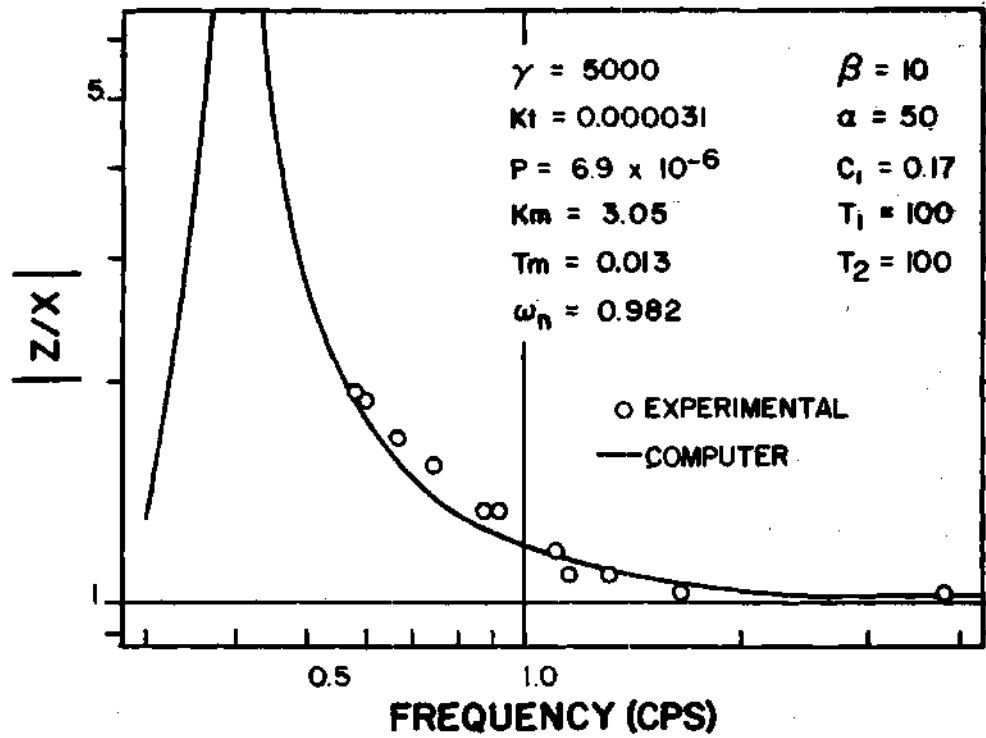


Figure 27. Frequency Response of the Servo Vibrograph

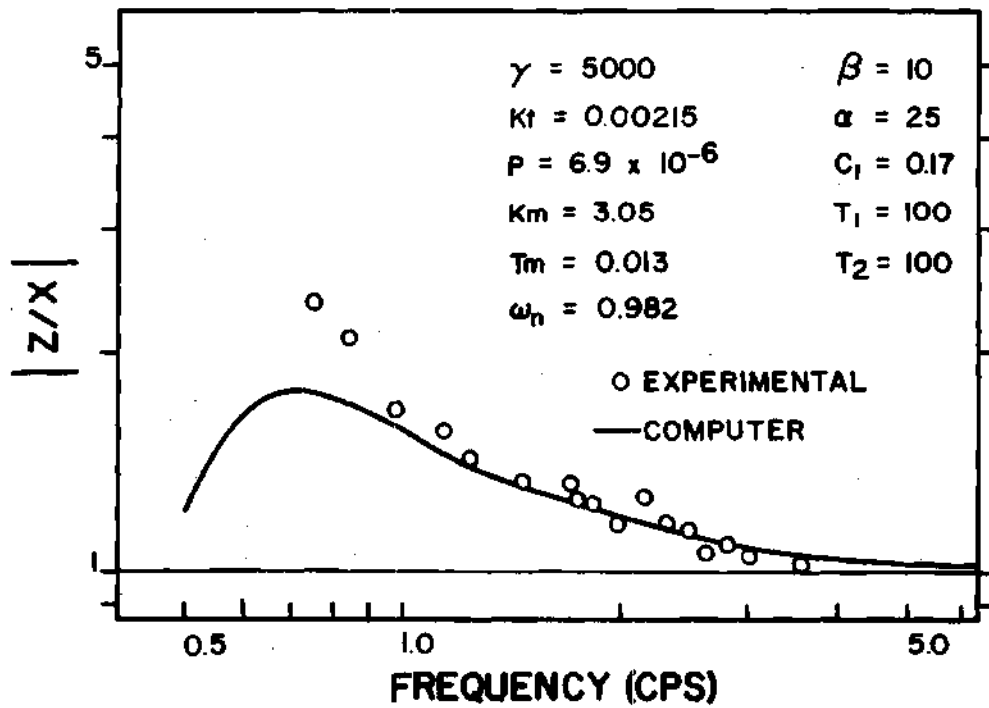
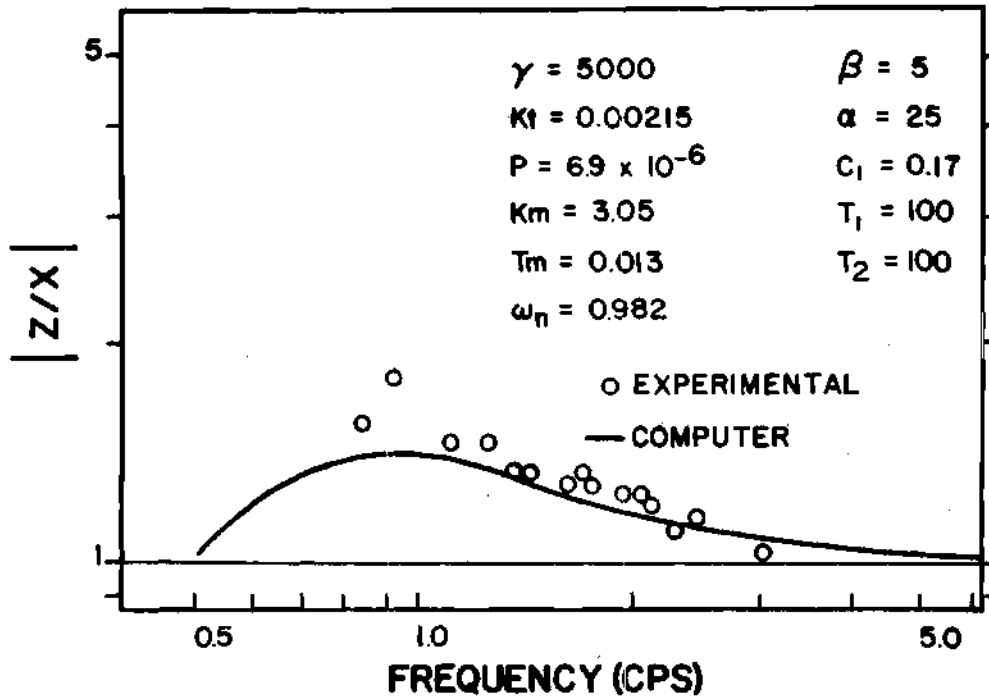


Figure 28. Frequency Response of the Servo Vibrograph

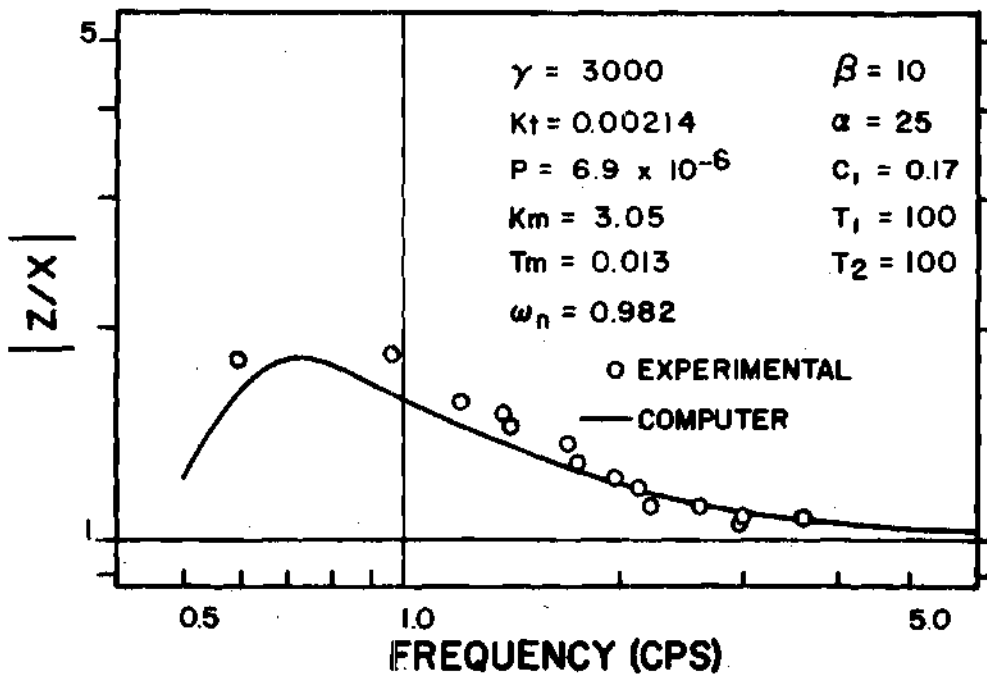
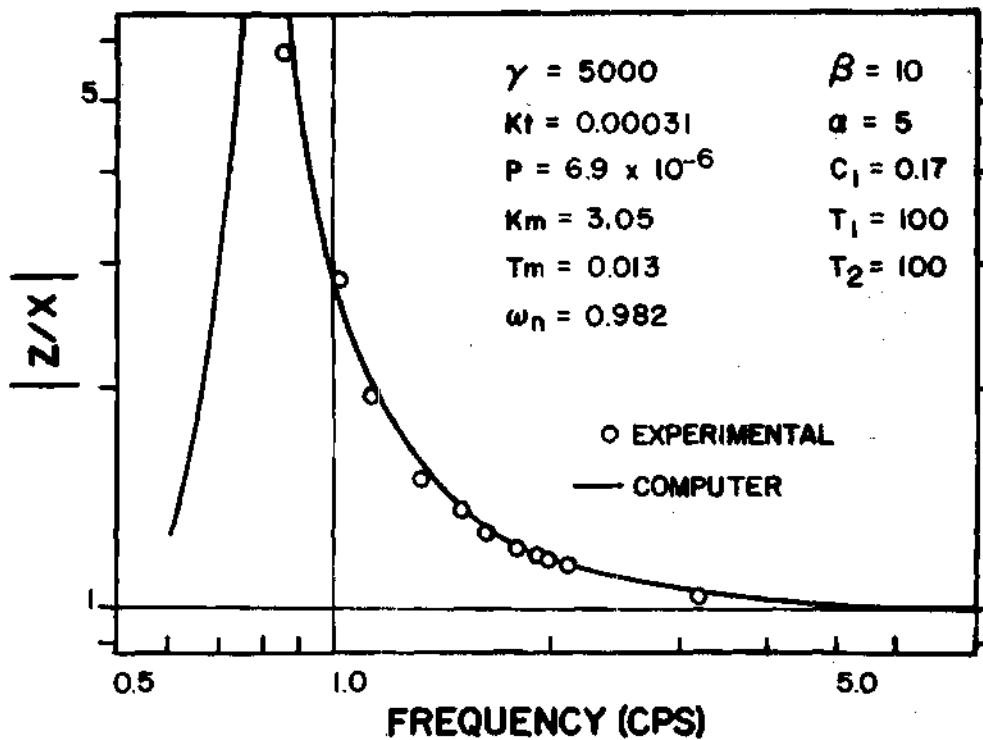


Figure 29. Frequency Response of the Servo Vibrograph

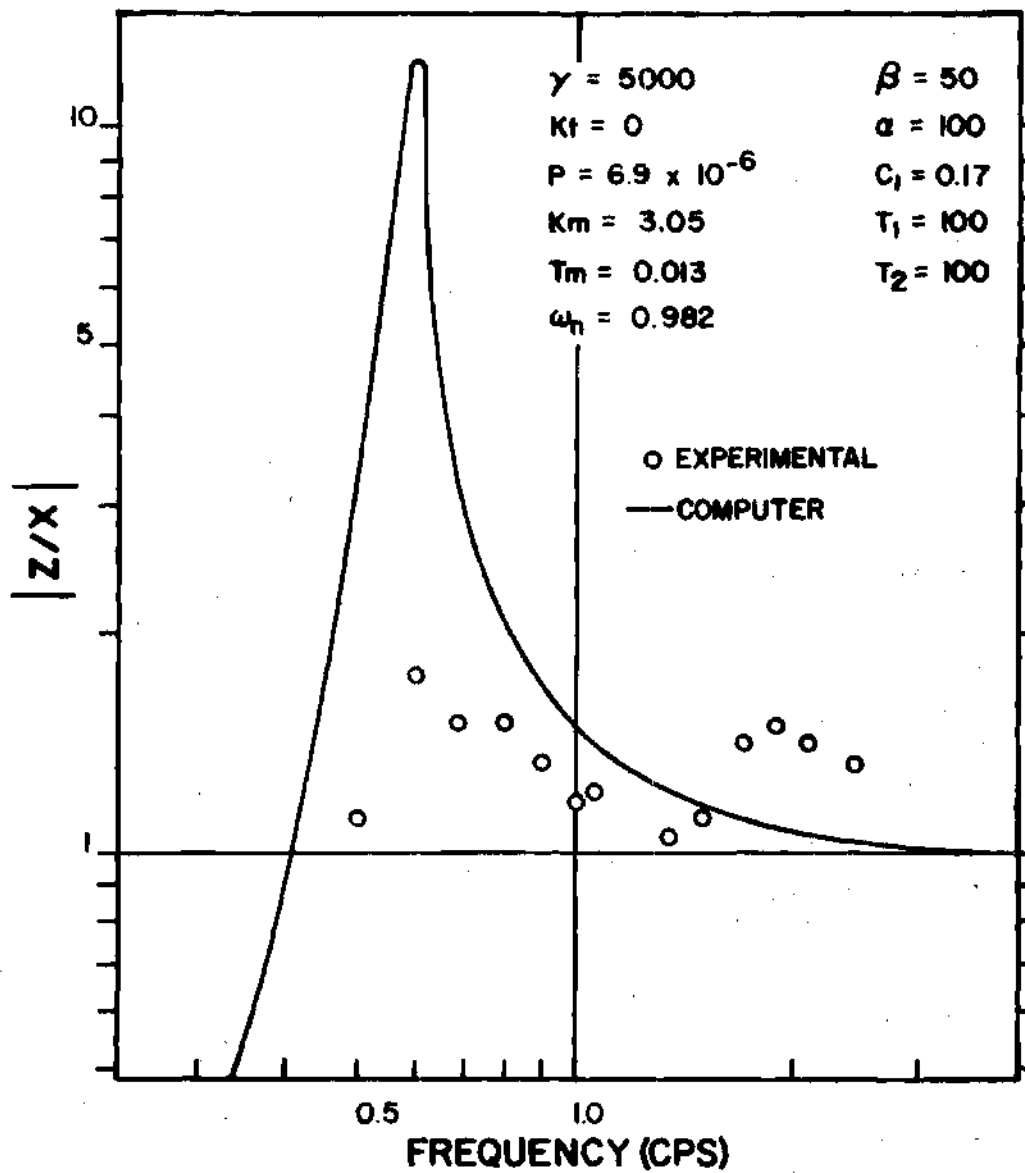


Figure 30. Frequency Response with Saturated Amplifiers

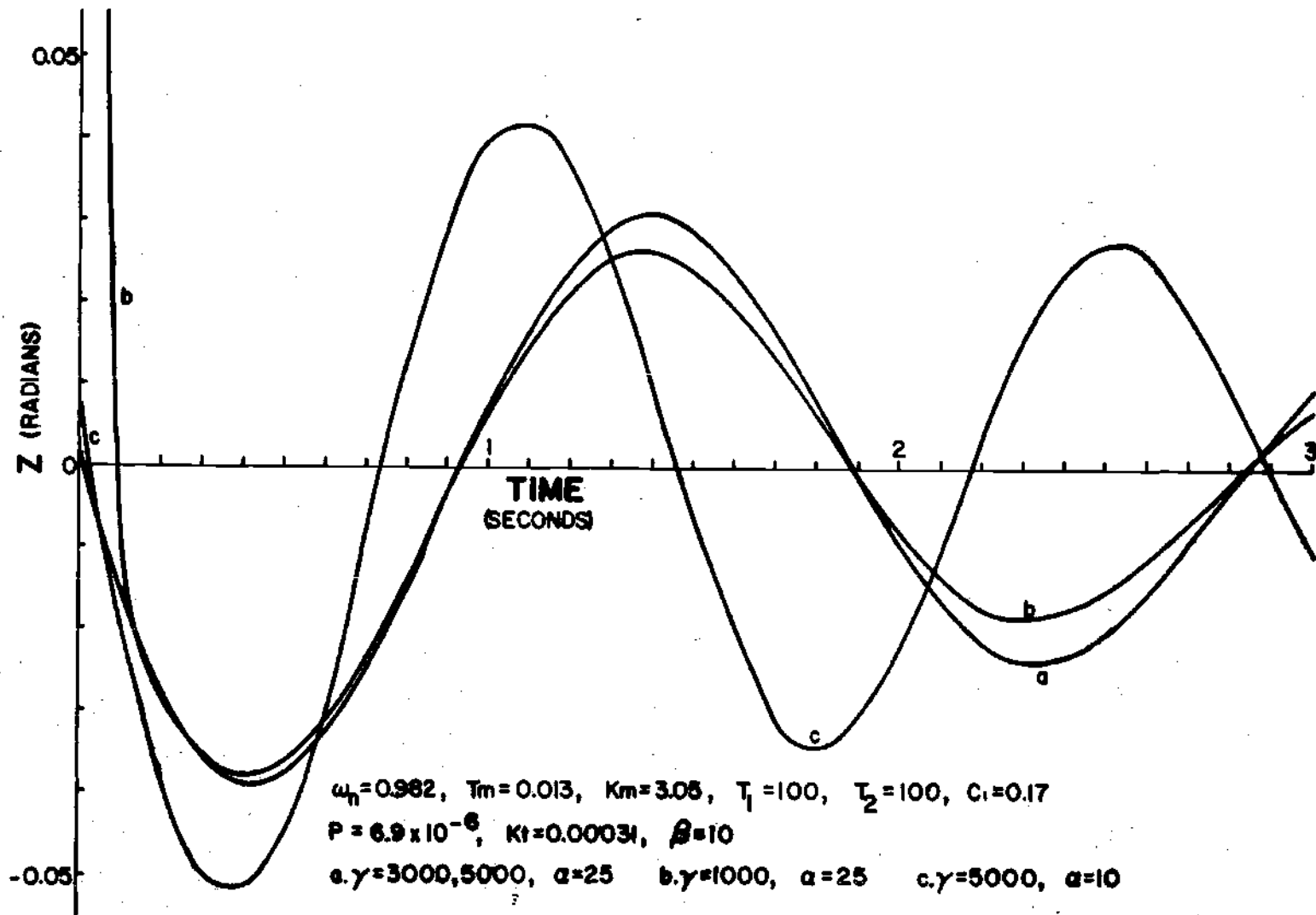


Figure 31. Theoretical Response of the Servo Vibrograph to a Unit Impulse

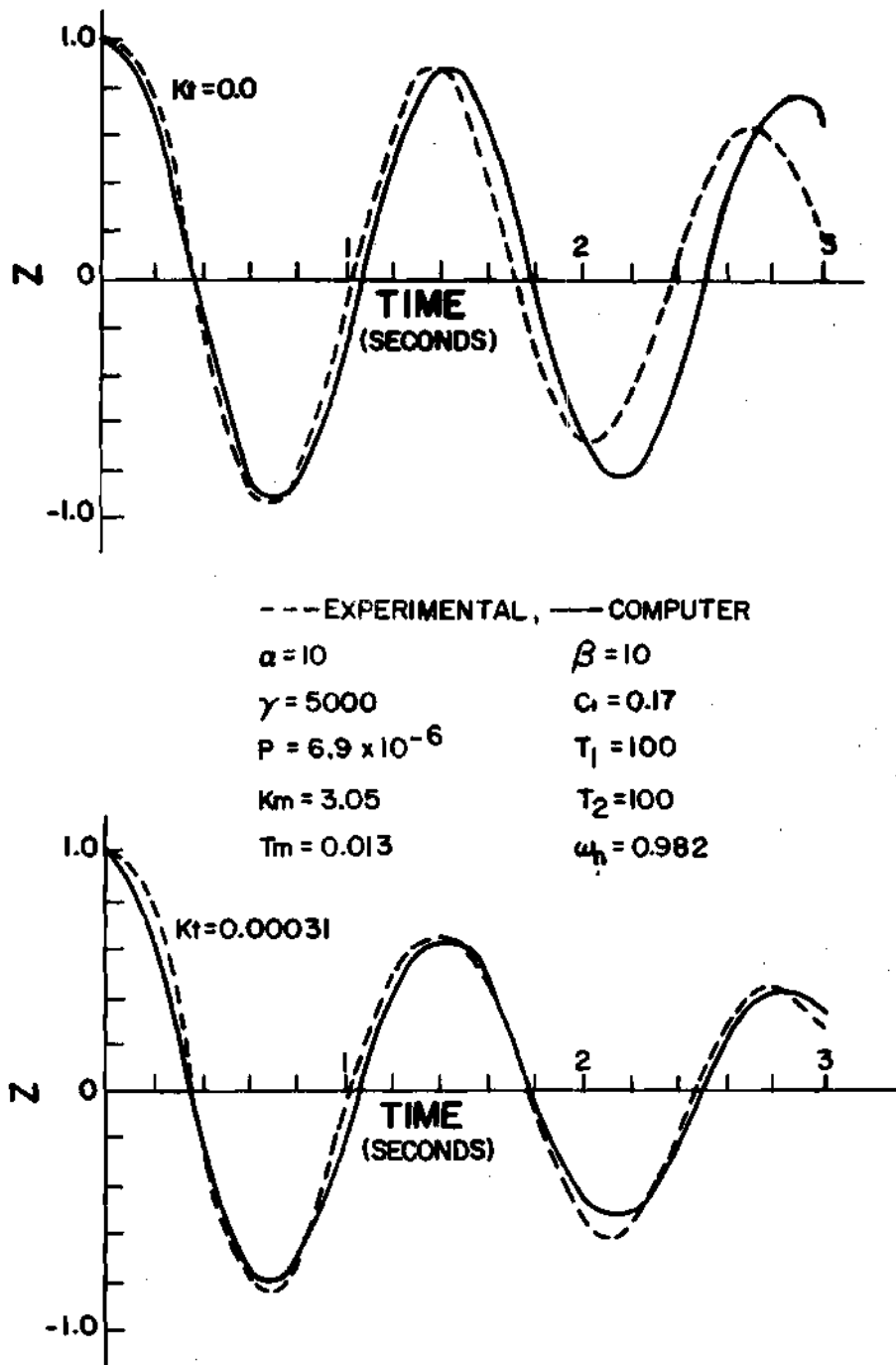
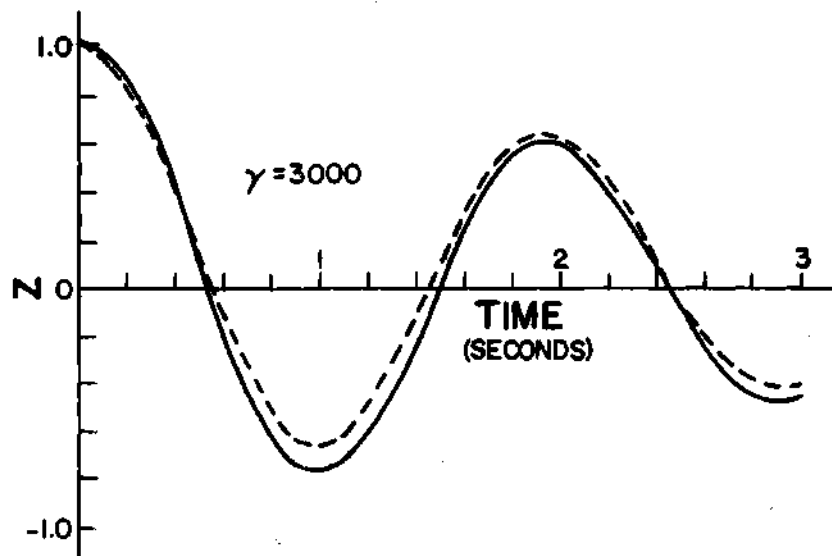


Figure 32. Transient Response of the Servo Vibrograph



--- EXPERIMENTAL, — COMPUTER

$$\alpha = 25$$

$$\beta = 10$$

$$K = 0.00031$$

$$C_1 = 0.17$$

$$P = 6.9 \times 10^{-6}$$

$$T_1 = 100$$

$$K_m = 3.05$$

$$T_2 = 100$$

$$T_m = 0.013$$

$$\omega_n = 0.982$$

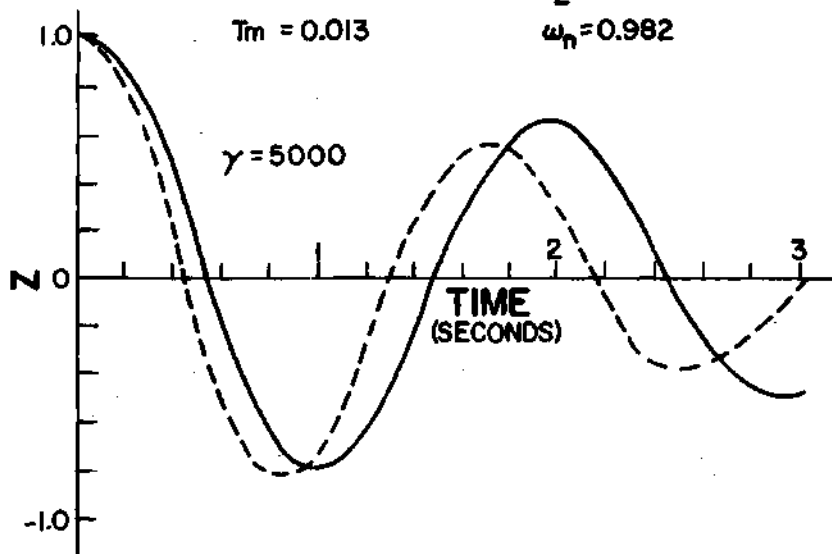


Figure 33. Transient Response of the Servo Vibrograph

APPENDIX B  
PROTOTYPE CONSTRUCTION

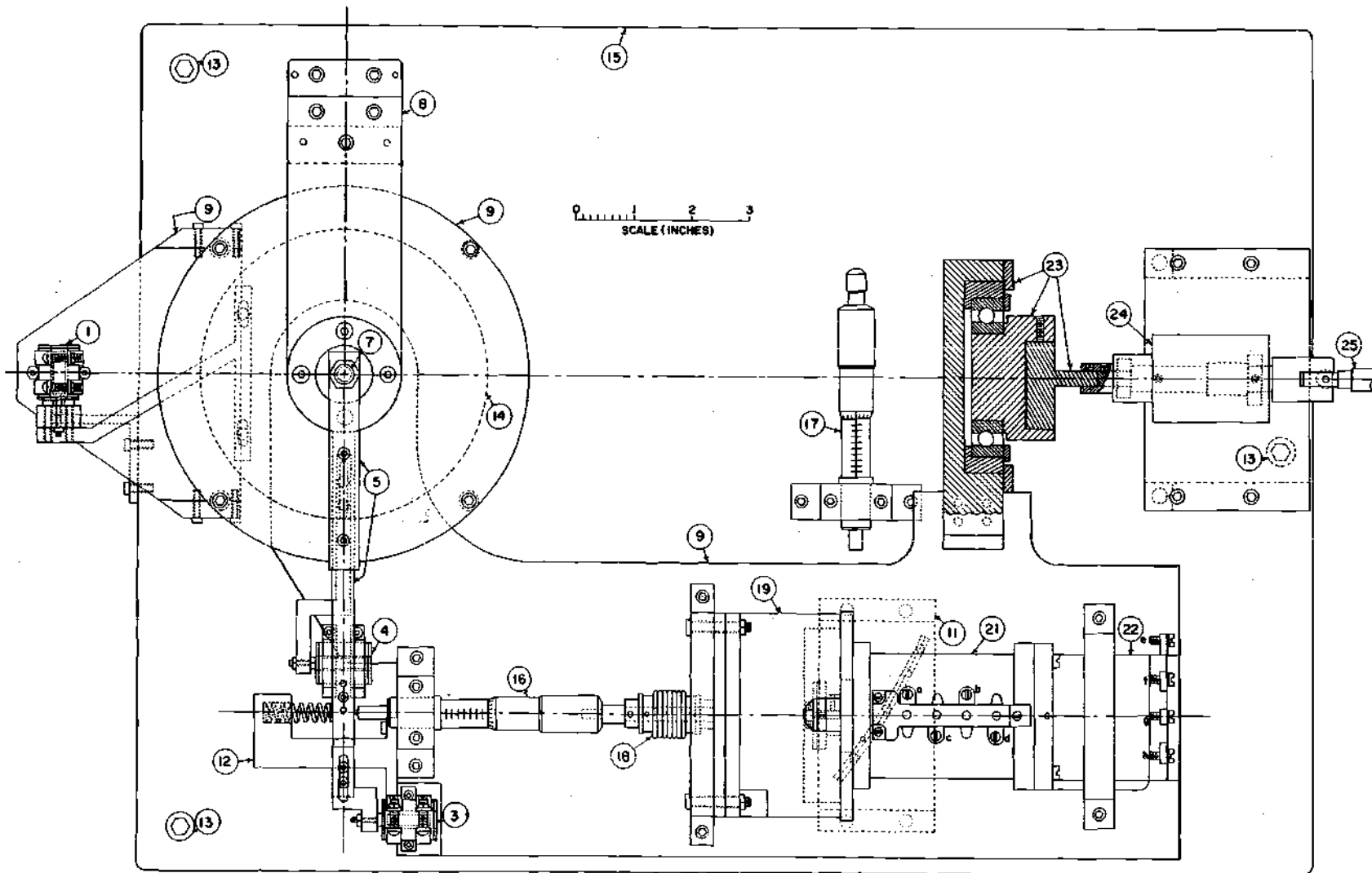


Figure 34. Top View of the Servo Torsional Vibrograph Prototype

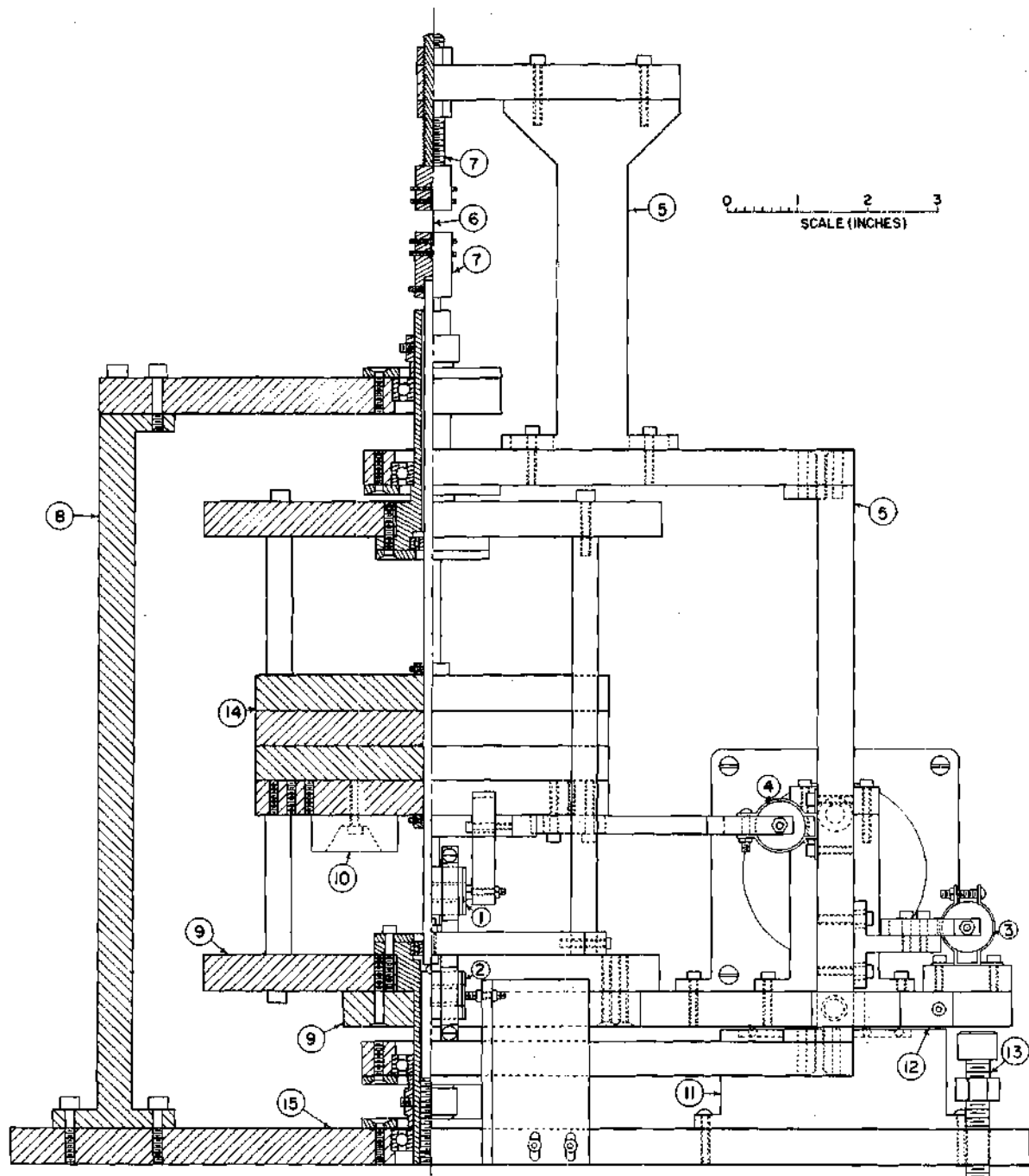
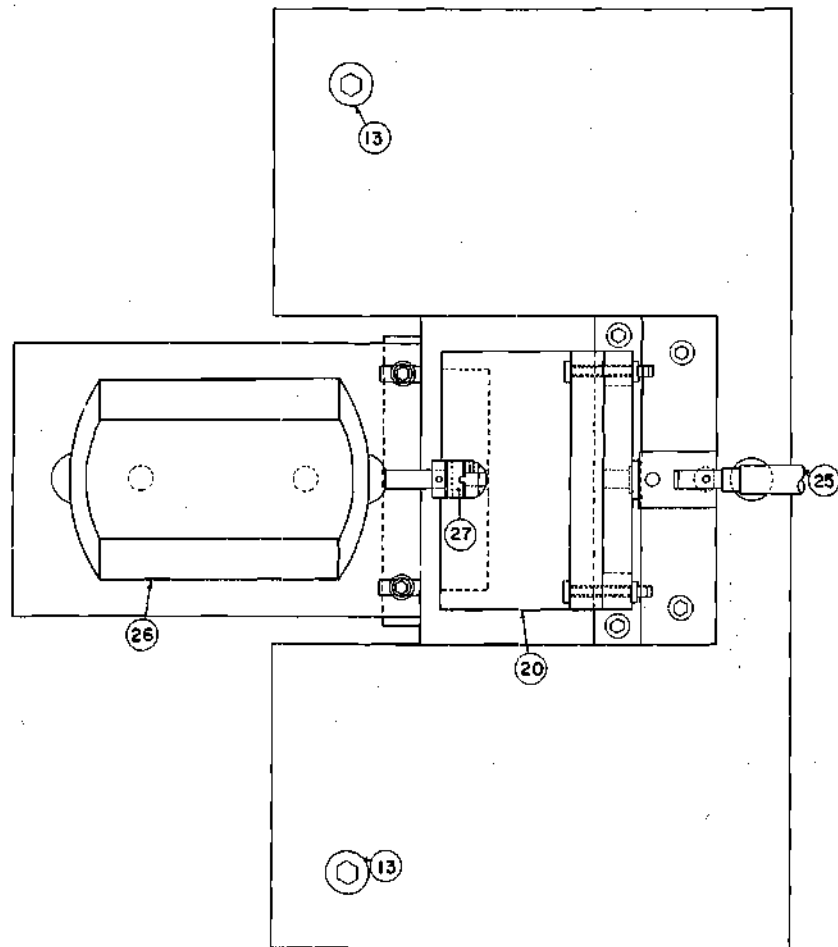


Figure 35. Front View of the Servo Torsional Vibrograph Prototype



0 1 2 3  
SCALE (INCHES)

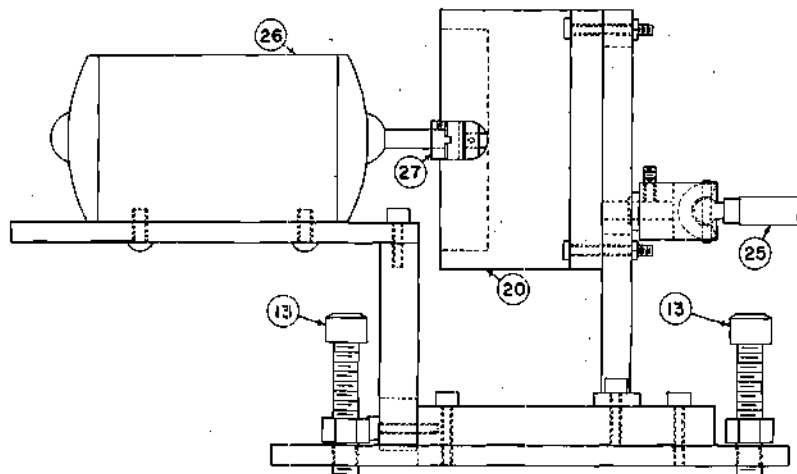


Figure 36. Driving Motor and Gear Box  
for the Sine Generator

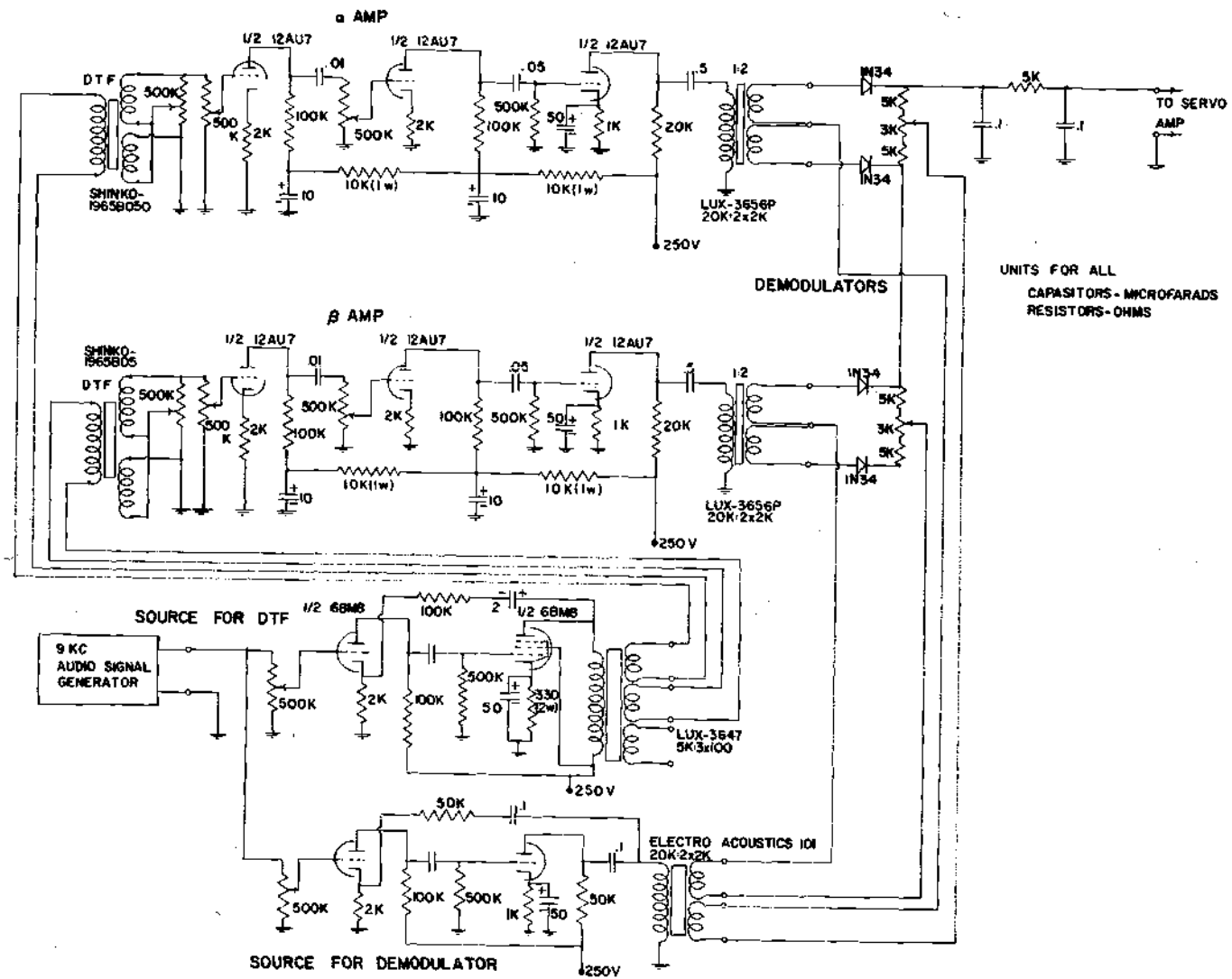


Figure 37. Amplifiers for the Servo Vibrograph



Table 5. Parts List

- 
1. Output linear differential transformer (LVDT), Shinko Electronics (Japan), Type 24L-L, No. 1965B05.
  2. Input LVDT, Shinko Electronics, Type 24L-L, No. 1965B050.
  3. Beta LVDT, Shinko Electronics, Type 24L-L, No. 1965B05.
  4. Alpha LVDT, Shinko Electronics, Type 24L-L, No. 1965B050.
  5. Spring Base, aluminum.
  6. Spring, piano wire.
  7. Spring holder, brass.
  8. Main Support, aluminum.
  9. Vibrometer base, aluminum.
  10. Balancing weight for inertial mass, brass.
  11. Vibrometer base ball bearing support, aluminum.
  12. Spring base spring holder, aluminum.
  13. Leveling screws.
  14. Inertial mass, four stainless steel disks.
  15. Ground plate, aluminum.
  16. Micrometer drive, Starrett, No. 263R micrometer head, 0-1 inch.
  17. Micrometer for determination of input amplitude, Starrett, No. 263R micrometer head, 0-1 inch.
  18. Bellows coupling, PIC Design Corp., No. T1-3.
  19. Servo motor gear box, Link Aviation Inc., Ratio-100:1, Part No. 88059, Serial No. 1-16918.
  20. Input gear box, Link Aviation Inc., Ratio-75:1, Part No. 88055, Serial No. 1-16258.

Table 5. Parts List (Continued)

- 
21. Servo motor, Kollsman Inc., Type 890F-0160230, 115 volts, 60 cycle, 2 phase, 2 pole, 3350 RPM, Stall torque-6.7 oz.in., Rotor Moment of Inertia-17.5 gram cm<sup>2</sup>.
  22. Tachometer generator, Kollsman Inc., Type 890F-0160230, Input Volts-32, Output-3.0 volts/1000 RPM.
  23. Sine cam, steel and aluminum.
  24. Sine cam support, magnesium and steel.
  25. Universal joints and connecting shaft.
  26. Input drive motor, Dayton Motor Co., A.C.-D.C. series motor, 115 volts, Model 2M034, 1/15 H.P., 5000 RPM.
  27. Oldham coupling.
  28. Signal generator, RCA audio signal generator, Type WA-44B.
  29. Power supply, Heathkit regulated power supply, Model 1P-32.
  30. Servo amplifier, Servo Systems Co., Model No. M-116, Serial No. 347, 115 volts, 60 cycle, Gain-5000 with 80 mv. input, A.C. or D.C. input.
  31. Sanborn preamplifiers and recorder; Preamplifiers, Model 350-1100B Carrier Preamplifier, Recorder, Model 296.
  32. Motor speed regulator, Seco Vari-Volt, Model 806, Seco Vari-Volt, Model 806, Seco Electronics, 1000 watts.
-

## APPENDIX C

## SUGGESTED DESIGN MODIFICATIONS

The more important design modifications are listed below:

1. In order to eliminate the mechanical constraints on the spring base the micrometer should be eliminated and in its place a high ratio worm gear should be substituted.
2. In order to decrease the possibility of the saturation of the servo amplifier and still maintain a high gain, the gain should be reduced and the gear ratio decreased. This change should be accomplished in conjunction with the worm gear modification.
3. In order to decrease the system's size and to lessen the effect of translational vibrations on the system the linear variable differential transformers should be replaced with rotary differential transformers mounted on the central shaft. The rotary differential transformers should have the smallest dead zone practicable.
4. The principal feedback amplifier (alpha) should have its overall gain increased in order to get large decreases in the natural frequency.

## APPENDIX D

## SENSITIVITY ANALYSIS USING SENSITIVITY FUNCTION

In order to investigate the servo vibrograph's response to small unexpected changes in the system parameters the sensitivity function was employed. The sensitivity expresses the ratio of the percentage variation in some specific quantity to the percentage variation in one of the system parameters. It may be defined mathematically as

$$S_K^M = \frac{dM/M}{dK/K} = \frac{dM \cdot K}{dK \cdot M}$$

where,

M = the system characteristic,

K = the specified parameter.

For the transfer function of the servo vibrograph the sensitivity function can be calculated for each of the system parameters if the transfer function is substituted for M, each of the system parameters (P,  $\omega_n^2$ , T<sub>m</sub>, K<sub>t</sub>,  $\alpha$ ,  $\beta$ ,  $\gamma$ , and C<sub>1</sub>) is substituted for K and the prescribed derivative is taken. Since the parameters K<sub>m</sub>,  $\gamma$  and  $\alpha$ , T<sub>1</sub> and  $\beta$ , T<sub>2</sub> occur in the same uninterrupted segment of the block diagram (Figure 5) the sensitivity functions will be the same for each set.

If

$$Q = T_m s^4 + C s^3 + D s^2 + E s + F$$

$$R = T_m s^2 + A s + B$$

$$M = Z/X$$

then the sensitivity functions are:

$$S_P^M = \frac{K_m P \alpha T_1 \gamma [C_1 T_m s^2 (\omega_n^2 T_m + C_1 A) s + \omega_n^2 A] s}{Q R}$$

$$S_{\omega_n^2}^M = \frac{-\omega_n^2 [T_m s^2 + A s + K_m P \beta T_2 \gamma]}{R}$$

$$S_{T_m}^M = \frac{-K_m P T_m \alpha T_1 \gamma [C_1 s + \omega_n^2] s^2}{Q R}$$

$$S_{K_t}^M = \frac{K_m^2 K_t P \alpha T_1 \gamma^2 [C_1 s + \omega_n^2] s}{Q R}$$

$$S_{K_m}^M = S_{\gamma}^M = \frac{K_m P \alpha T_1 \gamma [C_1 T_m s^2 + (\omega_n^2 T_m + C_1) s + \omega_n^2] s}{Q R}$$

$$S_{\alpha}^M = S_{T_1}^M = \frac{K_m P \alpha T_1 \gamma [C_1 T_m s^3 + (\omega_n^2 T_m + C_1 A) s^2 + E s + F]}{Q R}$$

$$S_{\beta}^M = S_{T_2}^M = \frac{K_m^2 P^2 \alpha T_1 \beta T_2 \gamma^2 [C_1 s + \omega_n^2]}{Q R}$$

$$S_{C_1}^M = \frac{-C_1 [T_m s^2 + A s + K_m P \beta T_2 \gamma] s}{R}$$

Since the equations are functions of all the parameters and the Laplace operator, a sine input is assumed and the sinusoidal transfer

function for each is calculated by setting  $s = j\omega$ . Since the phase angle of the sensitivity function has little significance, only the magnitude is calculated.

If

$$G = \sqrt{\begin{aligned} &[-Tm^2 \omega^6 + (D Tm + AC + BTm)\omega^4 \\ &- (FTm + AE + BD)\omega^2 + BF]^2 \\ &+ [Tm(C + A)\omega^5 - (ETm + AD + BC)\omega^3 \\ &+ (AF + BE)\omega]^2 \end{aligned}}$$

$$H = \sqrt{(Tm \omega^4 - D \omega^2 + F)^2 + (-C \omega^3 + E \omega)^2}$$

then the magnitude of each of the sensitivity functions is expressed as follows:

$$\left| S_{\frac{M}{P}} \right| = \frac{Km P \alpha T_1 \gamma \sqrt{(\omega_n^2 Tm + C_1 A)^2 \omega^4 + [-C_1 Tm \omega^3 + \omega_n^2 A \omega]^2}}{G}$$

$$\left| S_{\frac{M}{\omega_n^2}} \right| = \frac{\omega_n^2 \sqrt{(-Tm \omega^2 + Km P \beta T_2 \gamma)^2 + A^2 \omega^2}}{H}$$

$$\left| S_{\frac{M}{Tm}} \right| = \frac{Km P Tm \alpha T_1 \gamma \sqrt{C_1^2 \omega^6 + \omega_n^4 \omega^4}}{G}$$

$$\left| S_{Kt}^M \right| = \frac{K_m^2 K_t P \alpha T_1 \gamma^2 \sqrt{C_1^2 \omega^4 + \omega_n^4 \omega^2}}{G}$$

$$\left| S_{K_m}^M \right| = \left| S_{\gamma}^M \right| = \frac{K_m P \alpha T_1 \gamma \sqrt{(\omega_n^2 T_m + C_1)^2 \omega^4 + (-C_1 T_m \omega^3 + \omega_n^2 \omega)^2}}{G}$$

$$\left| S_{\alpha}^M \right| = \left| S_{T_1}^M \right| = \frac{K_m P \alpha T_1 \gamma \sqrt{[(-\omega_n^2 T_m + C_1 A)\omega^2 + F]^2 + [-C_1 T_m \omega^3 + E \omega]^2}}{G}$$

$$\left| S_{\beta}^M \right| = \left| S_{T_2}^M \right| = \frac{K_m^2 P^2 \alpha T_1 \beta T_2 \gamma^2 \sqrt{C_1^2 \omega^2 + \omega_n^4}}{G}$$

$$\left| S_{C_1}^M \right| = \frac{C_1 \sqrt{[A^2 \omega^4 + [-T_m \omega^3 + K_m P \beta T_2 \gamma \omega]^2}}{H}$$

The feedback system in the servo vibrograph causes each of the sensitivity functions to be of a very small amplitude and thus the instrument is not affected by small changes in the system parameters. Moreover, as the gains (alpha and gamma) are increased, the sensitivities are decreased to even lower values. The only sensitivity function which has a significantly large value is that of the sensitivity of Z/X with respect to the natural frequency of the basic vibrograph. Since this is set by the size of the inertial mass and spring and since both can be controlled and maintained at a constant value, there is no cause for concern.

As an example of the shape and magnitude of the sensitivity curves with respect to the input frequency, a sample is presented in Figure 39. The values for the parameters are as follows:

$$\begin{array}{ll}
 \alpha = 100 & K_t = 0.00031 \\
 \gamma = 5000 & T_m = 0.013 \\
 \beta = 10 & K_m = 3.05 \\
 \omega = 1 \text{ cps} & P = 6.9 \times 10^{-6} \\
 C_1 = 0.1 & T_1 = T_2 = 100
 \end{array}$$

For these values the 10%AME frequency is 0.49 cps, the 10%PHAE frequency is 0.165 cps and the maximum's frequency is 0.15 cps with an amplitude of 17.4.

The sensitivity reaches a maximum at a frequency (0.3 cps) slightly higher than the natural frequency and has the following values at the 10%AME frequency for an assumed 10 per cent variance in each parameter.

$$\begin{array}{ll}
 \gamma \text{ and } K_m = 1.11 \times 10^{-6} & \text{per cent} \\
 P = 6.38 \times 10^{-6} & \text{per cent} \\
 T_m = 4.45 \times 10^{-8} & \text{per cent} \\
 K_t = 5.26 \times 10^{-6} & \text{per cent} \\
 \alpha \text{ and } T_1 = 6.37 \times 10^{-6} & \text{per cent} \\
 \beta \text{ and } T_2 = 2.64 \times 10^{-10} & \text{per cent} \\
 \omega_n^2 = 1.01 & \text{per cent} \\
 C_1 = 7.90 \times 10^{-3} & \text{per cent}
 \end{array}$$

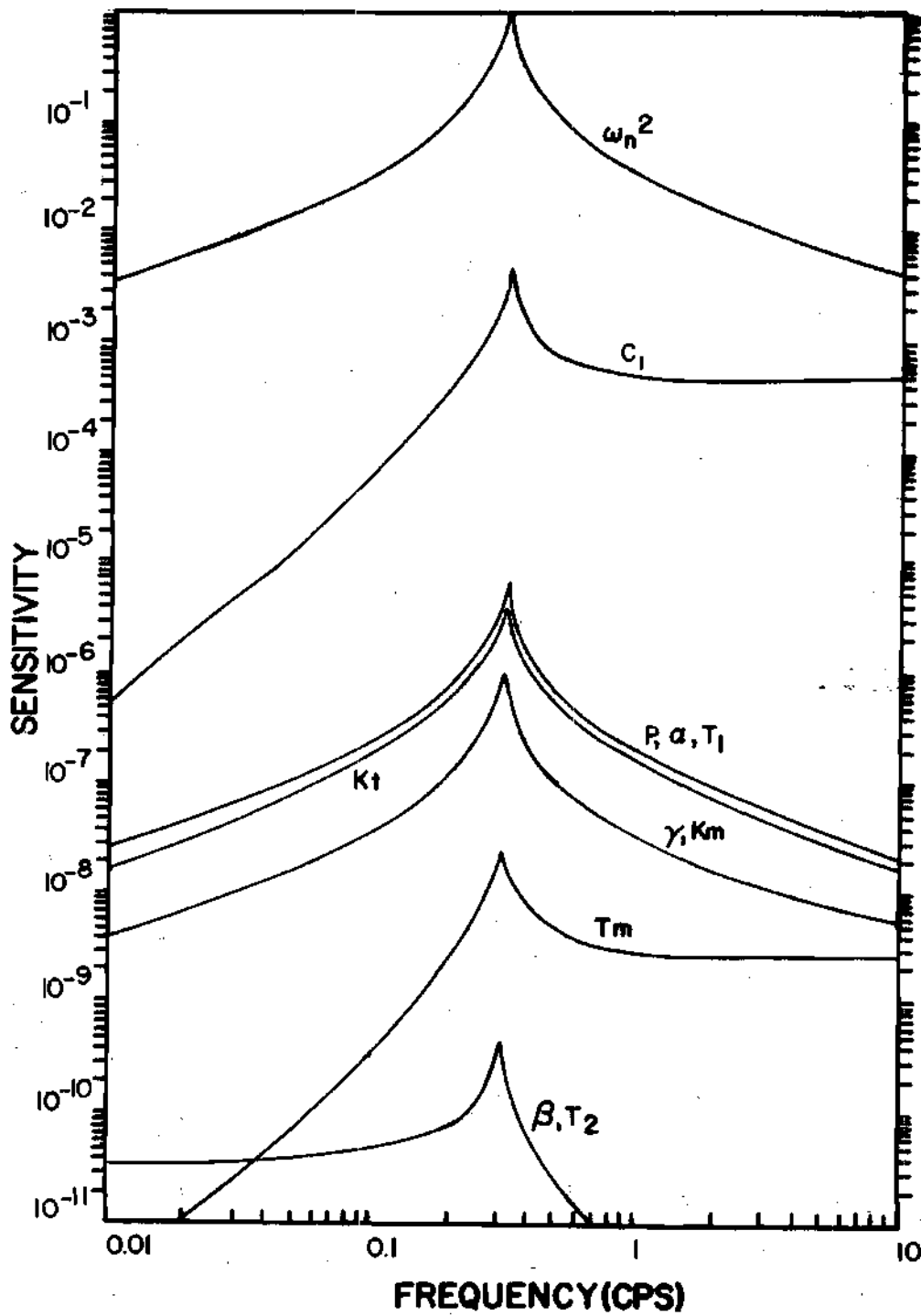


Figure 39. Sensitivity of the Servo Vibrograph

Due to the small values, the sensitivity with respect to the amplitude ( $Z/X$ ) is not an important factor in the design of the servo vibrograph.

APPENDIX E

SAMPLE COMPUTER PROGRAMS

```

BEGIN
COMMENT S H BYRNE ;
COMMENT FREQ RESPONSE CURVE ;
FILE OUT FO 6(2,15) ;
REAL OF,ALPHA1,GAMA,KT1A,BETA1,OM2P,C1,TM,KM,KT,OM2,P,BETA,ALPH,A,B,C,
D,E,F,FREQ,NUM1,DEN1,ZOX,NTAN,DTAN,PHI,PHID,ANG,ANGR,W ;
LABEL E1 ;
FORMAT OUT

```

```

FORM1("FREQ = ",E15.8," Z/X = ",E15.8," @ DEG = "
,E15.8),
FORM4(" ZERO DENOM DEN1" )
FORM6(X2,"ALPHA=",E15.8," GAMA =",E15.8," BETA =",E15.8),
FORM7(X2,"FREQ =",E15.8," C1 =",E15.8," KT =",E15.8),
FORM8(X2,"TM =",E15.8," KM =",E15.8," P =",E15.8) ;

```

LIST

```

ANS1(FREQ,ZOX,ANG),
ANS3(ALPHA1,GAMA,BETA1),
ANS4(OM2P,C1,KT1A),
ANS5(TM,KM,P) ;
KT1A + 0.00031 ;
OM2P + 0.982 ;
C1 + 0.17473 ;
TM + 0.0129793422 ;
KM + 3.050532 ;
BETA1 + 10 ;
OM2 + 38.07452 ;
P + 6.919780137e-6 ;
GAMA + 5000 ;
ALPHA1 + 100 ;

```

```

WRITE(FO,FORM6,ANS3) ; WRITE(FO,FORM7,ANS4) ; WRITE(FO,FORM8,ANS5) ;
ALPH + 100*ALPHA1*P ;
BETA + 100*BETA1*P ;
KT + KT1A ;
A+(KM*KT*GAMA + 1.0) ;
B+(GAMA*KM*(ALPH + BETA)) ;
C+(1.0+KM*KT*GAMA+C1*TM) ;
D+(GAMA*KM*(ALPH + BETA)+C1*(1.0+KM*KT*GAMA)+OM2*TM) ;

```

```

E+(C1×GAMA×KM×BETA+OM2×(1.0+KM×KT×GAMA)) ;
F+(GAMA×OM2×KM×BETA) ;
FOR FREQ + 0.1 STEP 0.1 UNTIL 5.0 DO BEGIN
W + FREQ×6.28318 ;
NUM1 + SQRT((TM×W+4-B×W+2)+2 + (A×W+3)+2) ;
DEN1 + SQRT((TM×W+4-D×W+2+F)+2 + (E×W- C×W+3)+2) ;
IF DEN1=0.0 THEN BEGIN WRITE(FO,FORM4) ; GO TO E1 END ;
ZOX + NUM1/DEN1 ;
QF + W ;
NTAN+((C×TM-A×TM)×QF+5-(B×C+E×TM-D×A)×QF+3+(B×E-A×F)×QF) ;
DTAN+((TM×TM×QF+6+(A×C-TM×D-TM×B)×QF+4+(F×TM+B×D-A×E)×QF+2-B×F) ;
IF DTAN=0.0 THEN ANGR+3.14159/2.0 ELSE
ANGR+ARCTAN(NTAN/DTAN) ;
IF (DTAN<0.0)AND(NTAN>0.0) THEN ANGR+ANGR+3.14159 ;
IF (DTAN<0.0)AND(NTAN<0.0) THEN ANGR+ANGR-3.14159 ;
ANG+ANGR×57.2958 ;
WRITE(FO,FORM1,ANS1) ;
E1:
END ;
END.

```

FREQUENCY RESPONSE FOR THE FOLLOWING PARAMETERS

ALPHA = 1.000000000+02    GAMA = 5.000000000+03    BETA = 1.000000000+01  
 FREQ = 9.820000000-01    C1 = 1.747300000-01    KT = 3.100000000-04  
 TM = 1.297934220-02    KM = 3.050532000+00    P = 6.919780140-06

FREQ =	1.000000000-01	Z/X =	1.286505850-01	DEG =	-2.190412610+00
FREQ =	2.000000000-01	Z/X =	6.327743340-01	DEG =	-7.105987990+00
FREQ =	3.000000000-01	Z/X =	9.763180490+00	DEG =	-1.047892090+02
FREQ =	4.000000000-01	Z/X =	2.181462670+00	DEG =	-1.706751190+02
FREQ =	5.000000000-01	Z/X =	1.532955810+00	DEG =	-1.747734350+02
FREQ =	6.000000000-01	Z/X =	1.318563780+00	DEG =	-1.762560170+02
FREQ =	7.000000000-01	Z/X =	1.215816340+00	DEG =	-1.770415690+02
FREQ =	8.000000000-01	Z/X =	1.157230260+00	DEG =	-1.775362940+02
FREQ =	9.000000000-01	Z/X =	1.120201780+00	DEG =	-1.778801370+02
FREQ =	1.000000000+00	Z/X =	1.095128040+00	DEG =	-1.781347820+02
FREQ =	1.100000000+00	Z/X =	1.077282840+00	DEG =	-1.783318980+02
FREQ =	1.200000000+00	Z/X =	1.064092830+00	DEG =	-1.784895300+02
FREQ =	1.300000000+00	Z/X =	1.054047520+00	DEG =	-1.786187730+02
FREQ =	1.400000000+00	Z/X =	1.046210320+00	DEG =	-1.787268530+02
FREQ =	1.500000000+00	Z/X =	1.039971650+00	DEG =	-1.788186950+02
FREQ =	1.600000000+00	Z/X =	1.034920570+00	DEG =	-1.788977840+02
FREQ =	1.700000000+00	Z/X =	1.030771210+00	DEG =	-1.789666550+02
FREQ =	1.800000000+00	Z/X =	1.027319420+00	DEG =	-1.790272060+02
FREQ =	1.900000000+00	Z/X =	1.024416100+00	DEG =	-1.790808650+02
FREQ =	2.000000000+00	Z/X =	1.021950190+00	DEG =	-1.791288160+02
FREQ =	2.100000000+00	Z/X =	1.019837550+00	DEG =	-1.791718890+02
FREQ =	2.200000000+00	Z/X =	1.018013430+00	DEG =	-1.792108180+02
FREQ =	2.300000000+00	Z/X =	1.016427330+00	DEG =	-1.792461790+02
FREQ =	2.400000000+00	Z/X =	1.015039390+00	DEG =	-1.792784470+02
FREQ =	2.500000000+00	Z/X =	1.013817800+00	DEG =	-1.793080160+02
FREQ =	2.600000000+00	Z/X =	1.012736880+00	DEG =	-1.793352130+02
FREQ =	2.700000000+00	Z/X =	1.011775780+00	DEG =	-1.793603150+02
FREQ =	2.800000000+00	Z/X =	1.010917350+00	DEG =	-1.793835560+02
FREQ =	2.900000000+00	Z/X =	1.010147440+00	DEG =	-1.794051390+02
FREQ =	3.000000000+00	Z/X =	1.009454240+00	DEG =	-1.794252350+02

```

BEGIN
COMMENT S H BYRNE - FREQUENCY RESPONSE CHARACTERISTICS
PROGRAM FINDS
1  FREQUENCY AND AMPLITUDE AT A 90 DEGREE PHASE ANGLE
2  FREQUENCY, AMPLITUDE, AND PHASE ANGLE AT MAXIMUM
3  10 PERCENT AMPLITUDE ERROR FREQUENCY WITH PHASE ANGLE
4  10 PERCENT PHASE ANGLE ERROR FREQUENCY WITH AMPLITUDE
LABEL  E2,E3,T1,T2,T6,T5,F2,F3,U8,U9,V8
INTEGER M,R1,R2,R3,R4,R5,S,R,IR,R6,R7,R8,R9
REAL  FREQ,PER,FRFQ,PFR,ANG,ZZ1,YYF,YYP,ALPHA1,GAMA,BETA1,DM2P,C1,KT1A,TM
,P,A,B,C,D,E,F,KM,KT,ALPH ,BETA,DM2,AR,BR,CR,DR,XF,X,NUM,DEN,ERROR,Q,Y,
Z0,Y1,I,Z1,QF,N,L,NTAN,DTAN,ANGR,ZZZ,IMA,IMAG,U1,U2,U3,U4,U5,U6,U7,ZO
INTEGER ARRAY BD(0:133,0:133)
REAL ARRAY  RSE(0:133,0:133)
FILE OUT  FD 6(2,15)
FORMAT OUT

```

```

FORM6(/,"GAMA(HOR) & ALPHA(VERT) = 10,25,50,100,250,500,750,"
1000,2000,3000,4000,5000,10000) BETA =" ,E15,8),
FORM7(X2,"FREQ =" ,E15,8," C1 =" ,E15,8," KT =" ,E15,8) ,
FORM8(X2,"TM =" ,E15,8," KM =" ,E15,8," P =" ,E15,8) ,
FORM9( 10(E12,4)) ,
FORM11(/,"NATURAL UNDAMPED FREQ",///) ,
FORM12(/,"Z/X MAX",///) ,
FORM13(/,"NATURAL DAMPED FREQ",///) ,
FORM14(/,"FREQ--10 % OFF FINAL VALUE",///) ,
FORM15(/,"ANG--10 % OFF FINAL VALUE",///) ,
FORM16(/,"FREQ--162 DEGREES",///) ,
FORM17(/,"Z/X--162 DEGREES",///) ,
FORM18(/,"ANG--MAX Z/X",///) ,
FORM19(X8,I2,9(X10,I2)) ,
FORM20(X58,I2,2(X10,I2)) ,
FORM21(/,"Z/X--90 DEGREES",///) ,
FORM10(X50,3(E12,4))

```

LIST

```

ANP3(BETA1) ,
ANS4(DM2P,C1,KT1A) ,
ANS5(TM,KM,P) ,

```

```

ANS6(FOR S+1 STEP 1 UNTIL 10 DO RS(R,S)) ;
ANS7(FOR S+11 STEP 1 UNTIL 13 DO RS(R,S)) ;
ANS8(FOR S+1 STEP 1 UNTIL 10 DO BO(R,S)) ;
ANS9(FOR S+11 STEP 1 UNTIL 13 DO BO(R,S)) ;
DEFINE ZOX=((((TM*Y+4-B*Y*Y)+2+A*A*Y+6)/((TM*Y+4-D*Y+2+F)*2 +
      (*C*Y+3+E*Y)*2)) #)
KT1A+ 0.01 ;
KT+KT1A ;
DM2P + 1.0 ;
DM2+39.478417612 ;
TM+0.01 ;
KM+ 1.0 ;
P+ 7.00-6 ;
C1+ 0.1 ;
BETA1+10.0 ;
BETA+ 100*BETA1*P ;
R1+0 ; R2+13 ; R3+26 ; R4+39 ; R5+52 ; S+0 ;
R6+65 ; R7+78 ; R8+ 91 ; R9+104 ;
FOR ALPHA1 + 10.0,25.0,50.0,100.0,250.0,500.0,750.0,1000.0,
      2000.0,3000.0,4000.0,5000.0,10000.0 DO BEGIN
      R1+R1+1 ; R2+R2+1 ; R3+R3+1 ; R4+R4+1 ; R5+R5+1 ; S+0 ;
      R6+R6+1 ; R7+R7+1 ; R8+R8 +1 ; R9+R9 + 1 ;
FOR GAMA + 10.0,25.0,50.0,100.0,250.0,500.0,750.0,1000.0,
      2000.0,3000.0,4000.0,5000.0,10000.0 DO BEGIN
      S+S+1 ;
      ALPH+ 100*ALPHA1*P ;
FOR M+ R1,R2,R3,R4,R5,R6,R7,R8,R9
      DO BEGIN BO(M,S) + 0 ; END ;
      A+(KM*KT*GAMA + 1.0) ;
      B+(GAMA*KM*(ALPH +BETA)) ;
      C+(1.0+KM*KT*GAMA+C1*TM) ;
      D+(GAMA*KM*(ALPH +BETA)+C1*(1.0+KM*KT*GAMA)+DM2*TM) ;
      E+(C1*GAMA*KM*BETA+DM2*(1.0+KM*KT*GAMA)) ;
      F+(GAMA*DM2*KM*BETA) ;
      AR+TM*TM ;
      BR+A*C-D*TM-B*TM ;
      CR+F*TM+B*D-A*E ;

```

```

DR+ =B*F ;
XF+100.0 ; M+0 ; X+0.1 ;
IF DR#0.0 THEN BEGIN
E2: NUM+ 2.0*X*X*X*AR + BR*X*X - DR ;
DEN+ 3.0*X*X*AR + 2.0*BR*X + CR ;
END
ELSE BEGIN BO[R1,S]+30 ;
IMAG+BR*BR - 4.0*AR*CR ;
IF IMAG<0.0 THEN BEGIN BO[R1,S]+ 31 ;
XF+0.0 ; GO TO E3 ; END ;
IMA +(-BR + SQRT(IMAG))/2.0*AR ;
XF+IMA ;
IF IMA <0.0 THEN BEGIN XF+0.0 ; BO[R1,S]+32 ; END ;
GO TO E3 ; END ;
IF (DEN#0.0) THEN
BEGIN X+X+0.1 ; M+M+1 ; GO TO E2 ; END ;
XF+ NUM/DEN ; ERROR + XF - X ;
IF XF<0.0 THEN XF+M + 1.0 ELSE BEGIN
IF ABS(ERROR) < 0.0005 THEN
GO TO E3 ; END ;
IF M > 100 THEN BEGIN BO[R1,S]+20 ; GO TO E3 ; END ;
M + M+1 ; X+XF ; GO TO E2 ;
E3: Q+SQRT(ABS(XF)) ;
FREQ + Q/6.28318 ;
IF Q=0.0 THEN RS[R9,S]+0.0 ELSE BEGIN Y+Q ; RS[R9,S]+SQRT(ZOX)
END ;
BO[R9,S]+BO[R1,S] ;
RS[R1,S]+FREQ ;
M+0 ;
Y+6.0 ; ZO+ZOX ; Y1+6.0 ;
I+2.0 ;
T1: Y1+Y1 + I ;
IF Y1 < 0.0 THEN BEGIN Y1+Y1 - I ; I+0.5*I ; GO TO T1 ; END ;
IF Y1>62.831853 THEN BEGIN BO[R2,S]+41 ;
ZZ1+SQRT(Z1) ; Y1+Y1/6.28318 ;
Y1+1.0 ;
IF ZO<1.0 THEN BO[R2,S]+49 ; GO TO T6 ; END ;

```

```

Y+Y1 ;
Z1+ZOX ;
M+M+1 ;
IF M > 100 THEN BEGIN BO[R2,S]+20 ; GO TO T2 ; END ;
IF Z1 > ZO THEN BEGIN ZO+Z1 ; GO TO T1 ; END ;
I+0.5*I ;
IF ABS(I)<0.00001 THEN GO TO T2 ;
ZO+Z1 ; GO TO T1 ;
T2: ZZ1+SQRT(Z1) ; YF+Y1/6.28318 ;
T6: RS[R2,S]+ZZ1 ; RS[R3,S]+YF ;
QF+Y1 ;
NTAN+((C*TM-A*TM)*QF+5-(B*C+E*TM-D*A)*QF+3+(B*E-A*F)*QF) ;
DTAN+-(TM*TM*QF+6+(A*C-TM*D-TM*B)*QF+4+(F*TM+B*D-A*E)*QF+2-B*F) ;
IF DTAN=0.0 THEN ANGR+=3.14159/2 ; ELSE
ANGR+ARCTAN(NTAN/DTAN) ;
IF (DTAN<0.0)AND(NTAN>0.0) THEN ANGR+ANGR+3.14159 ;
IF (DTAN<0.0)AND(NTAN<0.0) THEN ANGR+ANGR-3.14159 ;
ANG+ANGR*57.2958 ;
BO[R3,S]+BO[R8,S]+BO[R2,S] ;
RS[R8,S]+ANG ;
IF ABS(1.0 - ZZ1) < 0.1 THEN BEGIN BO[R4,S]+51 ;
Y1+1.0 ; END ;
Y+Y1 ; M+0 ; N+1.0 ; I+1.0 ;
F2: Y+Y+I ;
IF Y<0.0 THEN BEGIN Y+Y-I ; I+0.5*I ; GO TO F2 ; END ;
L+ABS(SQRT(ZOX) - 1.0) ;
M+M+1 ;
IF M > 100 THEN BEGIN BO[R4,S]+20 + BO[R4,S] ; GO TO F3 ; END ;
IF (N*L) < (0.1*N) THEN BEGIN
I+0.5*I ;
IF ABS(I)<0.00001 THEN GO TO F3 ;
N+N ; END ;
GO TO F2 ;
F3: FRFQ+Y/6.28318 ;
QF+Y ;
T5: RS[R4,S]+FRFQ ;

```

```
NTAN+=((C*TM-A*TM)*QF*5-(B*C+E*TM-D*A)*QF*3+(B*E-A*F)*QF) ;  
DTAN+=(TM*TM*QF*6+(A*C-TM*D-TM*B)*QF*4+(F*TM+B*D-A*E)*QF*2-B*F)  
;
```

```
IF DTAN=0.0 THEN ANGR+=-3.14159/2 ELSE  
ANGR+ARCTAN(NTAN/DTAN) ;  
IF (DTAN<0.0)AND(NTAN>0.0) THEN ANGR+ANGR+3.14159 ;  
IF (DTAN<0.0)AND(NTAN<0.0) THEN ANGR+ANGR-3.14159 ;  
ANG+ANGR*57.2958 ;
```

```
RS[R5,S]+ANG ;  
BO[R5,S]+BO[R4,S] ;  
Y+Y1 ; M+0 ; N+1.0 ; I+1.0 ;
```

```
U1+C*TM-A*TM ;  
U2+B*C+E*TM-D*A ;  
U3+B*E-A*F ;  
U4+TM*TM ;  
U5+A*C-TM*D-TM*B ;  
U6+F*TM+B*D-A*E ;  
U7+B*F ;
```

U9:

```
Y+Y+I ;  
IF YSO.0 THEN BEGIN Y+Y-I ; I+0.5*I ; GO TO U9 END ;  
NTAN+=(U1*Y*5 - U2*Y*3 + U3*Y) ;  
DTAN+=(U4*Y*6 + U5*Y*4 + U6*Y*2 - U7) ;
```

```
ANGR+ARCTAN(NTAN/DTAN) ;  
IF (DTAN<0.0)AND(NTAN>0.0) THEN ANGR+ANGR+3.14159 ;  
IF (DTAN<0.0)AND(NTAN<0.0) THEN ANGR+ANGR-3.14159 ;  
L+ABS(ANGR) ;  
M+M+1 ;
```

```
IF M > 100 THEN BEGIN BO[R6,S]+BO[R7,S]+20 ; GO TO U8 ; END ;  
IF (N*L)>(2.82743*N) THEN BEGIN
```

```
I+0.5*I ;  
IF ABS(I)<0.00001 THEN GO TO U8 ;  
N+N END ;  
GO TO U9 ;
```

U8:

```
RS[R6,S]+Y/6.28318 ;  
RS[R7,S]+SQRT(ZOX) ;  
END ; END ;
```

```

BEGIN INTEGER BREAKFORNEWSEGMENT ;
  WRITE(FO(PAGE)) ;
  FOR IR+1,105,27,14,92,40,53,66,79 DO BEGIN
    FOR R+IR STEP 1 UNTIL (IR+12) DO BEGIN
      WRITE(FO,FORM9,ANS6) ;WRITE(FO,FORM19,ANS8) ;END ;
    WRITE(FO,FORM6,ANS3) ; WRITE(FO,FORM7,ANS4) ; WRITE(FO,FORM8,ANS5) ;
    IF IR = 1 THEN WRITE(FO,FORM11) ELSE BEGIN
    IF IR = 14 THEN WRITE(FO,FORM12) ELSE BEGIN
    IF IR = 27 THEN WRITE(FO,FORM13) ELSE BEGIN
    IF IR = 40 THEN WRITE(FO,FORM14) ELSE BEGIN
    IF IR = 66 THEN WRITE(FO,FORM16) ELSE BEGIN
    IF IR = 79 THEN WRITE(FO,FORM17) ELSE BEGIN
    IF IR = 92 THEN WRITE(FO,FORM18) ELSE BEGIN
    IF IR = 105 THEN WRITE(FO,FORM21) ELSE BEGIN
    WRITE(FO,FORM15) END ; END ; END ; END ; END ; END ; END ; END ;
    FOR R+IR STEP 1 UNTIL (IR+12) DO BEGIN
    WRITE(FO,FORM10,ANS7) ; WRITE(FO,FORM20,ANS9) ; END ;
    WRITE(FO(PAGE)) ;
  END ;
END ;
COMMENT MEANING OF SUB-CONSTANTS
00+NO COMMENT 20+ITERATION OVER 100
30+ DR= 0 31+IMAG 32+NEG ALL FOR UNDAMPED NAT FREQ ROOTS
41+FREQ > 10 CPS 49+FREQ > 10 CPS AND Z/X < 1.0
51+MAX Z/X LESS THAN 10% OFF 71+ SAME AND OVER 100 ;
V8 ;
END.

```

138

3.3170e+00	3.3167e+00	3.3126e+00	3.3112e+00	3.3098e+00	3.3096e+00
0	0	0	0	0	0
3.3212e+00	3.2740e+00	3.1493e+00	3.1110e+00	3.0720e+00	3.0664e+00
0	0	0	0	0	0
3.3081e+00	4.3628e-01	2.1100e-01	1.8134e-01	1.6185e-01	1.5971e-01
0	51	51	51	51	51
3.2074e+00	2.2072e-01	1.9270e-01	2.3011e-01	2.5001e-01	2.5218e-01
0	51	0	0	0	0
3.5036e-01	1.1796e-01	1.3827e-01	1.3995e-01	1.4118e-01	1.4132e-01
51	0	0	0	0	0
1.7987e-01	9.4712e-02	1.0132e-01	1.0191e-01	1.0234e-01	1.0239e-01
51	0	0	0	0	0

GAMA(HOR) AND ALPHA(VERT) = 10,100,500,1000,5000,10000    BETA = 1.00000000e+01  
 FREQ = 1.00000000e+00    C1 = 1.00000000e-01    KT = 1.00000000e-02  
 TM = 1.00000000e-02    KM = 1.00000000e+00    P = 7.00000000e-06

FREQUENCY---10 PERCENT OFF FINAL VALUE

## LITERATURE CITED

1. W. Bradley and E. E. Eller  
*Shock and Vibration Handbook*  
McGraw-Hill Book Co., New York, 1961, pp. 12-1 to 12-24.
2. S.A.E. Technical Board  
*Cooperative Testing of Torsiographs and Calibrators*  
Society of Automotive Engineers, Inc., New York, 1947.
3. W. K. Wilson  
*Practical Solution of Torsional Vibration Problems*  
John Wiley and Sons, Inc., New York  
Second Edition, 1940, Vol. II, pp. 203-365.
4. C. H. Bradbury  
*Torsional Vibration in Diesel Engines*  
Charles Griffin and Co. Ltd., London, 1938.
5. E. E. Gross, Jr.  
*Measurement of Vibration*  
General Radio Co., Cambridge, Mass., 1955.
6. E. F. Sawarenski and D. P. Kirnos  
*Elemente der Seismologie und Seismometrie*  
Akademie-Verlag-Berlin, 1960, pp. 321-494.
7. H. Benioff  
"Earthquake Seismographs and Associated Instruments"  
*Advances in Geophysics*  
Vol. 2, 1955, pp. 219-275.
8. C. F. Richter  
*Elementary Seismology*  
H. Freeman and Co., San Francisco, 1958.
9. P. Byerly  
*Seismology*  
Prentice-Hall, Inc., Englewood Cliffs, N. J., 1942.
10. J. P. Eaton  
"Theory of the Electromagnetic Seismograph"  
*Bulletin Seismological Society of America*  
Vol. 47, 1957, pp. 37-75.

11. H. Benioff  
"A New Vertical Seismograph"  
*Bull. Seismol. Soc. Am.*  
Vol. 22, 1932, pp. 115.
12. P. Byerly  
"Theory of the Hinged Seismometer with Support in General Motion"  
*Bull. Seismol. Soc. Am.*  
Vol. 42, 1952, pp. 251.
13. A. Wolf  
"The Limiting Sensitivity of Seismic Detectors"  
*Geophysics*  
Vol. 7, April, 1942, pp. 115-122.
14. D. E. Hudson  
"The Measurement of Ground Motion of Destructive Earthquakes"  
*Bull. Seismol. Soc. Am.*  
Vol. 53, No. 2, pp. 419-437, February, 1963.
15. F. E. Romberg  
"Analytical Expression for Transients in Seismometer-Galvanometer Systems"  
*Bull. Seismol. Soc. Am.*  
Vol. 53, No. 3, pp. 563-576, April, 1963.
16. B. P. Bogert  
"Correction of Seismograms for the Transfer Function of the Seismometer"  
*Bull. Seismol. Soc. Am.*  
Vol. 52, No. 4, pp. 781-792, Oct., 1962.
17. J. Coulomb and G. Grenet  
"Nouveaux Principes de construction des seismographes electromagnetiques"  
*Annales de Physique*  
Ser. 11, No. 3, 1935, pp. 321-369.
18. B. P. Bogert  
"The Transfer Function of a Short-Period Vertical Seismograph"  
*Bull. Seismol. Soc. Am.*  
Vol. 51, No. 4, pp. 503-513, October, 1961.
19. D. Silverman  
"The Frequency Response of Electromagnetically Damped Dynamic and Reluctance Type Seismometers"  
*Geophysics*  
Vol. 4, 1939, pp. 53-68.

20. S. K. Chakrabarty and S. N. R. Choudhury  
"Response Characteristics of Electromagnetic Seismographs"  
*Bull. Seismol. Soc. Am.*  
Vol. 54, No. 5, Part A, pp. 1445-1458, October, 1964.
21. S. K. Chakrabarty  
"Response Characteristics of Electromagnetic Seismographs and  
their Dependence on the Instrumental Constants"  
*Bull. Seismol. Soc. Am.*  
Vol. 39, 1949, pp. 205-218.
22. L. Fleming  
"Feedback Vibrometer"  
*Journal Acoustical Society of America*  
Vol. 36, No. 9, pp. 1645-1648, September, 1964.
23. M. J. Tucker  
"An Electronic Feedback Seismograph"  
*Journal Scientific Institute*  
Vol. 35, No. 5, pp. 167-171, May, 1958.
24. G. H. Sutton and G. V. Latham  
"Analysis of Feedback-Controlled Seismometer"  
*Journal Geophysical Research*  
Vol. 69, No. 18, pp. 3865-3882, September, 1964.
25. R. Gilman  
"Report on Some Experimental Long-Period Seismographs"  
*Bull. Seismol. Soc. Am.*  
Vol. 50, No. 4, pp. 553-559, October, 1960.
26. H. E. Sheffield  
"An Electronic Vertical Long-Period Seismometer"  
*Institute of Electrical and Electronic Engineers Transactions*  
Vol. IM-13, No. 1, March, 1964, pp. 2-7.
27. P. Bernard  
"Sur l'amplification des séismographes dont la période est  
allongée par condensateurs,"  
*Annales De Géophysique*  
Vol. 11, 1955, pp. 374-375.
28. J. Coulomb  
"Accroissement de la période d'un galvanomètre par emploi d'un  
condensateur"  
*Mesures*  
Vol. 179, 1952, pp. 221-224.

29. H. Benioff  
"Long-Period Seismographs"  
*Bull. Seismol. Soc. Am.*  
Vol. 50, No. 1, pp. 1-13, January, 1960.
30. K. Matsushima and T. Nakada  
"Principle of Servo-Vibrograph of Long Natural Period"  
*Bulletin of the Tokyo Institute of Technology*  
No. 58, March, 1964, pp. 49-59.
31. Nakada, Asakura, Fukuda and Watanabe  
"Measurement of the Accuracy of Table Rotation of Gear Hobbing  
Machine and Apparatus for Correcting Errors in Rotation"  
*Japan Society of Mechanical Engineers*  
Vol. 66, No. 533, 1963.
32. K. Matsushima and T. Nakada  
"Very Low-Pass Mechanical Filter Applied Schuler Pendulum"  
Preparatory Reports of the 6th Associated Meeting for Automatic  
Control, 1963.
33. B. C. Kuo  
*Automatic Control Systems*  
Prentice-Hall, Inc., Englewood Cliffs, N. J., 1962.

#### Other References

34. K. E. Bullen  
*An Introduction to the Theory of Seismology*  
University Press, Cambridge, Third Edition, 1963.
35. A. H. Church  
*Mechanical Vibrations*  
John Wiley and Sons, Inc., New York, 1957, pp. 85-90.
36. R. E. Ingram  
"An Integral Solution of the Electromagnetic Seismograph Equation"  
*Bull. Seismol. Soc. Am.*  
Vol. 50, No. 3, pp. 461-465, July, 1960.
37. J. N. Macduff and J. R. Curreni  
*Vibration Control*  
McGraw-Hill Book Co., New York, 1958, pp. 50-53.
38. B. Morrill  
*Mechanical Vibrations*, The Ronald Press Co., New York, 1957,  
pp. 81-82.
39. F. H. Raven  
*Automatic Control Engineering*  
McGraw-Hill Book Co., Inc., New York, 1961.

40. W. T. Thomson  
*Mechanical Vibrations*  
Prentice-Hall, Inc., Englewood Cliffs, N. J., 1948, pp. 94-99.
41. K. N. Tong  
*Theory of Mechanical Vibration*  
John Wiley and Sons, Inc., New York, 1960, pp. 79-83.
42. F. S. Tse, I. E. Morse and R. T. Hinkle  
*Mechanical Vibrations*  
Allyn and Bacon, Inc., Boston, 1963, pp. 78-83.

## VITA

Sydnor Hummer Byrne, Jr. was born in Blacksburg, Virginia on February 20, 1941. There he attended elementary and secondary schools, graduating from high school in 1959. He immediately entered Virginia Polytechnic Institute and was graduated highest in his class in the school of Mechanical Engineering. In September of 1963 he entered the Georgia Institute of Technology, received a Master of Science Degree in 1965, and continued to pursue the Doctor of Philosophy Degree in the School of Mechanical Engineering.

During the summer months of this undergraduate study, he worked as an engineer for the Newport News Shipbuilding and Dry Dock Company, Newport News, Virginia; Esso Research and Engineering Company, Morristown, New Jersey; and Allegheny Ballistics, Cumberland, Maryland.

He married Mary Alice Kingrea in March of 1965 and presently has no children.

His primary interest is in the area of applied research in mechanical engineering with specific interest in machine design and allied subjects.